

KLAIPĖDA UNIVERSITY

Nikita DOBROTIN

EVOLUTION OF THE CURONIAN
SPIT DUNES

DOCTORAL DISSERTATION

BIOMEDICAL SCIENCES,
ECOLOGY AND ENVIRONMENTAL SCIENCES (03B)

Klaipėda, 2018

Doctoral dissertation was prepared during the period 2011–2018 at Klaipėda University, based on the conferment a doctorate right which was granted for Klaipėda University by the order of the Minister of Education and Science (Republic of Lithuania) No. V-574, signed on 17th July, 2017.

Academic advisor

prof. dr. Albertas BITINAS (Klaipėda University, Physical Sciences, Geology – 05P)

The doctoral dissertation will be defended at the Board of Klaipėda University in Ecology and Environmental Sciences:

Chairman

prof. dr. Zita Rasuolė GASIŪNAITĖ (Klaipėda University, Biomedical Sciences, Ecology and Environmental Sciences – 03B)

Members:

dr. Nerijus BLAŽAUSKAS (Klaipėda University, Physical Sciences, Geology Sciences – 05P),

doc. dr. Martynas BUČAS (Klaipėda University, Biomedical Sciences, Ecology and Environmental Sciences – 03B),

dr. Alar ROSENTAU (Tartu University, Estonia, Physical Sciences, Geology Sciences – 05P),

prof. habil. dr. Sergej OLENIN (Klaipėda University, Biomedical Sciences, Ecology and Environmental Sciences – 03B).

The doctoral dissertation will be defended in a public meeting of the Board in Ecology and Environmental Sciences, Klaipėda University, Aula Magna Conference hall at 1 p.m. on 19th of October, 2018.

Address: Herkaus Manto str. 84, LT-92294, Klaipėda, Lithuania.

The doctoral dissertation was sent out on 19th of September 2018.

The doctoral dissertation is available for review at the Library of the Klaipėda University.

KLAIPĖDOS UNIVERSITETAS

Nikita DOBROTIN

KURŠIŲ NERIJOS
KOPŪ RAIDA

DAKTARO DISERTACIJA

BIOMEDICINOS MOKSLAI,
EKOLOGIJA IR APLINKOTYRA (03B)

Klaipėda, 2018

Disertacija rengta 2011–2018 metais Klaipėdos universitete pagal suteiktą Klaipėdos universitetui Lietuvos Respublikos švietimo ir mokslo ministro 2017 m. liepos 17 d. įsakymu Nr. V-574 Ekologijos ir aplinkotyros mokslo krypties doktorantūros teise.

Vadovas

prof. dr. Albertas BITINAS (Klaipėdos universitetas, fiziniai mokslai, geologija – 05P)

Daktaro disertacija ginama Klaipėdos universiteto Ekologijos ir aplinkotyros mokslo krypties taryboje:

Pirmininkas

prof. dr. Zita Rasuolė GASIŪNAITĖ (Klaipėdos universitetas, biomedicinos mokslai, ekologija ir aplinkotyra – 03B)

Nariai:

dr. Nerijus BLAŽAUSKAS (Klaipėdos universitetas, fiziniai mokslai, geologija – 05P),

doc. dr. Martynas BUČAS (Klaipėdos universitetas, biomedicinos mokslai, ekologija ir aplinkotyra – 03B),

dr. Alar ROSENTAU (Tartu universitetas, Estija, fiziniai mokslai, geologija – 05P),

prof. habil. dr. Sergej OLENIN (Klaipėdos universitetas, biomedicinos mokslai, ekologija ir aplinkotyra – 03B).

Daktaro disertacija bus ginama viešame Ekologijos ir aplinkotyros mokslo krypties tarybos posėdyje 2018 m. spalio 19 d. 13 val. Klaipėdos universiteto Aula Magna konferencijų salėje.

Adresas: Herkaus Manto 84, LT-92294, Klaipėda, Lietuva.

Daktaro disertacija išsiųsta 2018 m. rugsėjo 19 d.

Disertaciją galima peržiūrėti Klaipėdos universiteto bibliotekoje.

Abstract

One of the unique places in Europe in both environmental and cultural terms is the Curonian Spit – a massive sandy barrier separating the Curonian Lagoon from the Baltic Sea. Straddling both the Lithuanian and the Russian parts, the Spit is included into the UNESCO list of cultural heritage monuments. From the geological point of view, it is still an “alive” environment dominated by aeolian deposits. Detailed investigations of the Dead (Grey) Dunes massif along the Lithuanian part of the Spit using ground-penetrating radar (GPR) and magnetic susceptibility (MS) surveys, supported by radiocarbon (^{14}C) chronological framework of paleosols and infrared optically stimulated luminescence (IR-OSL) ages of sand horizons, have advanced understanding of aeolian landscape evolution. The detailed analysis of the received data did not allow distinguishing separate soil-forming generations and supported the idea of only one long continuous period of permanent formation of palaeosols. According to the data of palaeodynamic reconstructions carried out in the Dead (Grey) Dunes massif, mid-Holocene phase of dune activity was of a local character and likely did not exceed several centuries. GPR surveys enabled a series of paleogeographic reconstructions of the massif for different time intervals of its evolutionary history.

Key words

Curonian Spit, palaeosol, ground penetrating radar (GPR), radiocarbon (^{14}C) dating, IR-OSL dating, Holocene, Dead (Grey) Dunes.

Reziumė

Kuršių Nerija yra vienas unikaliausių Lietuvos kampelių tiek kultūrine, tiek geologine prasme. Geologiniu požiūriu – tai „gyvas“, iki šiol besiformuojantis darinys, kurį sudaro eolinės (vėjo sunėšamos) nuogulos.

Detalus Mirusiujų (Pilkujų) kopų tyrimų kompleksas, susidedantis iš modernių geofizinių ir geochronologinių tyrimo metodų, apėmė geofizinius lauko tyrimus georadarui (GPR), eolinių smėlių magnetinio imlumo matavimus, paleodirvožemiu radiokarboninį (^{14}C) bei eolinių smėlių absoliutaus amžiaus nustatymą optiškai stimuliuotos liuminescencijos (IR-OSL) metodais. Detalios surinktų duomenų analizės metu nepavyko išskirti atskirų dirvožemų formavimosi generacijų, gauti duomenys palaiko vieno ilgo dirvodaros proceso modelį.

Tyrimo duomenys rodo, kad kopų reaktivacija paskatino lokalūs veiksniai, jie apėmė nedideles teritorijas, trūko nuo kelių dešimčių iki kelių šimtų metų. Sudarytos paleogeografinės rekonstrukcijos atkuriant skirtingais laikotarpiais buvusį kopų reljefą.

Reikšmingi žodžiai

Kuršių nerija, paleodirvožemis, georadaras, radiokarboninis (^{14}C) datavimas, IR-OSL datavimas, Holocenas, Mirusios (Pilkosios) kopos.

Contents

1. INTRODUCTION	9
1.1 Relevance of the thesis	9
1.2 Aim and objectives	10
1.3 Novelty of the study	11
1.4 Scientific and practical significance of the results	11
1.5 Scientific approval	12
1.6 Acknowledgment	14
1.7 Abbreviations	14
2. LITERATURE REVIEW	15
3. MATERIAL AND METHODS	25
3.1 Study area	25
3.2 Geological structure of the Curonian Spit	25
3.2.1 Stratigraphy of Quaternary sediments	25
3.2.2 Geomorphologic characteristics	28
3.3 Ground penetrating radar (GPR) survey	29
3.3.1 GPR operation basics	29
3.3.2 Survey of the Dead (Grey) Dunes	31
3.4 Magnetic susceptibility	33
3.5 Radiocarbon (^{14}C) analysis	33
3.6 Optically stimulated luminescence (IR-OSL) dating	34
3.7 GPR data interpretation and palaeogeographic reconstructions	34
3.8 Evaluation of aeolian palaeodynamics	41

4. GEOLOGICAL LAYERING OF THE PALAEOSOLS, THEIR AGE AND PALAEOODYNAMICS OF DUNE MASSIFS	43
4.1 Distribution and age of palaeosols	43
4.2 Interpretation of palaeosol age and formation	47
4.3 Aeolian palaeodynamics	51
4.4 Palaeogeographic reconstructions	57
5. DISCUSSION	61
5.1 Dune evolution and climate change	61
5.2 Ecogeology and dune formation	63
CONCLUSIONS	67
REFERENCES	69
ANNEXES	75
Annex No.1. Borehole No. 30 used in GPR data interpretation	76
Annex No.2. Control boreholes used to identify GPR reflections	76
Annex No.3. Borehole No. 18685 used in GPR data interpretation	77
Annex No.4. Results of radiocarbon (^{14}C) dating of palaeosols in the Curonian Spit	77
Annex No.5. Magnetic susceptibility (MS) measurements at the Vingis dune site	84
Annex No.6. Magnetic susceptibility (MS) measurements at the Naglis dune site	85
Annex No.7. GPR cross-sections	86
SANTRAUKA	89
Ivadas	89
Temos aktualumas	89
Tyrimo tikslas ir pagrindiniai uždaviniai	90
Naujumas	90
Darbo mokslinė ir praktinė reikšmė	90
Darbo rezultatų aprobatimas	91
Santrumpų sąrašas	93
Tyrimo medžiaga ir metodai	94
Tyrimų rajonas	94
Geomorfologija	94
Georadaro veikimo principas	95
Kopų tyrimas georadaru	95
Magnetinis imlumas	95
Paleodirvožemiu datavimas radiokarboniniu (^{14}C) metodu	96
Smėlių datavimas OSL metodu	96
Georadaro duomenų interpretavimas ir paleogeografinės rekonstrukcijos	96
Eolinių paleodinamikos vertinimas	97
Rezultatai	98
Paleodirvožemiu amžius ir paplitimas	98
Paleodirvožemiu amžiaus ir genezės interpretacija	98
Eolinių procesų paleodinamika	99
Paleogeografinės rekonstrukcijos	100
Rezultatų aptarimas	100
Kopų evoliucija ir klimato pokyčiai	100
Ekogeologija ir kopų formavimasis	101
Išvados	101

1

Introduction

1.1 Relevance of the thesis

The Curonian Spit is a narrow sandy barrier separating the Curonian Lagoon from the Baltic Sea. It is one of the most unique places in Europe in cultural and geological terms. The Curonian Spit, both the Lithuanian and the Russian parts, are included into the UNESCO list of Cultural Heritage Monuments. The whole territory of the Curonian Spit belongs to the National Parks (NP) established in both countries. The Curonian Spit dunes form the so-called Great Dune Ridge (GDR) that stretches out along the entire lagoon coast of the Spit. The history of geological development of the Great Dune Ridge is poorly known except the fact that during the XVI – XIX centuries, due to the strong impact of human activity (total cutting of forests in the biggest part of the Curonian Spit), an aeolian activity was extremely high. As a result, 14 villages have been buried beneath the sandy dunes along the Curonian Lagoon coast of the Spit (Gudelis, 1998a; Bučas, 2001). After that, starting from the beginning of the XIX century, a significant part of the Curonian Spit dunes was artificially forested. It suspended the aeolian activity and protected the fishermen villages against sand blizzards. At the same time, the artificial foredune was formed along the entire length of the marine coast of the Curonian Spit. This foredune protected (as a barrier) the inner part of the Spit from the seashore sand drift. However, a part of the aeolian massifs is not yet covered by vegetation and represents natural environmental “laboratories”

1. Introduction

where investigations of aeolian processes are still available. Due to recent aeolian processes a number of buried palaeosols, which are significant indicators of phase activity of the dune development, are outcropping in the unplanted areas. The reasons of ancient periodical activity (possible climate changes, natural or human stimulated hazards such as forest fires, etc.) are unknown and still are an object of discussions. An understanding of the mentioned issues is topical not only from the scientific point of view but for practical uses as well. The information on the Curonian Spit evolution and its present dynamics is valuable for the urban infrastructure development, estimation of stability of the lagoonal coasts, definition the boundaries of protected areas, formation of touristic routes, regulation of visitors' traffic, etc.

The Curonian Spit is ecologically sensitive territory with a number of protected areas - due to these circumstances not all of the traditional geophysical and geological methods can be used during scientific investigations. So, the researches have become possible thanks to the development of non-invasive methods that allow research in ecologically sensitive areas without any harm to the environment. Therefore, the investigations of sandy dunes by a ground-penetrating radar (GPR) and dating of sediments with modern methods of absolute geochronology (^{14}C , IR-OSL) were chosen as the main methods for reconstruction of the geological evolution of the Curonian Spit dunes. One of still active aeolian dune massif – a so-called Dead (Grey) Dunes which is located between Juodkrantė and Pervalka settlements and has a status of Nature Reserve – has been chosen as a key area for this study.

1.2 Aim and objectives

The aim of this study is to investigate the geological structure of the Curonian Spit dunes, to establish the peculiarities of their evolution and factors that influenced it during the Holocene, as well as assess the existing hypotheses about soil-forming processes in sandy environment.

The following objectives were undertaken:

- Mapping of the palaeosols and determination of their spatial position.
- Determination of the age of palaeosols and identification of possible generations of palaeosols formation.
- Reconstruction of the palaeo-relief of the dune massifs for various periods of the past.
- Evaluation of the palaeo-dynamic rate and nature of aeolian processes.
- Determination of the main factors of the Curonian Spit dunes evolution.

1.3 Novelty of the study

The studies have shown that the latest state-of-the-art technologies (GPR combined with precision GPS systems) can be particularly detailed and accurately capture the palaeosols terrain without boring or digging, which is important for planning works in protected areas. Covering a whole survey area with a detailed GPR grid would enable to restore the surface of buried soils found in the area of interest with a high degree of reliability, which would correspond exactly to the surface of the former dunes during the stable formation period. It is the first time when such detailed palaeogeographic reconstructions are carried out in Lithuania, as well as in the eastern Baltic region.

1.4 Scientific and practical significance of the results

Despite the abundance of research carried out in the Curonian Spit, the geological development of this peninsula is not yet fully clear. A large part of the Spit formed due to intense aeolian processes caused by several reasons.

Understanding the aeolian and soil forming processes which took place during the Holocene allows reconstructing the Curonian Spit evolution. This valuable data could be used to reconstruct evolution for other similar spits in southern and south-eastern Baltic region (for example Leba, Hell, Vistula).

Curonian Spit, as a famous site included into the UNESCO list of Cultural Heritage Monuments, is one of the most visited tourist attractions in Lithuania. The reconstruction of palaeo-geographical conditions could result in substantial updates of the information on the evolution of the Curonian Spit, provided by the Curonian Spit National Park (NP) for visitors.

Archaeological studies show that geological layers associated with buried soils, especially below the groundwater level, contain well-preserved archaeological artefacts of the Stone and Bronze Age. Consequently, the new information on the prevalence of palaeosols would also be useful for archaeologists enhancing their understanding of palaeo-geographic situation (dune distribution, alteration of palaeo-coastline, etc.) during various periods of time, which will allow more targeted research.

1.5 Scientific approval

The results of this study were presented in ten international conferences and six national local seminars and PhD students' conferences.

International conferences:

Dobrotin, N. Reconstruction of palaeodynamics of the Curonian Spit dunes based on the ground-penetrating radar (GPR) survey and LIDAR data. *ECSA 51th International Symposium "Research and management of transitional waters"*, Klaipeda, Lithuania, September 2012.

Dobrotin, N., Bitinas, A., Michelevičius, D., Damušytė, A. Reconstruction of palaeodynamics of the Curonian Spit dunes based on the ground-penetrating radar (GPR) survey and geochronological data. *11th Colloquium on Baltic Sea Marine Geology*, m/s "Silja Serenade", 18-19.09.2012.

Bitinas, A., Molodkov, A., Buynevich, I. V., Damušytė, A., **Dobrotin, N.**, Gregorauskienė, V., Mažeika, J., Pupienis. D. Aeolian landscape evolution in the Curonian Spit, Baltic Sea. *The Baltic Sea a Mediterranean of Northern Europe: In the Light of Natural Sciences, Archaeological and Historical Research from Ancient to Medieval Times*, 4-7 June 2014, Gdańsk, Poland.

Bitinas, A., Molodkov, A., Buynevich, I., V., Damušytė, A., **Dobrotin, N.**, Gregorauskienė, V., Mažeika, J., Pupienis. D. Dune palaeodynamics and chronological control, Curonian Spit, South-eastern Baltic. *9th Baltic Sea Science Congress „New Horizons for Baltic Sea Science“*, 26-30 August 2013, Klaipeda, Lithuania.

Buynevich, I.V., Gnivecki, P., Curran, H.A., Savarese, M., Bitinas, A., **Dobrotin, N.**, Pupienis, D., Boush, L.P., Brūniņa, L., Damušytė, A., Lloyd, G., Brake, M., Felgar, C. Geoarchaeological implications of biogenically-induced GPR signal interference in Baltic and Bahamian coastal dunes: comparative sedimentology and internal structure. *10th Baltic Sea Science Congress*, Riga, Latvia, 15-19 June 2015.

Buynevich, I.V., Bitinas, A., Tõnisson, H., Brūniņa, L., Pupienis, D., **Dobrotin, N.**, Damušytė, A., Molodkov, A., Vilumaa, K., Vandel, E., Anderson, A., Orviku. K. Early stage of mega-ridges at cape Kolka, Latvia. *10th Baltic Sea Science Congress*, Riga, Latvia, 15-19 June 2015.

Buynevich, I.V., Gregorauskienė, V., Bitinas, A., Damušytė, A., **Dobrotin, N.**, Pupienis, D., Pickett, W.J. Diagnostic magnetic susceptibility signatures of episodic pedogenesis in aeolian slipface sequences, Great Dune Ridge, Lithuania. *10th Baltic Sea Science Congress*, Riga, Latvia, 15-19 June 2015.

•Buynevich, I.V., Bitinas, A., Tõnisson, H., Brūniņa, L., Pupienis, D., **Dobrotin, N.**, Damušytė, A., Vilumaa, K., Vandel, E., Anderson, A. Coastal relicts in the Baltic woods: Early stage palaeo-shorelines of cape Kolka, Latvia. *North-eastern Section - 50th Annual Meeting of the Geological Society of America*, 23–25 March 2011, Bretton Woods, New Hampshire, USA.

1. Introduction

Buynevich, I.V., Bitinas, A., Pupienis, P., Damušytė, A., Brūniņa, L., Sivkov, V., **Dobrotin, N.**, Tõnnisson, H., Orviku. K. Paraglacial mega-barriers of the Baltic Sea: a decade of collaborative research. *North-eastern Section - 50th Annual Meeting of the Geological Society of America*, 23–25 March 201, Bretton Woods, New Hampshire, USA.

Dobrotin, N. Palaeodynamics of Curonian Spit eastern coastline during the Holocene according GPR data. *11th Baltic Sea Science Congress*, Rostock, Germany, June 2017.

National scientific events:

Dobrotin, N. Kuršiu nerijos kopų geologinė raida ir jos ryšys su klimato kaita holoceno metu. *Seminar at Faculty of Natural Sciences and Mathematics, Klaipėda University*, Klaipėda, Lithuania, September 2013.

Bitinas, A., **Dobrotin, N.**, Michelevičius, D., Damušytė, A. Kuršių Nerijos kopų geologinė raida. *Jūros ir krantų tyrimai 2013*. Klaipėda, Lithuania, April 2013.

Dobrotin, N. Kuršiu nerijos kopų geologinė raida ir jos ryšys su klimato kaita holoceno metu. *Seminar at the Faculty of Natural Sciences and Mathematics*, Klaipėda University, Klaipėda, Lithuania, September 2013.

Bitinas, A., **Dobrotin, N.** Kuršių nerijos kopos: susiformavimas, vystymasis, dabartinių geologiniai procesai. *Kuršių nerijos nacionalinio parko įkūrimo 25-mečio konferencija „Kuršių nerijos kraštovaizdžio pokyčiai”*. Nida, Lithuania, 3-4 November 2016.

Dobrotin, N. Palaeodynamics of Curonian Spit eastern coastline during the Holocene according GPR data. *Seminar at Faculty of Natural Sciences and Mathematics*, Klaipėda University, Klaipėda, Lithuania, March 2017.

Dobrotin, N. Kuršių nerijos rytinio kranto paleodinamika holoceno metu pagal georadarą ir ^{14}C datavimo duomenis. *Annual Conference of PhD Geology Students, Faculty of Chemistry and Geosciences*, Vilnius University, Vilnius, Lithuania, November 2017.

Materials of the study were presented in 4 original publications, published in peer-reviewed scientific journals:

Dobrotin, N., Bitinas, A., Michelevičius, D., Damušytė, A., Mažeika, J. 2013. Reconstruction of the Dead (Grey) Dune evolution along the Curonian Spit, Southeastern Baltic, *Bulletin of the Geological Society of Finland*, 85, 49–60.

Buynevich, I.V., Savarese, M., Curran, H.A., Bitinas, A., Glumac, B., Pupienis, D., Kopczynski, K., **Dobrotin, N.**, Gnivecki, P., Boush, L.P., Damušytė, A. 2017. Sand incursion into temperate (Lithuania) and tropical (the Bahamas) maritime vegetation: Georadar visualization of target-rich aeolian lithosomes, *Estuarine, Coastal and Shelf Science*.

Morkūnaitė, R., Bautrėnas, A., Česnulevičius, A., **Dobrotin, N.**, Baubinienė, A., Jankauskaitė, M., Kalesnikas, A., Mačilevičiūtė - Turlienė, N. 2018. Changes in quantitative parameters of active wind dunes on the south-east Baltic Sea coast during the last decade (Curonian Spit, Lithuania), *Geological Quarterly*, 62 (1).

Bitinas, A., **Dobrotin, N.**, Buynevich, I.V., Molodkov, A., Damušytė, A., Pupienis, D. Coastal dune dynamics along the northern Curonian Spit, Lithuania: toward an integrated database (in press, accepted).

1. Introduction

1.6 Acknowledgment

I would like to sincerely thank my supervisor Dr. Albertas Bitinas for his guidance and support during my studies. I am grateful to Dr. Nerijus Blažauskas and Dr. Petras Šinkūnas for reviewing the thesis and providing with valuable comments. I am also thankful to my colleagues Dr. Dainius Michelevičius, Mantas Budraitis, Juozas Bičkūnas, Julius Aukštuolis and all “Geobaltic” stuff for the assistance during fieldworks and data processing.

I express my gratitude to Dr. Ilya Buynevich, Dr. Aldona Damušytė, Dr. Donatas Pušienis and Dr. Virgilija Gregorauskienė for the scientific cooperation. Thanks to Dr. hab. Jonas Mažeika and Dr. Anatoly Molodkov for the dating of sediments. Many thanks to the Directorate of Curonian Spit National Park for work permit in protected areas. Finally, I would like to thank to all colleagues in Klaipėda University for support.

This study was funded by the project of the Research Council of Lithuania “Geological development of the Curonian Spit dunes” (No. MIP-11131).

1.7 Abbreviations

Abbreviation	Explanation
¹⁴ C method	radiocarbon dating
m.s.l.	mean sea level
AD	Anno Domini, number years in the Julian and Gregorian calendars
AMS method	radiocarbon dating using atom mass spectrometry
BP	before present
GD	Grey (Dead) Dunes, or Grey Dunes
GDR	Great Dune Ridge
GISP2	Greenland Ice Sheet Project 2, global temperature curve
GPR	ground penetrating radar
GPS	global positioning system
HMC	heavy minerals concentration
IR-OSL	dating by infrared optically stimulated luminescence
ka	kilo age, thousand years
LIDAR	light imaging, detection, and ranging: method to make high-resolution elevation maps
MS	magnetic susceptibility
NP	national park
PDR	Protective Dune Ridge
SAR	synthetic aperture radar

2

2. Literature review

From the geological point of view, the Curonian Spit is a typical sand barrier separating the sea and freshwater lagoon – in this case the Curonian Lagoon. Mentioned situation is characteristic for the entire south-eastern part of the Baltic Sea where the similar Vistula, Hell and Leba Spits exist. The first results of the geological surveys of the Curonian Spit and the closely related Curonian Lagoon were obtained in the end of XIX century – the first decades of XX century when the first publications on this subject were published by Prussian investigators J. Shumann (1861), G. Berendt (1869), A. Tornquist (1910), H. Wichdorff (1919), K.H. Paul (1944), and others. A few aspects of the geological structure were touched in the first papers about the Curonian Spit written by Lithuanian researchers and published in the first half of the 20th century (Viliamas, 1932; Šimoliūnas, 1939). The beginning of the systematic geological investigations of the Curonian Spit should be considered the sixth decade of the XX century, with the first appearance of publications prepared by V. Gudelis (1955) and M. Kabailienė (1959a, 1959b). In these papers the geological development of the Spit, stratigraphy of sediments, peculiarities of the relief, biodiversity of soils, etc. were examined. The Curonian Spit and adjacently littered Curonian Lagoon waters were studied not only from the scientific point of view but also from practical requirements, first of all related to the prospecting of amber deposits (Tamkutonis, 1960; Rimša, 1994; Valiukevičienė & Gasiūnienė, 1995). The Curonian Spit was also investigated by different projects

2. Literature review

of geological mapping: a number of boreholes were drilled, the detailed studies of the whole Quaternary thickness were carried out, a set of different geological maps were compiled, etc. (Šimėnas *et al.*, 1989; Bitinas *et al.*, 2000).

The question of the Curonian Spit origin and its geological development until present is still under discussion. A few hypotheses on this issue were published. One of them states that at the initial stages of the Baltic Sea development, when the sea level was lower than the present one, two short spits were formed. One of the spits, like recent Curonian Spit, started to grow from the Sembà peninsula, and the other one takes its beginning from morainic peninsula left by the last glacier (Upper Nemunas) between the Šarkuva (present Lesnoje) and Rasytė (current Rybachi) settlements. Subsequently, during sea transgression and rise in water level, these two spits merged and occupied the current Spit situation (Blazhchishin, 1998). The other investigator V. Gudelis (1998a) also had a similar point of view and expressed his opinion that the Curonian Spit had originally formed a little more westward, at the current Curonian Spit offshore, and only lately has been dislocated into the current position due to the Baltic Sea transgression. As far as another possible development of the Curonian Spit is described by M. Kabailienė (1967, 1995), according to which, in the present place of the Curonian Spit the chain of several separate islands was formed first, which later merged into a continuous body – the present Spit. V. Lavrushin (1993) has raised a hypothesis about the possible glaciotectonic origin of the Curonian Spit, which states that the spit foundation could have been squeezed out under the influence of the glacier at the very end of the Last Glacial (Upper Nemunas). According to this hypothesis, the process was held at the junction between the melting, dead ice mass located in the area occupied by the current Curonian Lagoon and the still active moving glacier sheet in the current depression of the Baltic Sea.

Recently, despite the aforementioned, often controversial, approaches to spit formation, researchers have more or less unanimously agreed that the Spit formation began when water level in the former Baltic Sea basin was much lower than the current sea water level. This is evidenced by the layers of ancient lagoon sediments which are found on the resent underwater marine slope of the Spit, also by the remnants of trees and peat layers (age 3.7 thousand the years BP) outcropping on the Baltic Sea coast near Rasyte (present Rybacy, territory of the Russian Federation) (Sergeev *et al.*, 2015, 2016). Most of researchers associate the Curonian Spit formation with one of the last stages of the formation of the Baltic Sea – the Litorina Sea and its maximal transgression approximately 7.5-7 thousand ago years ago (Damušytė, 2011). The data of archaeological research testifies that already in the Middle Neolithic, just a little more than 5 thousand years BP, people settled the Curonian Spit (Rimantienė, 1999; Piličiauskas, 2015).

The age of the Curonian Spit dunes differs – dunes have formed during different periods of time; hence dunes of different age are separated by palaeosols. J. Schumann

2. Literature review

(1861) was the first to mention this fact. Later Hess von Wichdorff described distribution, formation and reasons of evolution of the old dunes; the monograph also contained the detailed description of ancient forest soils (Wichdorff, 1919). The detailed data on palaeosols was presented in K. H. Paul's (1944) monograph which contained a scheme of outcropping palaeosols located southwards from Nida settlement.

More detailed scientific investigations of the Curonian Spit dunes were initiated only after the Second World War and were generally focused on the geomorphologic studies and recent dynamics of the development of the dunes. Significant studies of the dunes and palaeosols of the Curonian Spit were carried out by the Lithuanian scientist V. Gudelis (1989 – 1990, 1998a, 1998b, etc.). He carried out a visual mapping of palaeosols in some areas (Gudelis *et al.*, 1993), determining three so-called aeolodynamic stages of the development of the dunes of the Curonian Spit (Gudelis, 1998a):

- 1) period of intensive dune formation (5000 – 4000 years BP),
- 2) period of dune stabilization (from 4000 to 500 years BP),
- 3) period of intensive regeneration (after 500 years BP).

The results of pollen analysis revealed that the formation of palaeosols started by the end of Atlantic period and continued during the Sub-Atlantic and Sub-Boreal periods (Gudelis *et al.*, 1993; Gaigalas *et al.*, 1991; Moe *et al.*, 2005). The conclusions of pollen analysis were confirmed by the results of radiocarbon (^{14}C) dating of palaeosols (Chichiagova & Cherkinski, 1988; Gerasimov & Zavelski, 1980; Gaigalas *et al.*, 1991). In 2007 palaeosol studies using a ground penetrating radar (GPR) were initiated in the aeolian massif of the Dead (Grey) Dunes (Buynevich *et al.*, 2007a, 2007b). Recently, based on the geochronological dates of dunes and palaeosols by A. Gaigalas and A. Pazdur (Gaigalas & Pazdur, 2008), six periods (generations) of palaeosol formation have been identified:

- 1) 4600 – 4000 years BP,
- 2) 3400 – 2900 years BP,
- 3) 1900 years BP,
- 4) 1200 – 1000 years BP,
- 5) 600 – 400 years BP,
- 6) 290 – 120 years BP.

Older palaeosols are found in the base of the GDR western slope, whereas, the youngest palaeosols are widespread more eastward, in the middle part of the GDR western slope. The palaeosols of different age contain a big amount of charcoal (Figure 2.1). According to some researchers, forest fires were the main reason behind the destruction of palaeosols, which resulted in suitable conditions for aeolian activity (Gudelis, 1998b; Gaigalas & Pazdur, 2008).

2. Literature review

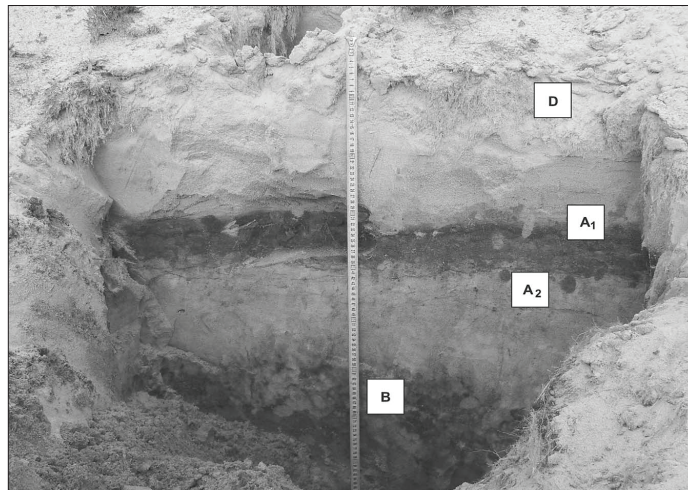


Figure 2.1 Buried soil in the Vinkis dune. The ancient soil layers: (A1) the forest litter (humus layer) with charcoal small pieces (980–1190 AD), (A2) a podzol layer, which is composed of grey fine sand, and (B) an illuvial horizon, which is of reddish and brown colour due to high content of iron and manganese. D – dune cover sand. Photo by Alfred Uchman (Gaigalas & Pazdur, 2008).

According to earlier investigations, in 1910 – 1984 the average annual drift of the dune ridge was 2.5 – 3.8 m/year eastwards (Michaliukaite, 1962). The overall dynamics of shifting dunes was higher in the southern part of the Curonian Great Dune Ridge (GDR) than in its northern part. For example, in 1910 – 1955 the northern part of the Grey Dunes would shift 0.5 – 2.8 m/year, while the southern and central part – 3 – 5 m/year (Michaliukaite, 1967).

The first basic GPR survey in the Curonian Spit was conducted in 1994 by geophysicists of the Geological Survey of Norway (NGU) (Figure 2.2). Reflectors are identified using data obtained from the borehole no. 30 (the borehole data presented in the annex No.1). Strong reflector (1) is identified as a boundary between medium grained and fine grained aeolian sediments, it also represents a ground water table: boundary has strong amplitude due to the high difference between the relative permittivity of dry and wet sand. Dipping reflectors (2) are recognized as slipfaces. Weak reflection (3) in the beginning of the cross-section is described as boundary between aeolian sediments and marine sediments (Mauring *et al.*, 1994).

In the last decade many GPR surveys in the Curonian Spit were conducted by the investigator from Temple University (United States) I. V. Buynevich together with Lithuanian colleagues from Klaipėda and Vilnius Universities and Lithuanian Geological Survey. Studies show GPR capabilities to detect palaeosols and slipfaces

2. Literature review

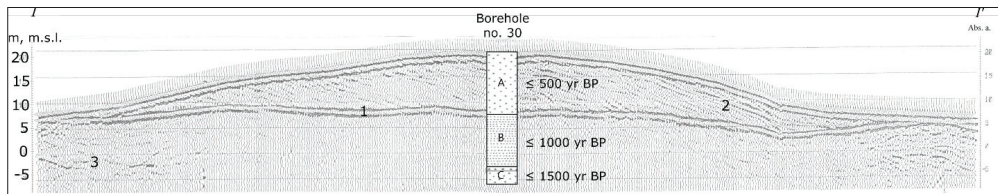


Figure 2.2. GPR cross-section of dune near Pervalka (I-I'): 1 – groundwater table, 2 – slipfaces, 3 – boundary between aeolian and marine sand, A – aeolian sediments, medium gained greyish yellow sand, B – aeolian sediments, fine grained greyish yellow sand, C – marine sediments, medium gained greenish grey sand. Numbers along the borehole section represents IR-OSL age of aeolian sediments (after Mauring et al., 1994; modified).

(Buynevich *et al.*, 2007a). High-amplitude reflections on GPR images were captured. Two types of major anomalies were identified (Figure 2.3): (1) palaeosols and (2) slipfaces. Study shows, that GPR technique allows not only locate buried palaeosols and determine dip angles, but to reconstruct their geometry and thickness as well.

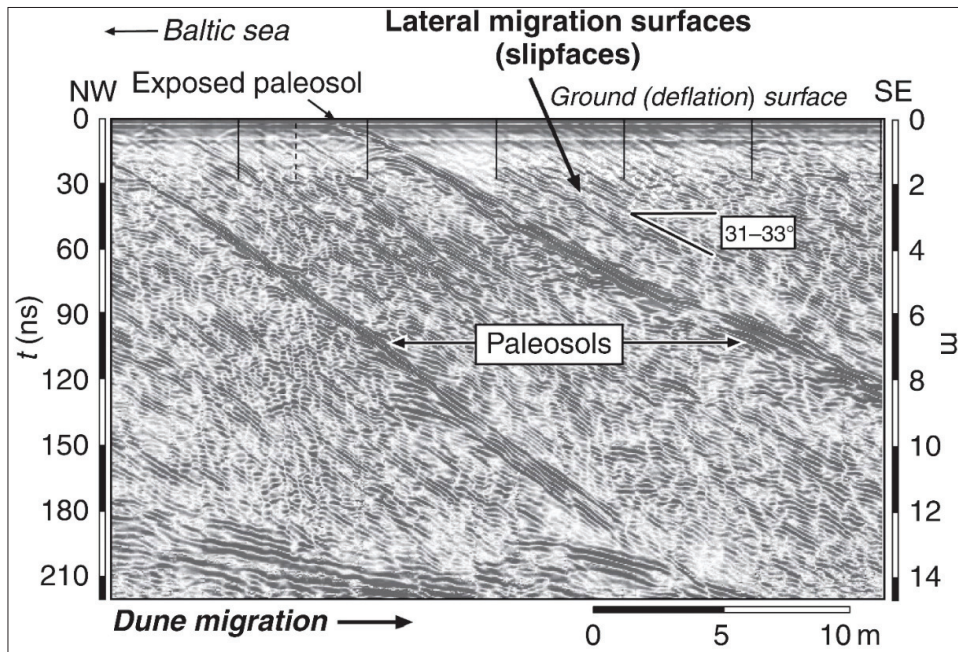


Figure 2.3. GPR radargram across the part of the relic dune. Palaeosols P1 and P2 are clearly visible, slipfaces, slipface dipping angle $31 - 33^\circ$ (Buynevich *et al.*, 2009).

2. Literature review

The most recent study demonstrates a capability of GPR to identify buried vegetation (Buynevich *et al.*, 2017). Radargrams reveal high-amplitude point-source anomalies and signal scattering characteristic to buried trees.

Previous investigations provide valuable information about geology of the Curonian Spit and its evolution. Geological mapping was done using outcrops, test pits and boreholes. Gathered data helps to understand only general geological situation. Geophysical investigations enable to study the palaeomorphology of the Curonian Spit, but the recent GPR surveys were conducted in relatively small areas as well as GPR cross-sections were not interconnected, so it is hard to see the whole geological picture of the Spit.

Coastal dunes developed in the spits like Curonian Spit are found in the whole Baltic Sea region. Massif sand leftovers after region deglaciation led to the formation of various sandy barriers. The longest sandy barriers are found in the southern coast of the Baltic Sea (Labuz *et al.*, 2018) and besides Curonian Spit, are represented by Vistula, Hel and Swina spits (Figure 2.4).

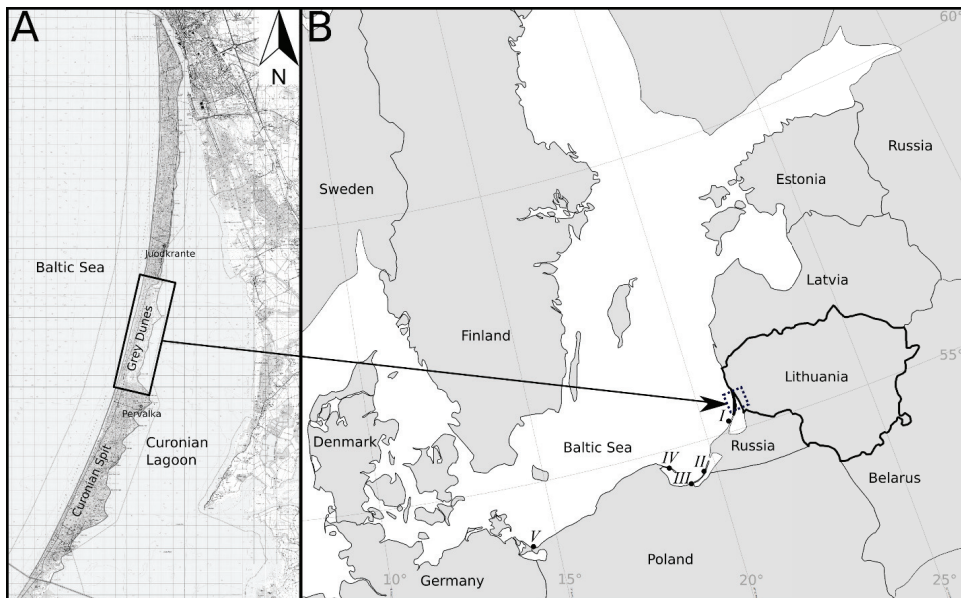


Figure 2.4. Location of the Curonian Spit (A) and of Dead (Grey) Dunes. Position of the Curonian Spit in the Baltic Sea region and location of main spits in the Southern Baltic (B). Roman numbers indicate places of typical geomorphological cross-sections of the spits: I – Curonian Spit, II, III – Vistula Spit, IV – Hel Spit, V – Swina Barrier Ridge.

2. Literature review

The geomorphological cross-sections of the main Baltic Sea region spits are presented in Figure 2.5. Most spits have common geomorphological features: seafront with foredune, interdune and the main dune ridge.

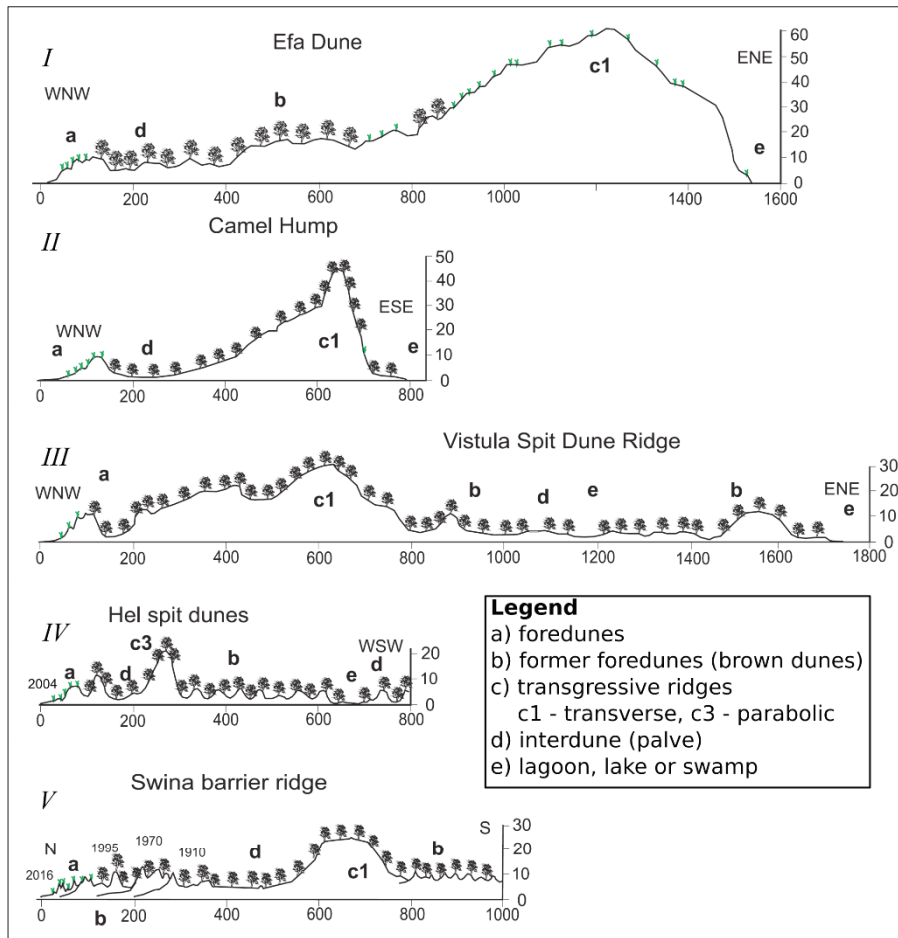


Figure 2.5. Cross-sections of the Baltic Sea spits with main geomorphological features, locations are provided in Figure 2.4 (after Labuz et al., 2018, modified). 1910, 1970, 1995 and 2016 in the cross-section V shows where in that year was the marine coast and foredune.

However, these common geomorphological features are different in shape and size, as well as different relationship between them. It depends on the peculiarities of geological development of the particular spit, also it shows that dune massifs in separate spits had a different evolution.

2. Literature review

Vistula Spit is the most similar sandy barrier to the Curonian Spit, according to its length, width, geomorphological features and geological structure. It is 110 km long sandy strip that stretches from cliff coast in the Gulf of Gdańsk and to the Sambian Peninsula cliffs in the Kaliningrad Oblast. The Vistula Spit aeolian landforms according to their age and morphological features can be separated into three groups (Figure 2.6) (Starkel, 1990):

Brown dunes. Internal (landward) dunes are straight and flat ridges up to 4 m high, exceptionally up to 10 m high.

Yellow dunes. Irregularly shaped ridges and depressions. Dune ridges up to tens of meters high. Dune ridges frequently overlap.

White dunes. External (coastal) blowout dune ridge, rises to several meters.

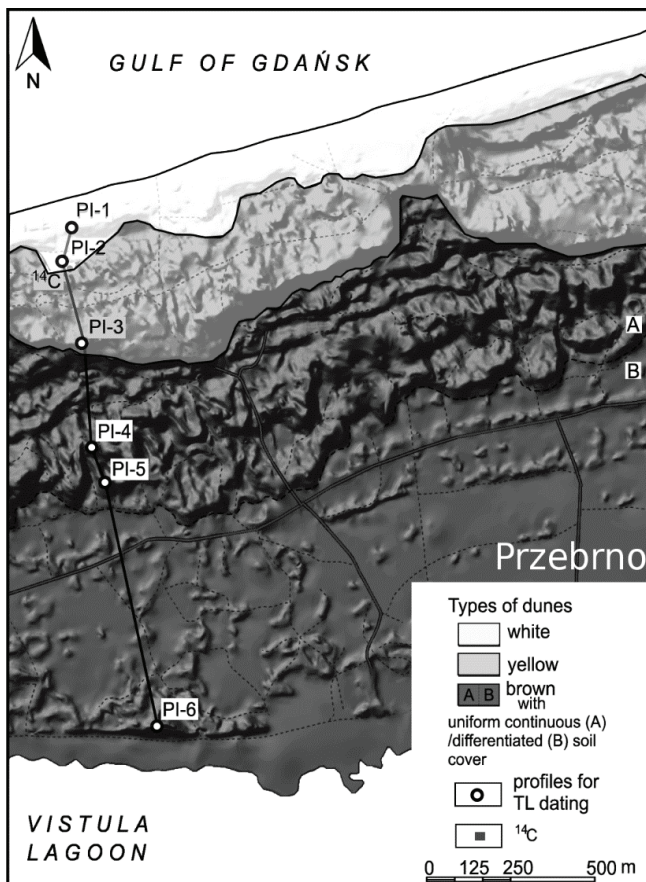


Figure 2.6. Location of research sites and line of geological cross-section (Fig. 2.7) shown on the digital elevation model of the Vistula Spit near Przebrno (after Fedorowicz et al., 2012; modified).

2. Literature review

Detailed thermo-luminescence studies (Fedorowicz *et al.*, 2012) showed that the brown dune ridge formed approximately 5.5 ka BP, whereas the youngest white dunes were formed approximately 0.5 – 0.3 ka BP. The geological profile through the Vistula Spit is presented in the Figure 2.7.

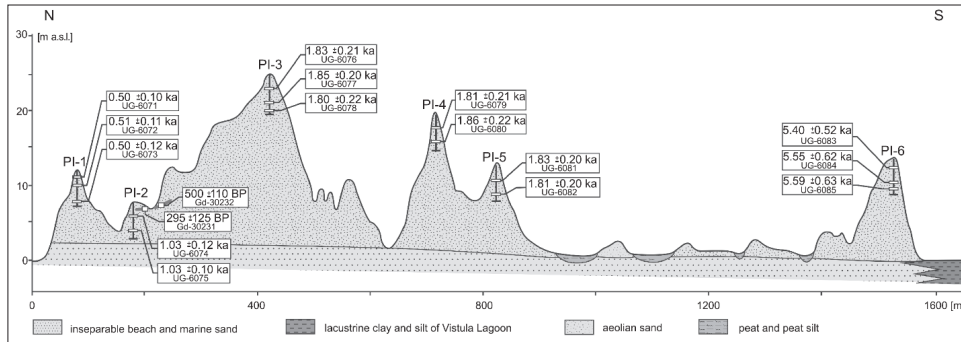


Figure 2.7. Simplified geological cross-section through the Vistula Spit and results of TL dating (after Fedorowicz *et al.*, 2012).

Based on TL dating, four phases of intensification of aeolian processes were distinguished (Figure 2.8):

- 1) 5860 – 5400 years BP,
- 2) 1930 – 1610 years BP,
- 3) 1200 – 900 years BP,
- 4) from 500 years BP.

Geochronological data shows that a principal difference is between the location of older and younger dune massifs. It is possible to maintain, that a significant brake of aeolian sedimentation – close to three thousand years – has taken place during the Vistula Spit development.

Comparing the Curonian and Vistula Spits, the significant differences in geomorphological shape and geological structure are an obvious. The Curonian Spit dunes are transgressing towards lagoon, i.e. the youngest dunes have developed along the Curonian Lagoon coast, whereas in the Vistula Spit the dune massifs are in an opposite situation –the oldest dunes are located along the lagoon coast (Figs 2.6. and 2.7.). It means that the Vistula Spit increased in width because of its growth at the sea coast: the new dune massif was formed along the marine coast, after having short migration towards lagoon, relatively quickly were stabilized (i.e. covered by vegetation), and then no more transformations occurred. An example of such a spit development is obvious in the Swina Barrier Ridge where resent new dune massifs are forming due to the progressive accretion of new and new foredunes along the marine coast (Fig. 2.5., cross-section V).

2. Literature review

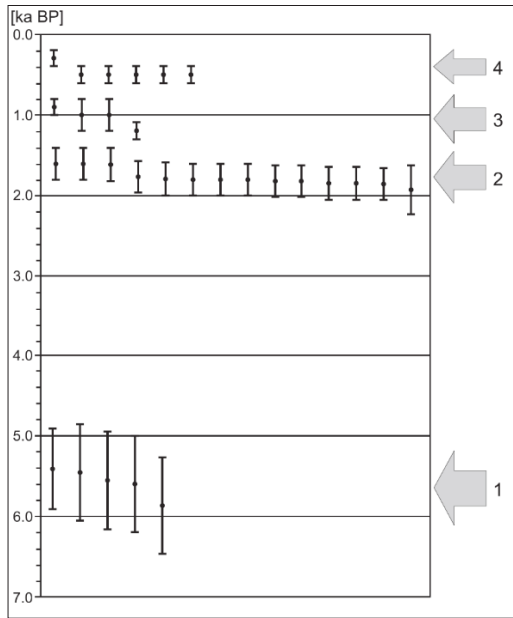


Figure 2.8 The TL ages classified into four distinct periods/phases of intensified aeolian accumulation (after Fedorowicz et al., 2012)

3

Material and methods

3.1 Study area

The Curonian Spit is a 98 km long sand dune peninsula that separates the Curonian Lagoon from the Baltic Sea. It is situated in the south-eastern part of the Baltic Sea and stretches from the Sambian Peninsula (territory of the Russian Federation) towards the north – north-east (western part of territory of the Republic of Lithuania). Dunes of the Curonian Spit are the highest dunes in the North Europe and reach more than 60 meters (Gudelis, 1998a). The highest “Senosios smuklės” (i.e. “Old Inn”) dune, also known as Vecekrugo Dune, is 67.2 meters high and is situated a few kilometers to the south from Preila. The research was carried out in the so-called Dead (Grey) Dunes massif which is located between Juodkrantė and Pervalka (Figure 2.4 A).

3.2 Geological structure of the Curonian Spit

3.2.1 Stratigraphy of Quaternary sediments

The stratigraphics of Quaternary sediments and their indexes are presented according to the geological and geomorphological legend accepted for practice in the Lithuanian Geological Survey (Guobytė, 2007). The lithological description of sediments was performed according to Wentworth classification presented in Table 1.

3. Material and methods

Table 1. The Wentworth sediment classification scheme (Wentworth, 1922).

Wentworth size class		ϕ	Millimeters
Gravel	Boulder	-12 -- 8	4096 – 256
	Cobble	-8 -- 6	256 – 64
	Pebble	-6 -- 2	64 – 4
	Granule	-2 -- 1	4 – 2
Sand	Very coarse sand	-1 – 0	2 – 1
	Coarse sand	0 – 1	1 – 0.5
	Medium Sand	1 – 2	0.5 – 0.25
	Fine Sand	2 – 3	0.25 – 0.125
	Very fine sand	3 – 4	0.125 – 0.0625
Silt	Coarse silt	4 – 5	0.0625 – 0.031
	Medium silt	5 – 6	0.031 – 0.0156
	Fine silt	6 – 7	0.0156 – 0.0078
	Very fine silt	7 – 8	0.0078 – 0.0039
Mud	Clay	8 – 14	0.0039 – 0.00006

The thickness of Quaternary sediments is highly dependent on the nature of the pre-Quaternary relief. In the Curonian Spit Quaternary deposits are 80 –100 meters thick, sometimes reaching up to 140 meters – in places where the current terrain (dune massifs) has risen high above sea level. The stratigraphy of Quaternary sediments is presented in the geological cross-section carried out in perpendicular to the Spit (Figure 3.2.1 A), whereas the thickness of Quaternary – in the separate scheme (Figure 3.2.1 B): both were carried out during the geological mapping of Quaternary sediments at the scale of 1:50 000 when a set of geological maps of different content was compiled for the southern part of the Lithuanian Maritime Region (Bitinas *et al.*, 2000).

The Quaternary thickness is lying on the pre-Quaternary deposits (Upper Cretaceous) and is presented by sediments of different genesis. They age varies from Middle Pleistocene to the resent Holocene sediments. The oldest Pleistocene sediments are represented by till (morainic loam) formed during the Medininkai Glaciation (geological index in the cross-section – g II md). The glaciofluvial sediments represented by fine-grained sand of the same age (f II md) are also widespread beneath the part of the Spit.

The layer of glaciolacustrine sediments of the Baltija Stage of Upper Nemunas glaciation (lg III bl) consists of greyish brown fine-grained sand, silty sand and sandy silt. The layer bed occurs on glaciogenic sediments, an altitude of its roof varies about 20 – 25 meters below sea level.

3. Material and methods

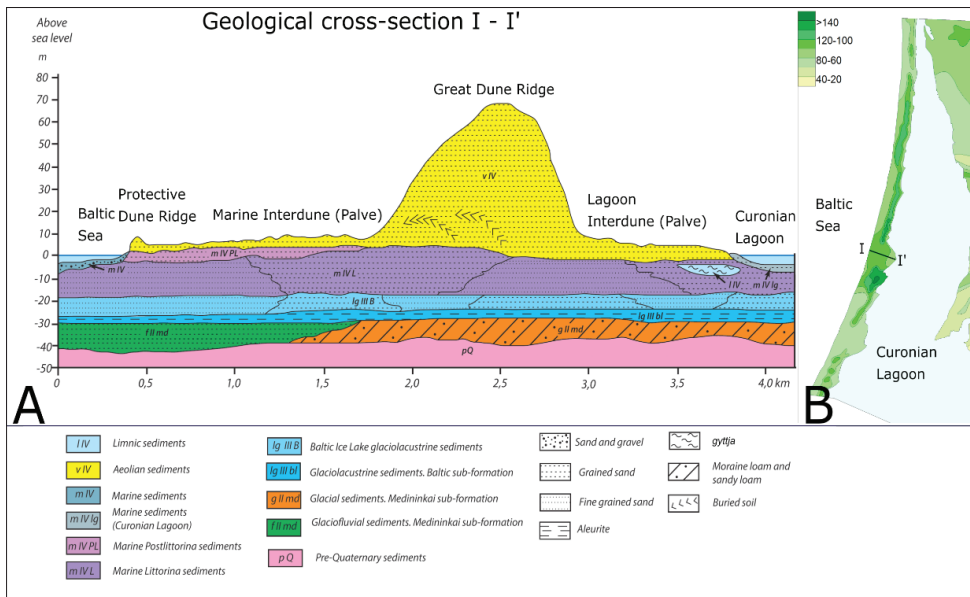


Fig. 3.2.1. Geological structure of the Curonian Spit: A – geological cross-section of the Curonian Spit near Pervalka, B – thickness of Quaternary sediments (Bitinas et al., 2000).

The layer of the Baltic Ice Lake sediments (lg III B) consists of fine-grained and very fine-grained sand. It might reach up to 7 meters in thickness, while the layer roof is approximately 18 meters below sea level.

The layer of Litorina Sea sediments (m IV L) consists of fine-grained and very fine-grained sand. The layer is 15 –18 meters thick, its roof varies at an altitude from 4 meters below sea level up to 4 meters above sea level. The layers of the last three mentioned stratigraphic units are widespread beneath the entire territory of the Curonian Spit.

The layer of Post-Litorina Sea sediments (m IV PL) consists of fine-grained sand. Post-Litorina sediments are usually deposited on the marine Litorina sediments and are covered with recent marine and aeolian sediments. The sediments are developed only along the western half of the Spit. The bed of this layer is usually situated no more than 3 meters below sea level. The sediments might reach up to 5 meters in thickness.

Below a big part of the Curonian Spit ancient lagoonal sediments (l IV) – so-called “lagoon marl” represented by carbonate sandy silt, with remnants of wood, freshwater molluscs, fish relicts, etc. are present. These sediments, as the most important indicator for understanding the stratigraphy and geological development of the entire Curonian Spit, is one of the main objects of geological investigations of the Spit (Wichdorff, 1919; Kabailiènè, 1995; Damušytè, 2011; Kaminskas & Bitinas, 2013; Sergeev et al., 2015; Bitinas et al., 2017; Kaminskas et al., 2017; etc.). The layers of

3. Material and methods

the “lagoon marl” are up to 6-8 meters thick, the roof of this layer is 7-8 meters below the present sea level. Somewhere these sediments, due to the high pressure of moving dunes, are squeezed out to the dune foots and recently extend along the lagoonal coast of the Spit (Linčius, 1993; Buynevich *et al.*, 2010; Sergeev *et al.*, 2016).

The recent marine sediments (m IV) are deposited in the Baltic Sea coast of the Spit during the last 1.0 – 1.2 thousand years. These sediments are called as a “recent” and separated from the sediments of the Post-Litorina Sea to emphasize their young age (formal boundary is drawn approximately 1000 years BP).

Aeolian sediments (v IV) consist of the re-deposited sediments of limnoglacial, liminic, marine or fluvial origin and cover practically the all territory of the Spit (Bitinas *et al.*, 2000). The Great Dune Ridge (GDR), reaching up to 67.2 meters above sea level at its highest point, consists of drifted sand from Litorina, Post-Litorina and recent marine washout sediments. Aeolian sediments are composed from fine- to medium-grained light grey, feldspar-quartz sand, with glauconite impurities. Sub-horizontal or diagonal layering is characteristic for aeolian sediments. Palaeosols, heavy-mineral concentrations and glauconite-rich layers can also be observed in the Great Dune Ridge.

3.2.2 Geomorphologic characteristics

The western shore of the Curonian Spit is concave, whereas the eastern shore is carved up into horns and bays. The horns are generally orientated west-east, demonstrating the effects of western winds. The width of the Curonian Spit varies from 0.4 (near Lesnoje, Russian part of the Spit) up to 3.8 km (Bulvikio horn, near Nida, Lithuanian part of the Spit). The Curonian Spit has a highly differentiated relief. The main morphological elements are oriented longitudinally, i.e. along the Spit. Five genetic-morphological sections are being distinguished going from the Baltic Sea coast to the Curonian Lagoon coast (Figure 3.2.1 A):

1) Seafront with an artificial Protective Dune Ridge (PDR). Seafront is 25-70 meters wide, composed of medium grain sized sand. The artificial protective dune ridge is up to 15 m in height and continuously stretches along the entire Spit.

2) Interdune (Palve). This plain, sometimes called as Marine Palve, occupies an area between the PDR and GDR. The hummocky relief of the Palve is the relict of re-blown ancient parabolic dunes. The area is composed of the aeolian sand and covered with vegetation. The sand thickness reaches 6 – 7 meters, the relief is 2 – 5 meters above sea level.

3) The Great Dune Ridge. It is the largest form of the Curonian Spit relief. The average height of the ridge is 30 – 40 meters, width of the dune ridge varies from 0.4 to 1.2 km. Usually dunes consist of a long and slight wind-ward slope, wide crest and steep (approximately 30° angle) slip face. Palaeosols are mostly found in the wind-ward slope. Near Juodkrantė settlement the GDR and Marine Palvė are absent and the

3. Material and methods

biggest part of the Spit is occupied by an ancient relict parabolic dune massif (Gudelis & Michaliukaite, 1976; Gudelis, 1989-1990).

4) Lagoon interdune and beach. Lagoon beaches are poorly developed, their width usually varies from 3 to 6 meters. In some places the lagoon beach reaches up to a few hundred meters in width and forms the fragments of the so-called Lagoon Palve. This plain is composed from marine (lagoon) sediments covered by a thin layer of aeolian sand.

3.3 Ground penetrating radar (GPR) survey

Assumptions for the implementation of this survey arose due to several methodological studies of Ground Penetrating Radar (GPR) in small areas, the results of which have shown the great effectiveness of this method in the investigation of buried soils (Buynevich al., 2007b).

3.3.1 GPR operation basics

Ground Penetrating Radar (GPR) is a synthetic aperture radar (SAR) system for subsurface reflections investigation. A short electromagnetic pulse is emitted to the environment, once the pulse reaches a layer (or an object) where the relative permittivity differs from the environment, a part of the pulse is reflected and returned to the antenna, the other part goes on, until it reaches the next layer (or object) (Figure 3.3.1). The higher the difference of relative permittivity, the greater the energy reflected from a boundary between different layers (or an object). In general, any dielectric discontinuity can be detected.

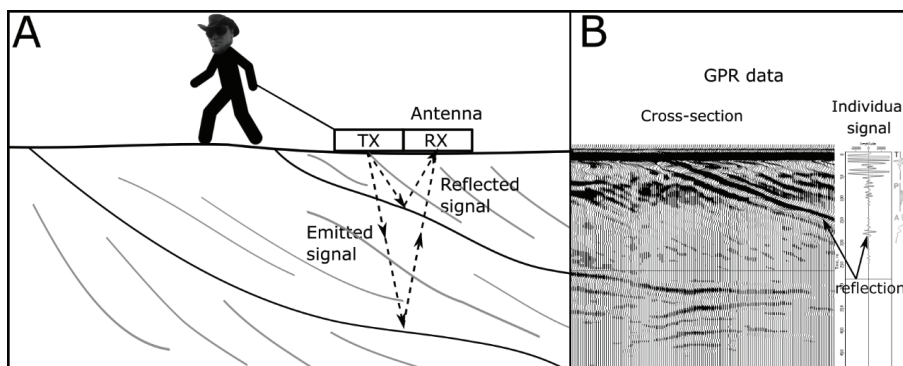


Figure 3.3.1. The main scheme of GPR (A). Transmitted signal travels through the media, part of the signal reflects from the boundary between different layers, the remaining part keeps travelling until the next layer. Tx – transmitting antenna, Rx – receiving antenna. GPR data (B) – cross-section and individual signal.

3. Material and methods

Signal attenuation and relative dielectric constant are the main factors that can pre-determine the quality of the research. Material that has a high value of low-frequency conductivity will have large signal attenuation (Table 2). Therefore gravel, sand, dry rock and fresh water are suitable environment for radar methods, while clay, salt water and other conductive materials are practically unsuitable for GPR survey (Daniels, 1996).

Table 2. Attenuation and relative dielectric constants of various materials measured at 100 MHz (Daniels, 1996).

Material	Relative permittivity ϵ_r
Air	1
Clay dry	2-6
Clay wet	5-40
Freshwater	81
Sand dry	2-6
Sand wet	10-30
Sea water	81
Soil sandy dry	4-10
Soil sandy wet	10-30

Maximum penetration depth depends on GPR operational frequency. The higher the frequency – the greater the attenuation per meter. Material loss at 100 MHz and 1 GHz are presented in Table 3. Most GPR devices generate short pulse signals with broad frequency spectrum; the final signal depends on the choice of the antenna.

Table 3. Material loss at 100 MHz and 1 GHz (Daniels, 1996).

Material	Loss at 100 Hz	Loss at 1 GHz
Clay	5-300 dB/m	50-3000 dB/m
Loamy Soil	1-60 dB/m	10-600 dB/m
Sand	0.01-2 dB/m	0.1-20 dB/m
Ice	0.1-5 dB/m	1-50 dB/m
Fresh Water	0.1 dB/m	1 dB/m
Sea Water	1000 dB/m	10000 dB/m

When a GPR signal reaches the boundary between two media, some of it is reflected and some of it is transmitted across the boundary. The amplitude of the reflected wave proportional to that of the incident wave is defined by the reflection coefficient (R). The reflection coefficient can be expressed as a function of the relative permittiv-

3. Material and methods

ity on each side of the interface. Assuming the GPR signal arrives at an angle perpendicular to the interface, the reflection coefficient is given by:

$$R = \frac{A_r}{A_i} = \frac{\sqrt{\epsilon_{r2}} - \sqrt{\epsilon_{r1}}}{\sqrt{\epsilon_{r2}} + \sqrt{\epsilon_{r1}}} \quad (1)$$

Where A_r is amplitude of reflected signal, A_i is amplitude of incident signal, ϵ_{r1} and ϵ_{r2} are the relative permittivity of the 1 and 2 media respectively. The bigger the difference between relative permittivity – the higher the amplitude of the reflected signal.

The relative permittivity presented in the table 2 is very approximate and can vary depending on various factors such as water content or mineralogical composition. In most situations the relative permittivity is unknown, thus the velocity of propagation must be measured *in-situ*, by the direct measurement of the depth to a target. In cases, when electrical permittivity is already determined, the depth to the target (d) can be calculated as follows:

$$d = \frac{c}{\sqrt{\epsilon_r}} \frac{t_r}{2} = v_r \frac{t_r}{2} \quad (2)$$

where c is the speed of light in vacuum, ϵ_r is the relative permittivity, t_r is the transit time to and from the target and v_r is the propagation velocity of the electromagnetic wave.

More detailed explanations of properties of earth materials and material-attenuation are presented in literature (Daniels, 1996).

3.3.2 Survey of the Dead (Grey) Dunes

Most of the GPR data was collected during project “Geological development of the Curonian Spit dunes” funded by the Research Council of Lithuania. At the beginning of the investigation, the area of 15 km² was surveyed with a ground-penetrating radar using a grid with 500 m spacing. Later the parts, where palaeosols were observed, were investigated using a denser 200 m grid (Figure 3.3.2). Approximately 180 linear kilometers of subsurface profiles were collected during the study period.

The GPR surveys were carried out using the RADAR Systems GPR Zond 12-e. 300 MHz antenna with 400 V pulse generator was selected for the best ratio of resolution and depth. Time window (range) was set to 500 ns.

The electromagnetic wave refractive index in the sand of the Curonian Spit was obtained by coring data – several boreholes were drilled for this purpose in various places of the spit (list of boreholes is presented in the annex No.2). The electromagnetic wave average refractive index $n = 2.3$ (relative permittivity $\epsilon_r = 5.33$) was adopted for the sandy layers.

3. Material and methods

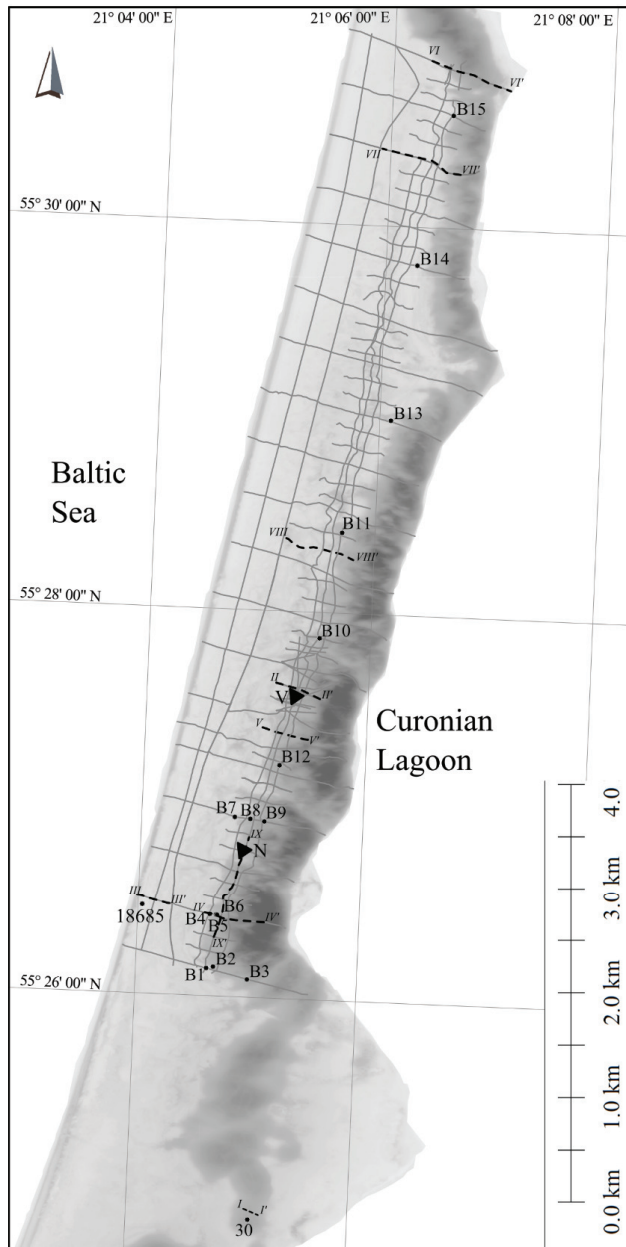


Figure 3.3.2. Location of the study area. Grey lines represent the GPR profiles grid, black dots represent boreholes locations (coordinates and description are presented in annex No.2), dashed lines with roman numbering (I – I' to IX-IX') shows location of GPR cross-section fragments presented in the text or annex (annex No.7), black triangles show sites of detailed investigations (N – the Naglis dune site, V – the Vingis dune site).

3. Material and methods

3.4 Magnetic susceptibility

The measurements of bulk volume low-field magnetic susceptibility (MS) were collected *in situ* along the GPR profiles using Bartington MS3 meter with a MS2K field scanning sensor (Buynevich *et al.*, 2007a). The MS value was obtained on the exposed sections of dune slipfaces at all visually distinct lithological changes. At quartz-dominated intervals, the measurements were obtained every 30 cm, with additional samples from the places with obvious lithological differences. This has allowed for a direct comparison of magnetic properties (primarily magnetite content in HMC) of specific horizons with their electromagnetic signal response as they are traced along the dip in the GPR images. All measurements are expressed as bulk susceptibility (mSI). The magnetic susceptibility values are presented in the annex No.5 and annex No.6.

3.5 Radiocarbon (^{14}C) analysis

Radiocarbon dating is one of the most widely used methods of absolute geochronology. It was developed by J. R. Arnold and W. F. Libby (Libby *et al.*, 1949) and has become an irreplaceable tool for archaeologists. Its development revolutionized archaeology by providing the means of dating deposits independent of artefacts and local stratigraphic sequences. This allowed for the establishment of world-wide chronologies.

During this study, 13 bulk samples for radiocarbon (^{14}C) analysis were collected from different palaeosols. The pre-treatment of the samples included crushing and Acid-Alkali-Acid (AAA) washing in order to remove carbonate and humic acid contamination. The remaining bulk organic carbon was used for benzene production (Kovaliukh & Skripkin, 1994). The specific ^{14}C activity in benzene was measured using the liquid scintillation counting (LSC) method described by Gupta & Polach (1985) and using a Tri-CarbÒ 3170TR/SL in the Radioisotope Research Laboratory of the Institute of Geology and Geography of the Nature Research Centre in Vilnius, Lithuania.

Some of the radiocarbon dating results were obtained by Accelerated Mass Spectrometry (AMS). The AMS radiocarbon dating technique is suited for a very small sample (0.2 milligrams to 0.3 grams) of final carbon. The AMS method is recommended for the radiocarbon dating of grains, seeds, small artefacts. Prior to the analysis, samples must be burnt to convert them into graphite. (<https://www.radiocarbon.com>, 1/25/2018)

Some of dating results, especially those analysed several decades ago, were published as uncalibrated data (conventional radiocarbon age). Thus, due to the unification of the radiocarbon chronology, all the radiocarbon dates were recalibrated using the ^{14}C calibration program OxCal v. 3.1 (Bronk Ramsey *et al.*, 2001) and the calibration curve IntCal09 (Reimer *et al.*, 2009).

3. Material and methods

3.6 Optically stimulated luminescence (IR-OSL) dating

The luminescence technique allows evaluating time since mineral grains were crystallized, heated to a few hundred degrees or were last exposed to sun radiation. The method uses an optically and thermally sensitive light or luminescence signal in minerals such as quartz and feldspar. During the exposure to a light or heat the luminescence signal in the grains is bleached until it is removed. When grains are not exposed to a light or heat, the luminescence signal accumulates again. The luminescence signal is induced by natural radiation. The luminescence dating has been applied and used in a variety of different fields including landscape evolution, palaeoclimate, quaternary geology and archaeology. Optically stimulated luminescence dating methods have demonstrated their suitability for the determination chronologies from aeolian deposits, assuming that most grains have been exposed to sufficient daylight to bleach their initial luminescence signal (Koster, 2005). More information about the luminescence method is presented in Preusser *et al.*, 2008.

The potassium feldspar-based infrared optically stimulated luminescence (IR-OSL) age determination was carried out at the Research Laboratory for Quaternary Geochronology (RLQG), Institute of Geology, Tallinn University of Technology. The presented palaeodosimetric dating techniques have been successfully used in previous investigations in the south-eastern Baltic region (Molodkov *et al.*, 2010; Bitinas *et al.*, 2011), including the dunes of the Curonian Spit and the vicinities of the Curonian Lagoon (Molodkov & Bitinas, 2006; Bitinas *et al.*, in press). The IR-OSL dating procedure used in RLQG is presented in detail as the subject of a separate methodological paper (Molodkov & Bitinas, 2006).

Two sites were chosen for IR-OSL dating. At each site sand samples were taken between two palaeosols, 10 samples were collected altogether. At the site of Vingis dune, five bulk samples were collected from the depth of ~0.4 m below the dune surface, at 5 m spacing. At the site of the Naglis dune, five bulk samples were collected from the depth of ~0.4 m below dune surface at 7 m spacing.

3.7 GPR data interpretation and palaeogeographic reconstructions

All post-processing was performed with Halliburton Geographix software. The real topography of the GPR profiles was added using LIDAR data (Figure 3.7.1). During this procedure, the groundwater table was flattened and palaeosol surfaces began to depict the real morphology of palaeodunes. The groundwater table and palaeosols were interpreted referring to the strength of the signal returns and characteristic geometry in radargrams.

3. Material and methods

After these corrections, some elevation errors in the relief of the dunes are visible, as well as some irregularities in the groundwater table. During the field works a simple GPS device without RTK data corrections was used, also LIDAR data was a few years old. Yet these corrections remain a useful tool to understand the general morphology of palaeodunes.

The investigations carried out with the ground-penetrating radar enabled to identify and map the palaeosols and groundwater table, as well as to characterize the inner structure of sand layers. In some instances, it was possible to differentiate coarse-grained marine sand from fine-grained lagoon sand enriched in organic matter. The difference of electric permittivity can be caused by grain size, mineralogical composition, organic matter and water content. Thus, in some cases the reflective boundary between different sand layers can be seen (Figure 3.7.2). These boundaries are identified by the control excavations or boreholes.

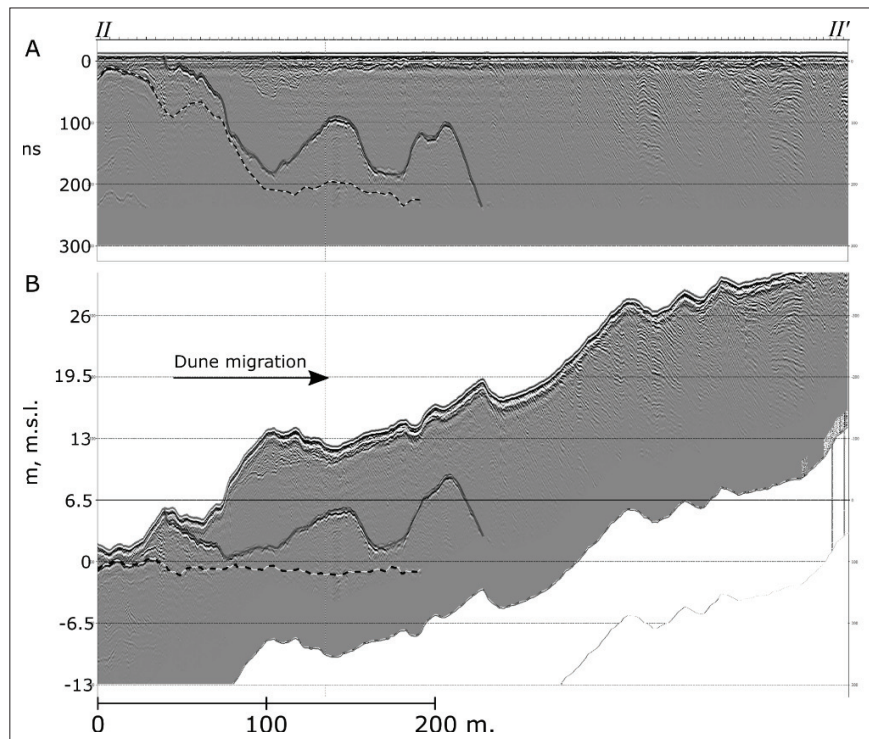
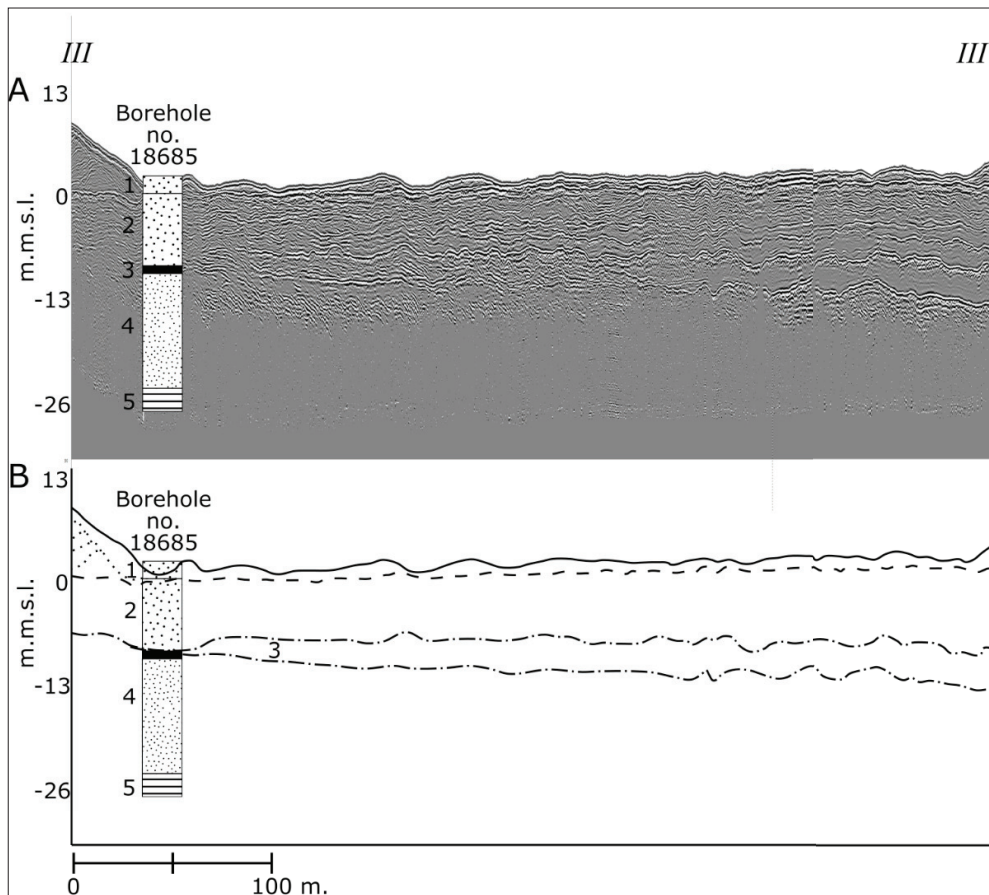


Figure 3.7.1. Primary view of ground penetrating radar (GPR) profile (II-II') (A) (vertical scale – in nanoseconds; 100 ns = 6.5 meters; wave refractive index $n = 5.33$), and the same profile with altitudes corrected according to LIDAR data (B). The groundwater table is indicated by dashed line, the buried palaeosol (KNP-V4A) – by grey line.

3. Material and methods

Two geological boreholes (no. 30 and no. 18685) with a detailed lithological record were used to identify the groundwater table. The borehole no 18685 description is presented in the technical annex No. 3. The GPR cross-section with the borehole no 30 is presented in Figure 2.2. The GPR cross-section III-III' intersected the borehole no 18685. This enabled to compare the borehole stratigraphy data with the reflections observed in the GPR data (Figure 3.7.2). The GPR cross-section III-III' represents the western part of the survey area, the section starts at the top of the artificial Protective Dune Ridge.



*Fig. 3.7.2. GPR cross-section (III-III') with borehole no 18685 lithological section (A).
1 – aeolian sand, 2 – marine sand, 3 – lagoon gyttja, 4 – glaciolacustrine fine-grained sand,
5 – glaciolacustrine sandy silt, GPR data interpretation (B): dotted line – protective dune ridge
reactivation surfaces, dashed line – ground water table, dashed line with dots – layer of gyttja.*

3. Material and methods

Based on the borehole stratigraphy, the first strong reflector represents the boundary between aeolian sand (1) and marine sand (2). This reflection is approximately at 0 meters m.s.l. and has a strong return signal (amplitude) based on previous investigations (Mauring *et al.*, 1994); it also represents the ground water table. The second strong reflection approximately -9 m, m.s.l. represents the layer of lagoon gyttja (3). In this example of the GPR cross-section, the reflections below 13 m have low amplitudes and low signal to noise ratio, this effect is caused by the signal attenuation by high water content in the sediments.

In some cases, the reflections from buried palaeosols and sand layers enriched with heavy minerals have similar shape and strength (Buynevich *et al.*, 2007a). Thus, 15 reflectors established on the radargrams were verified using control excavations and boreholes ((Figure 3.2.1, B1 – B15). For example, Figure 3.7.3 shows the fragment of the GPR cross-section II-II', five elements of aeolian sand layering can be distinguished: ground water table horizon (1), palaeosols (2), HMC horizon (3), dune slipfaces (4) and slipface complexes caused by different wind directions (5). The reflections (2) and (3) have similar signal strength, thus, those reflections were examined with test boreholes (B5 and B6). The borehole B5 revealed that the reflection (3) is sand with high HMC, while the borehole B6 revealed that the reflection (2) is palaeosol. All the test boreholes are presented in the annex No. 2.

The ground water table (Figure 3.7.3, dashed line) can be observed approximately 1 meter below the surface in the interdune area. Whereas in the GDR, the water table can be observed only in its slopes, but not visible under the crest of dunes due to high altitudes – the GPR signal is not powerful enough to travel more than 20 meters into the sand.

After the GPR radargrams were corrected according to LIDAR database, palaeosols were picked out. In some GPR cross-sections, palaeosols cross the groundwater table and descend below the present sea level (Figure 3.7.4). Such zones were interpreted as the former eastern base of GDR.

3. Material and methods

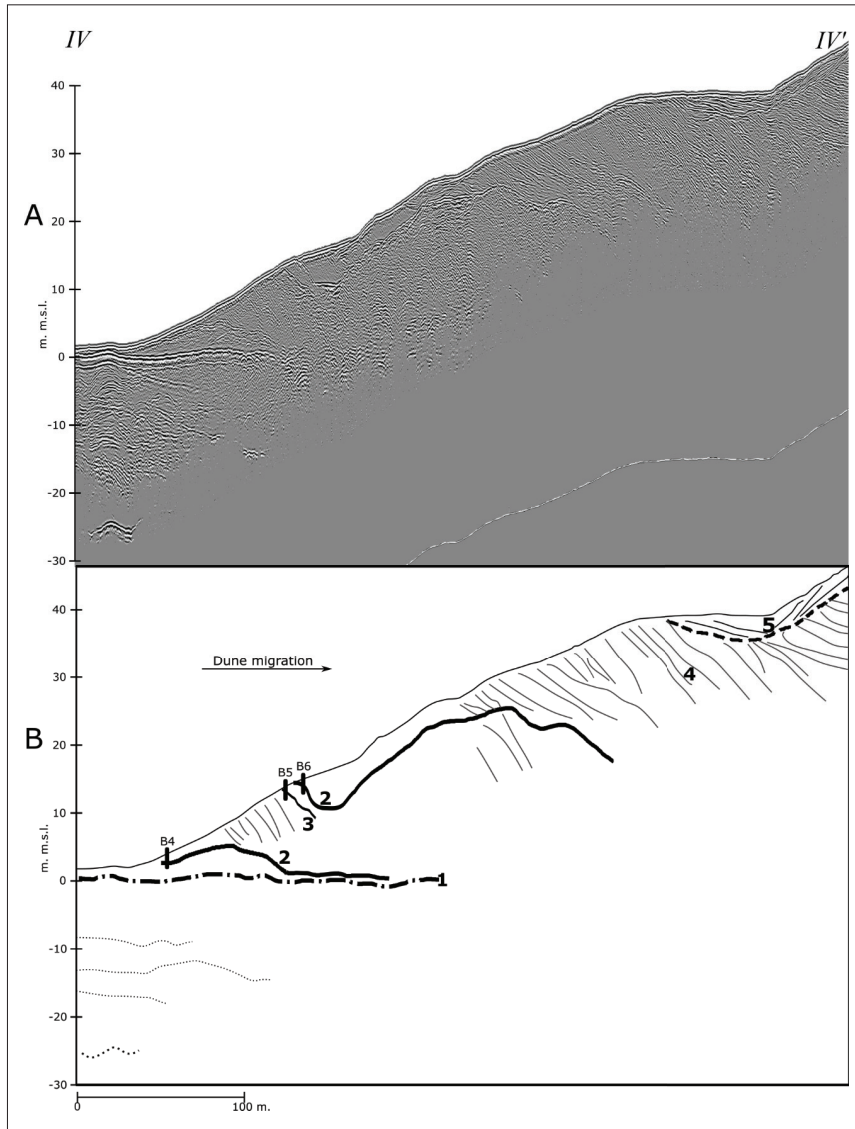


Figure 3.7.3. GPR cross-section fragment with visible reflectors. GPR data (A) and interpretation (B). B4, B5 and B6 are the control boreholes. The main layering elements of aeolian sediments: ground water table horizon (1), palaeosols (2), HMC layer (3), dune slipfaces (4), boundary between different slipface complexes caused by different wind direction (5).

3. Material and methods

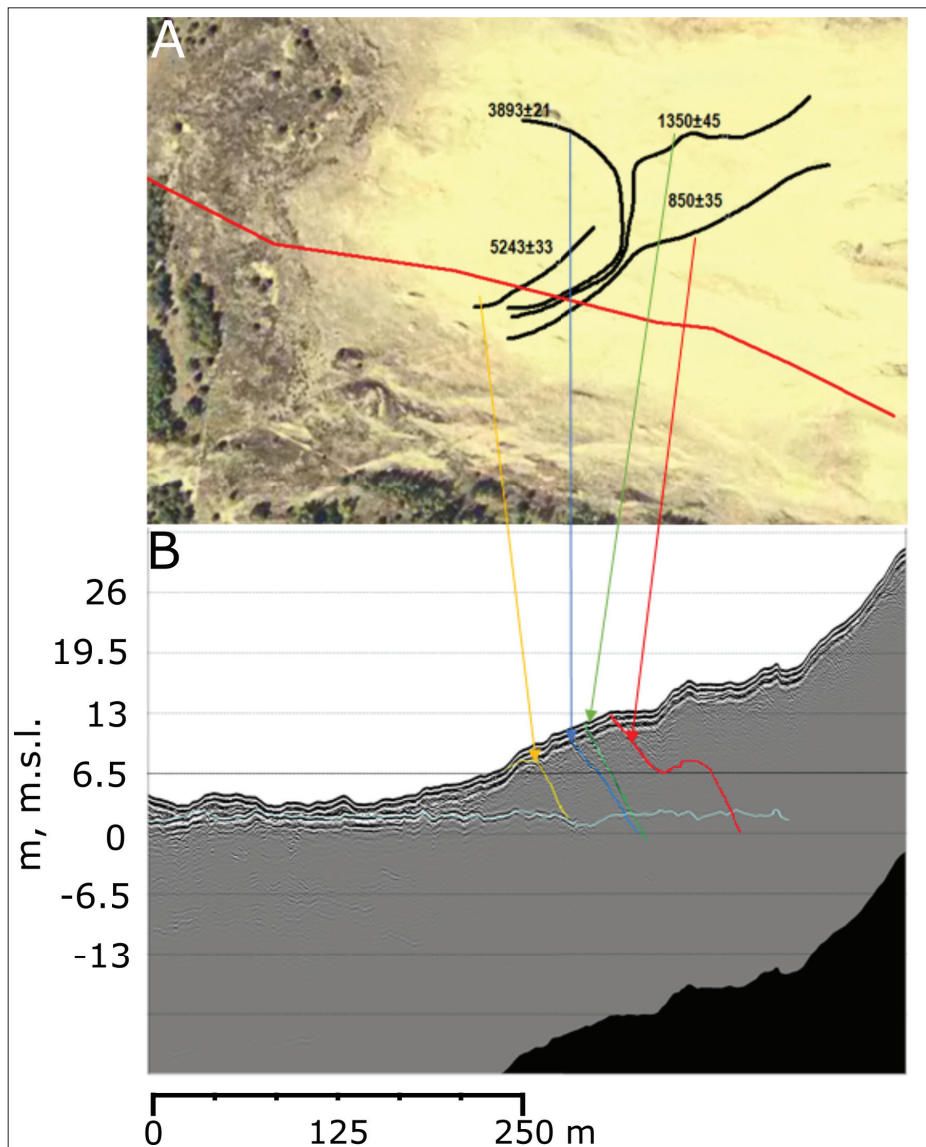


Figure 3.7.4. Palaeosols of different age in the GPR profiles: A – distribution of palaeosols and their radiocarbon (^{14}C) age (in years BP). Red line indicates GPR profile location depicted in the lower (B) section: age of palaeosols (Table 4): yellow – 5243 ± 33 cal. years BP; blue – 3893 ± 25 cal. years BP; green – 1350 ± 45 cal. years BP; red – 850 ± 35 cal. years BP. Teal line indicates the groundwater table.

3. Material and methods

Palaeosols were traced in the intersecting GPR cross-sections. After the tracing procedure, a palaeogeographic reconstruction was performed using the built-in interpolation function. Figure 3.7.5 shows the palaeogeographic reconstruction of a palaeodune.

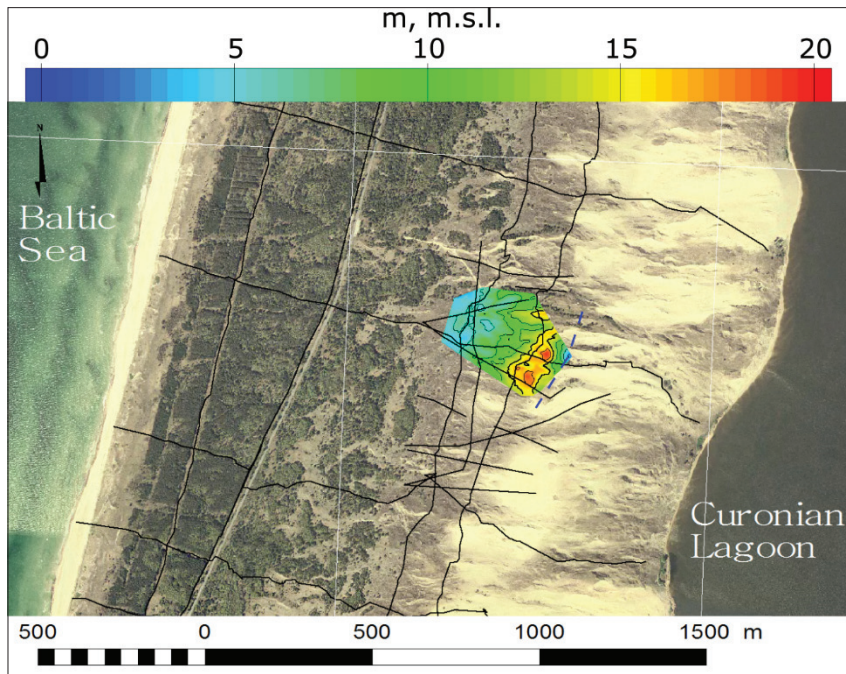


Figure 3.7.5. Distribution map of palaeosol V (930 ± 90 Cal. years BP).

Blue dashed line indicates possible eastern base of palaeodune.

Colour indicates palaeosol surface elevation above sea level (m, m.s.l.).

The palaeodune is covered with palaeosol V (930 ± 90 Cal. years BP, Annex No. 4, Vs-2251). The palaeosol is distributed over the area of 2830 m^2 . The palaeogeographic reconstruction reveals, that 930 yr. BP the palaeodune was situated in the western slope of GDR, red colour indicates the maximum height of the palaeodune (up to 20 m. m.s.l.), the palaeodune has a low-angle stoss slope and steep slipface. According to the palaeosol distribution, and a steep slipface angle, the possible eastern base of a palaeodune is established (Figure 3.7.5 a blue dashed line).

3. Material and methods

3.8 Evaluation of aeolian palaeodynamics

Two sites for the detailed palaeodynamics investigations were chosen in the stoss (western) slope of the GDR where a few palaeosol generations of different ages had been recognized and mapped (Figure 3.2.1, V and N). At each site, the investigations were conducted across the outcrops of palaeosols (start – end coordinates of the profile):

Vingis dune site: 55° 27' 35.07" N, 21° 05' 20.13" E – 55° 27' 36.44" N, 21° 05' 23.98" E;

Naglis dune site: 55° 26' 47.64" N, 21° 05' 01.51" E – 55° 26' 48.88" N, 21° 05' 04.15" E.

The above-mentioned sites selected for the detailed investigations were chosen between the neighbouring palaeosols that already had been dated by radiocarbon (AMS) method during the previous investigations of this dune ridge (Buynevich *et al.*, 2007a). The recent stage of investigations included a detailed ground penetrating radar (GPR) survey along the chosen profiles, visual lithological examination and description of aeolian sediments, as well as the measurements of magnetic susceptibility (MS) of sediments. During the laboratory investigations, the samples of the aeolian sediments were dated using the infrared optically stimulated luminescence (IR-OSL) technique.

The GPR data were collected in both locations between two palaeosols, perpendicular to the palaeosols strike. The palaeosols were interpreted based on their strong signal returns and characteristic geometry in radargrams. The reflectors established on the radargrams were identified by the means of control tranches in sediments.

The outcropping sections of the aeolian sediments are represented by yellow or grey sand, mainly quartz (96-98%). The medium-grained and coarse-grained sand occasionally contains thin horizons (usually 0.5-3.0 cm thick) of black or dark grey fine-to-medium-grained heavy-mineral concentrations (HMCs). According to previous mineralogical studies (Gudelis, 1989-1990), these HMCs are represented by hornblende, garnet, magnetite, ilmenite, and epidote. In some cases, lithological anomalies are represented by glauconite-coated quartz that can be recognized due to its green colour. Previous studies (Van Dam *et al.*, 2013) show that magnetite layers are clearly visible in the GPR data.

4

Geological layering of the palaeosols, their age and palaeodynamics of dune massifs

Aeolian sediments cover about 97-98% of the Curonian Spit territory – except a narrow belt along the Baltic Sea onshore where marine sand occurs, also in the particular segments along the Curonian Lagoon onshore. It is possible to distinguish a few zones with the different layering of aeolian sediments which are closely linked with the geomorphologic structure of the Curonian Spit (Figure 3.2.1). The specific layering of aeolian sediments is characteristic for the Protective Dune Ridge where the target-oriented influence of human activity (i.e. wooden reinforcements) left their tracks. In the Interdune area, or Palvė, both Marine and Lagoon, aeolian sediments form a flat plain alternating with a small hummocky relief where the aeolian sand does not exceed the first meter in thickness. The biggest thickness of aeolian sediments is concentrated in the Great Dune Ridge, including the fragment of relict parabolic dunes in the Juodkrantė surroundings.

4.1 Distribution and age of palaeosols

To identify more GPR reflections, the mapping of palaeosol outcrops was carried out. After the mapping was done, the data showed that the majority of outcrops were concentrated in the southern part of the investigation area (Figures 4.1.1 and 4.1.2). After the detailed palaeosol mapping and tracing in the GPR data thirteen palaeosol bulk samples were gathered and dated.

**4. Geological layering of the palaeosols,
their age and palaeodynamics of dune massifs**

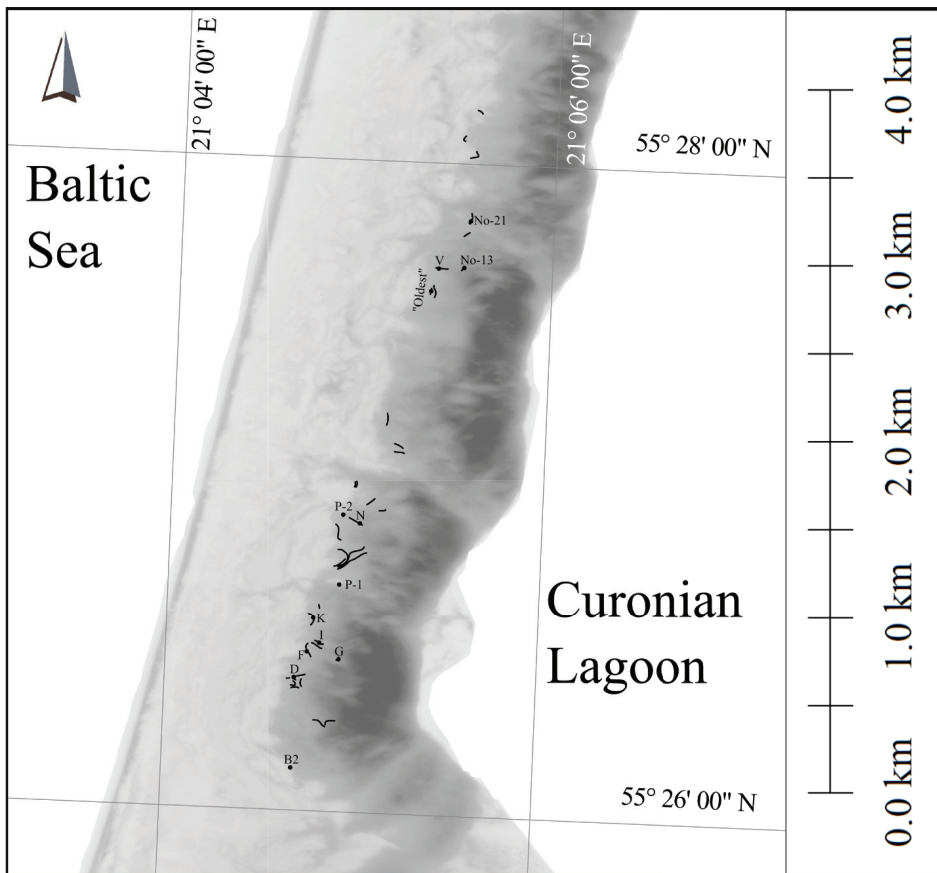


Fig. 4.1.1. Southern part of investigation area in the Dead (Grey) Dunes. Palaeosol outcrops are indicated by black lines, dots show sampling sites of dated palaeosols (Table 4).

4. Geological layering of the palaeosols, their age and palaeodynamics of dune massifs

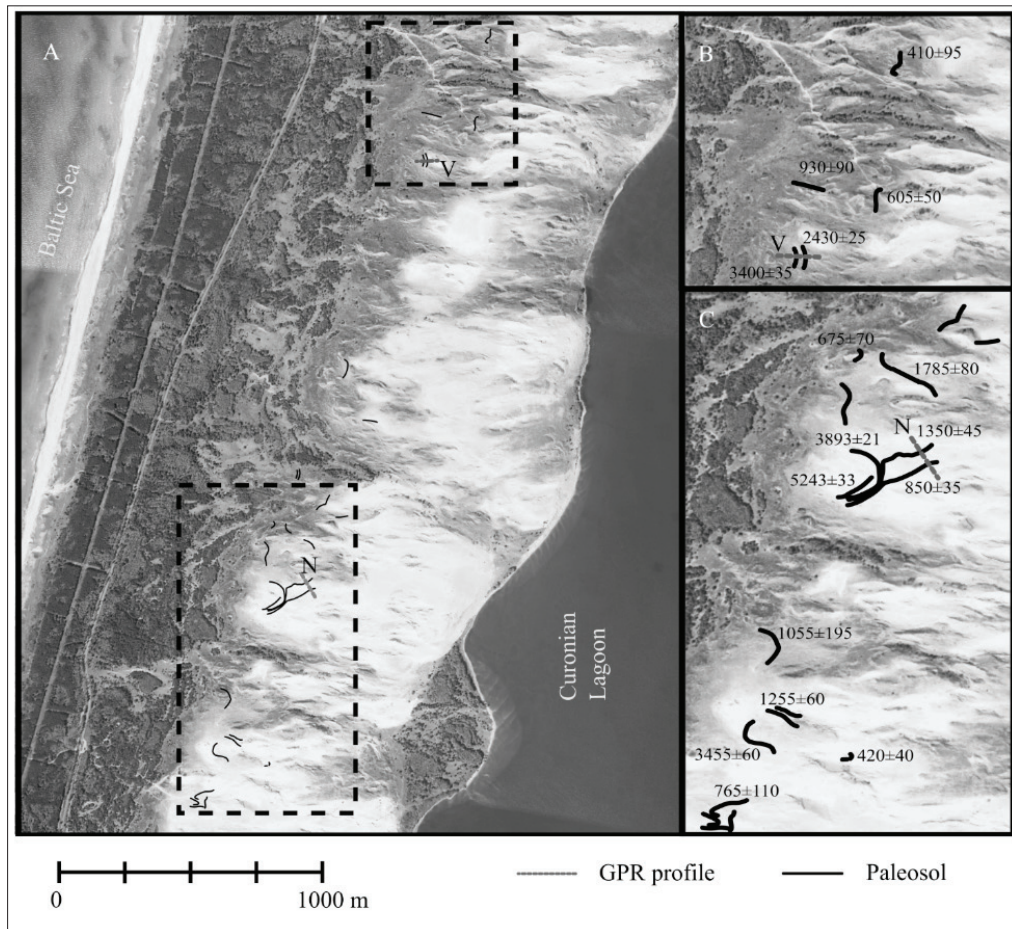


Figure 4.1.2. Distribution of outcropped palaeosols along the western slope of the Great Dune Ridge – a brighter shade on the photographic image reflect areas uncovered by vegetation. Dotted rectangles (A) indicate enlarged inserts in the surroundings of the site of Naglis dune (B) and the site of Vingis dune (C): GPR profiles of both sites are marked by letters V and N respectively; numbers next to palaeosols show their age (in calendar years BP) established by ^{14}C dating (after Buynevich et al., 2007a).

Thirteen dated palaeosol samples are presented in Table 4. Six dates fall into the time span of 400 – 900 years BP, four dates fall into the time span of 1000 – 2000 years BP and three dates fall into the time span of 3400 – 3900 years BP. The location elevation of the gathered samples ranges from 9 m to 33 m above the present sea level.

**4. Geological layering of the palaeosols,
their age and palaeodynamics of dune massifs**

Table 4. Results of radiocarbon (^{14}C) dating of palaeosols in the Curonian Spit

No.	Coordi-nates	Eleva-tion m, m.s.l.	Sampling site, Palaeosol code, depth, etc.	Method, analysed matter	^{14}C age, years (BP) ($\pm 1\sigma$)	Calibrated age (1σ range)
1	Vingis dune	10.7	“Oldest” palaeosol	Bulk, soil humus	3180 \pm 120	3560-3316 BP (59.2%) 3310-3262 BP (9.0 %)
2	55° 26' 42" 21° 04' 53"	11.1	Palaeosol-1	Bulk, soil humus	3545 \pm 70	3913-3720 BP (68.2%)
3	55° 26' 55" 21° 04' 55"	11.1	Palaeosol-2	Bulk, charcoal	675 \pm 70	606-556 BP (36.9 %) 668-624 BP (31.3%)
4	55° 26' 28" 21° 04' 56"	26.8	Palaeosol, G	Bulk, wood	420 \pm 40	518-459 BP (63.1%) 348-340 BP (5.1%)
5	55° 26' 35" 21° 04' 48"	13.6	Palaeosol, K	Bulk, charcoal	1055 \pm 195	1174-788 BP (68.2%)
6	55° 26' 29" 21° 04' 45"	10.1	Palaeosol, F	Bulk, charcoal	3455 \pm 60	3778-3678 BP (40.5%) 3828-3788 BP (16.5%) 3669-3640BP (11.3%)
7	55° 27' 40" 21° 05' 31"	33	Exposure No.13, depth 0.6 m	Bulk, wood	605 \pm 50	648-584 BP (54.2%) 568 550 BP (14.0%)
8	55° 26' 31" 21° 04' 49"	18.1	Palaeosol, I	Bulk, charcoal	1225 \pm 60	1184-1070 BP (52.0%) 1240-1204 BP (16.2%)
9	55° 26' 24" 21° 04' 42"	16.71	Palaeosol, D	Bulk, charcoal	765 \pm 110	796-640 BP (60.4%) 590-564 BP (7.0%) 891-887 BP (0.9%)
10	55° 26' 09" 21° 04' 42"	9.6	B 2, depth 1.7 m	Bulk, soil humus	1735 \pm 150	1826-1516 BP (63.3%) 1458-1442 BP (2.3%) 1860-1850 BP (1.4%) 1432-1422 BP (1.2%)
11	55° 26' 53" 21° 05' 02"	23.9	Palaeosol, N	Bulk, soil humus	1785 \pm 80	1818-1684 BP (46.6%) 1678-1615 BP (21.6%)
12	55° 27' 49" 21° 05' 32"	17.1	B10 near exposure No.21, depth 0.6 m	Bulk, soil humus	410 \pm 95	523-426BP (41.4%) 392-319 BP (26.8%)
13	55° 27' 41" 21° 05' 22"	15.9	Palaeosol, V	Bulk, soil humus	930 \pm 90	927-765 BP (68.2%)

4. Geological layering of the palaeosols, their age and palaeodynamics of dune massifs

4.2 Interpretation of palaeosol age and formation

Besides 13 radiocarbon dates obtained during this survey, additional 40 dates were found in literature. All the 53 results of the radiocarbon dating range from modern times to approximately 5800 calendar years BP (list of all radiocarbon dates is presented in the annex No.4). Following the hypothesis developed by Gaigalas and Pazdur (2008), as well as by other investigators in the Western Europe (Borowka, 1975; Tolksdorf & Kaiser, 2012), that the dune massifs were formed in changeable palaeogeographic conditions – calm periods with soil formation were changed by periods of intensive aeolian activation, four soil-forming generations were distinguished in the Curonian Spit dunes according to palaeosols age distribution (Figure 4.2.1):

- 1) 4500 – 5800 years BP;
 - 2) 3900 – 3100 years BP;
 - 3) 2600 – 2400 years BP;
 - 4) 1900 – 400 years BP;

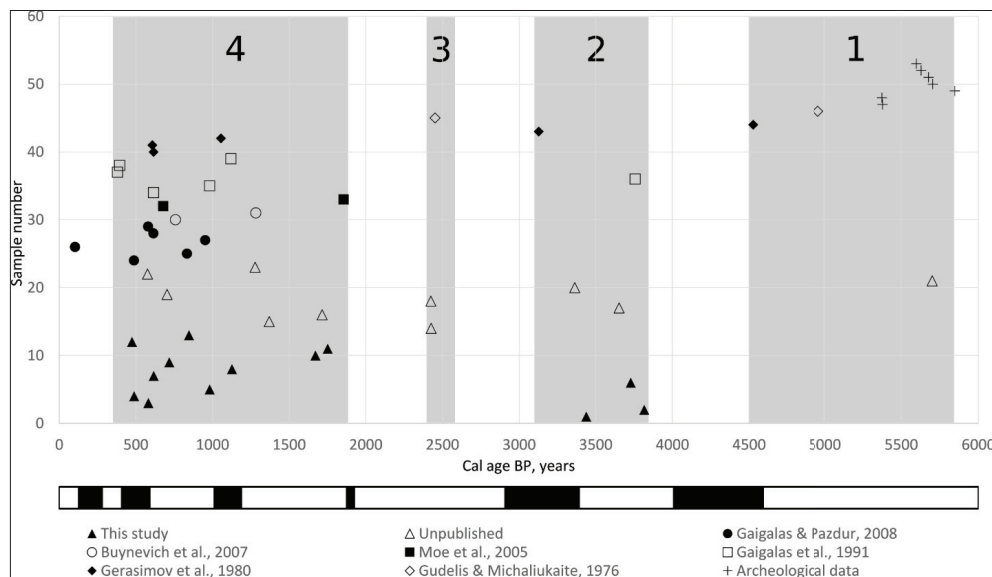


Figure 4.2.1. Results of radiocarbon (^{14}C) dating of palaeosols in the Curonian Spit. X-axis represents age BP, the number in the Y-axis corresponds to the number of sample in Table 4 (1-13) and Annex No.4 (14-53). Established soil-forming generations are marked as grey sections; soil-forming generations established by Gaigalas and Pazdur (2008) are marked by black rectangles below the graph.

4. Geological layering of the palaeosols, their age and palaeodynamics of dune massifs

The primary version about the possible existence of soil-forming generations in the Curonian Spit was published in 2013 (see author's publication list). The established soil-forming generations were based on the bigger amount of radiocarbon ages of palaeosols, thus, the amount of soil-forming generations and their time frames is different from Gaigalas and Pazdur (2008) version (Figure 4.2.1).

The second stage of palaeosols' radiocarbon age interpretation was linked to the comparison of the established soil-forming generations with the variation of global temperature. The reactivation of aeolian processes and re-deposition of dunes in the Curonian Spit started at least in the mid-Holocene and according to the theoretical assumptions could be linked with long-lasting climate fluctuations that occurred during this period. Due to lack of information about the marine climate fluctuation (such as humidity, storminess, etc.) during the last 6000 years, an attempt has been made to link palaeosols generations with global temperature change (GISP2) only (Figure 4.2.2).

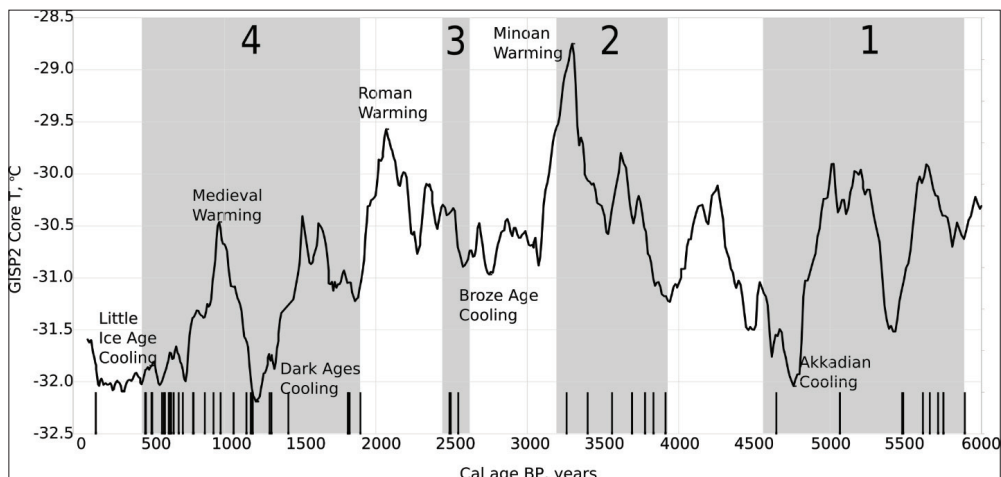


Figure 4.2.2. Comparison of the GISP2 core global temperature curve with the results of radiocarbon (^{14}C) dating of palaeosols age (black dashes). Grey sections indicate established palaeosol generations (1, 2, 3, 4), when dune surface used to be covered by vegetation and palaeosols were formed (GISP2 data after Alley, 2004; modified).

However, a visual comparison of the global temperature curve based on the GISP2 core data and the soil-forming generations based on the radiocarbon (^{14}C) dating results of palaeosols in the Curonian Spit shows that there is no connection between them. The comparison shows no visible pattern between cool or warm periods and palaeosol generations: the 2nd palaeosol generation occurred during the Minoan Warming, the 3rd generation occurred between the Roman Warming and the Dark Age Cooling periods, and the 4th generation corresponds to the Dark Ages cooling, the Medieval Warming and the Little Ice Age periods.

4. Geological layering of the palaeosols, their age and palaeodynamics of dune massifs

After that, trying to explain an uneven distribution of the received data of the radiocarbon analysis of the palaeosols, the main attention was concentrated on the peculiarities of the palaeosols development, their geological layering and radiocarbon dating technique, including palaeosols sampling, possible analysis errors, etc. According to previous investigations (Peyrat, 2007), soil forming processes take approximately from 600 to 800 years. Therefore, there could be a huge difference from which part of the palaeosol the sample was taken. Figure 4.2.3 demonstrates the possible radiocarbon age variations from the same palaeosol layer: if the ^{14}C sample was taken from the upper part of the palaeosol – the date will represent the last stage of the palaeosol formation; if the ^{14}C sample was taken from the lower part of the palaeosol – the date could represent the early stage of palaeosol formation. Especially it is characteristic for the radiocarbon dating by the AMS method.

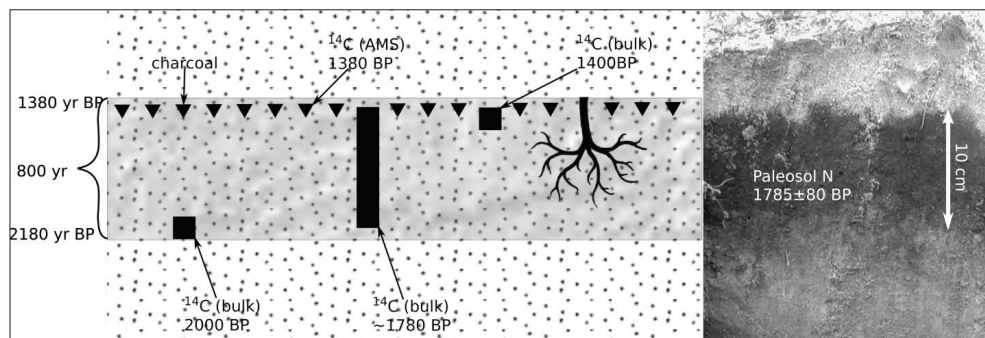


Figure 4.2.3. Dating of the palaeosol. Grey colour represents palaeosol, triangles represents charcoal, squares – bulk samples.

Considering that the majority of samples were collected from the uppermost part of the palaeosols, usually more enriched by organic matter, often by charcoal, radiocarbon ages more represent the latest stages of palaeosols development. Thus, it is possible to make an assumption that in the majority cases the palaeosol formation started, possibly, up to 800 years earlier as the received radiocarbon age from this layer. As a result, the palaeosol-forming generation time span should be extended, and the beginning of each generation should be advanced up to 800 years. The radiocarbon (^{14}C) dates obtained during this survey could represent any stage of soil formation. Generally, only one bulk sample from each palaeosol layer was collected and dated during this study, also during the previous investigations. Hence, this sample potentially could represent early or late stage of palaeosol development or could show a particular “average” age of the palaeosol layer.

4. Geological layering of the palaeosols, their age and palaeodynamics of dune massifs

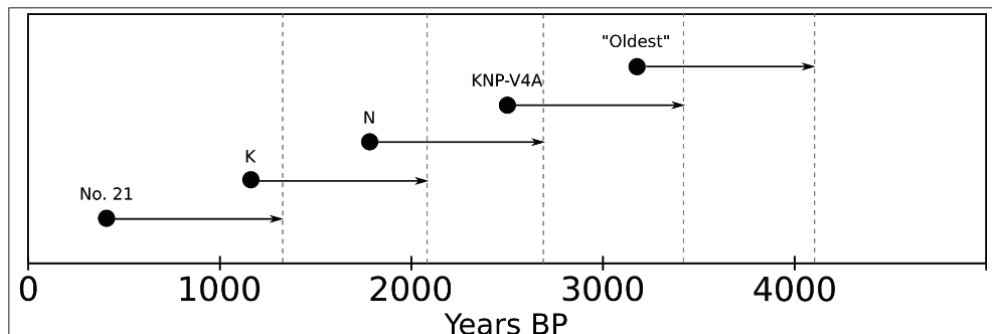


Figure 4.2.4. Interpretation of ^{14}C dating results of a few palaeosols (Table 4). Black dots represent palaeosols radiocarbon age (bulk sample), arrows show possible “beginning” of the palaeosol formation – correction (“oldering”) by 800 years of each sample is done according to Peyrat, 2007.

Figure 4.2.4 shows radiocarbon (^{14}C) age of a few palaeosols with possible initial moment of palaeosol formation, indicated by arrows. Thus, after the presented correction, the palaeosol N (1785 ± 80 years BP, Annex No. 4, Vs-2249) and palaeosol K (1055 ± 195 yr BP, Annex No. 4, Vs-2240) could represent the same soil-forming generation, as well as could represent the same generation as palaeosol KNP-V4A (2430 ± 25 years BP). As the result, the detailed analysis of the determination of palaeosols age and peculiarities of radiocarbon dating technique shows that the interpretation of the data received using ^{14}C is problematic – the palaeosols of different age previously attributed to the separate soil-forming generations could represent the same continuing soil-forming period.

Thus, taking into account the time span of palaeosol formation (800 – 1000 years) and that there is no information from which palaeosol part (lower, middle or upper) the ^{14}C bulk samples were gathered, it was assumed, that an unknown number of dated samples could represent only the last stage of palaeosol formation. Therefore, the time limits of established soil-forming generations could be extended (“oldered”) by above mentioned 800 years at least. Figure 4.2.5 presents extended range of distinguished soil-forming generations limits.

The graph shows that there are no gaps between generations: the 3rd palaeosol generation overlaps with the 2nd generation, as well as the 2nd generation overlaps the 1st generation. Consequently, all palaeosols from all 4 generations could be combined to one single generation stretching from more than 6000 years BP to modern days.

The presented analysis of palaeosols radiocarbon (^{14}C) data decline the hypothesis about multi-stage model of soil-forming processes in the Curonian Spit. On the other hand, it supports an idea of V. Gudelis (1998a) that it was only one long continuous period of permanent formation of palaeosols, and only a bigger amount of radiocarbon (^{14}C) analysis collected during the latest several decades enable to extend the

4. Geological layering of the palaeosols, their age and palaeodynamics of dune massifs

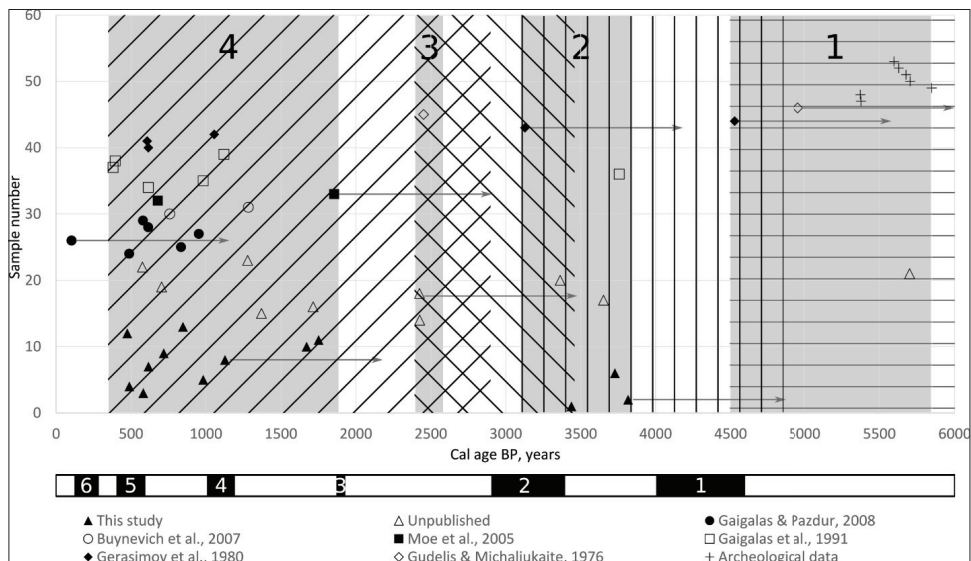


Figure 4.3.5. Results of radiocarbon (^{14}C) dating of palaeosols in the Curonian Spit. X-axis represents age BP in years, the number in the Y-axis corresponds to the number of samples in Table 4 (1-13) and Annex No.4 (14-53). Established soil-forming generations are marked as grey sections. Arrows attached to a few radiocarbon (^{14}C) dates show possible time span extension (“oldering”) of palaeosol formation. A horizontal hatch shows the possible extension of 1st generation, vertical hatch shows possible extension of 2nd generation, a forward diagonal hatch shows possible extension of 3rd generation, a backward diagonal hatch shows possible extension of 4th generation.

beginning of this period from 4000 to 6500-6700 years BP. An uneven distribution of radiocarbon (^{14}C) ages of palaeosols can be explained by the fact that the palaeosols of particular age were better developed than other ones, better survived during the activation of aeolian processes, or are more often outcropping in the recent aeolian relief, and, as a result, a significantly bigger number of samples was collected from the particular palaeosol layers during different investigations.

4.3 Aeolian palaeodynamics

The site of Vingis dune is located on the windward slope of the aeolian massif with minor relief, at the altitude of about 10 – 11 m above sea level. The situation of the site of Naglis is somewhat similar, except that it takes place higher – at the height of ~20 – 22 m m.s.l. From the geological point of view, the geophysical profiles at both sites were established along the inner sections of ancient dunes where the uppermost parts were deflated (Figure 4.1.2).

4. Geological layering of the palaeosols, their age and palaeodynamics of dune massifs

Results

Geophysical images from the site of Vingis dune reveal two main types of subsurface reflectors (Figure 4.3.1). The most noticeable reflectors are the palaeosols that outcrop along the present dune surface at horizontal distances of ~ 8 and 32 m. Both reflections dip east approximately of 6° (older palaeosol) and 12° (younger one). Meanwhile the series of less well expressed and shorter reflectors (occurring at intervals from 2 to > 20 cm) correspond to thin heavy-mineral concentrations (HMCs) that also dip in the eastern direction.

The age of the dune sand located between two palaeosols in the site of Vingis dune generally falls into the time span before 2.4 ± 0.2 and 2.2 ± 0.2 ka (Figure 4.3.1, Table 5), except for one sample (Figure 4.3.3, KOPOS-6), located directly below the palaeosol dated by 2430 ± 25 cal y BP, which shows an older age – 2.8 ± 0.2 ka.

The measurements of MS along the Vingis profile showed a range of values from 8-10 to 20-30 mSI. The MS value increase was largely associated with HMCs.

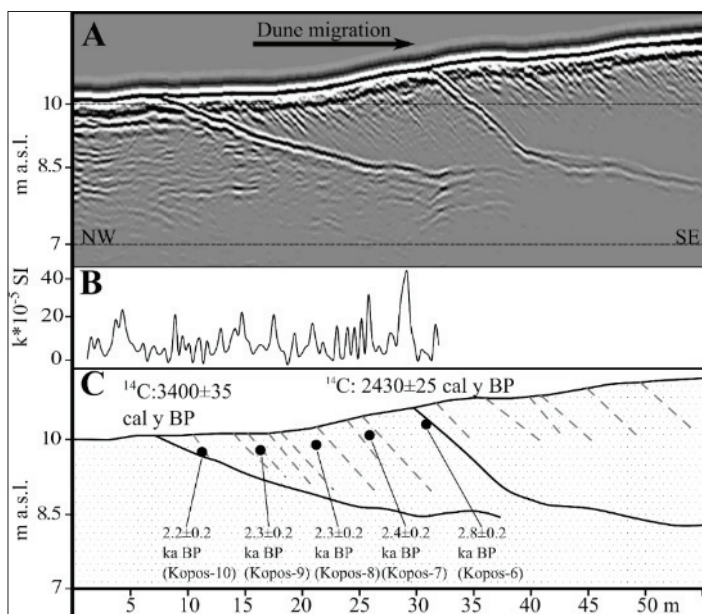


Figure 4.3.1. Profile of detailed investigations in the Vingis dune site: A – ground penetrating radar (GPR) image (radarogram), B – curve of magnetic susceptibility (MS), C – interpretation of radarogram. In the latter section palaeosols are marked by solid lines, interlayers with high concentration of heavy minerals – by dashed lines; radiocarbon age of the palaeosols is indicated above the surface identifying line. Sampling locations for IR-OSL dating is indicated by black dots. Distance along the horizontal scale is marked from the beginning of GPR profile.

4. Geological layering of the palaeosols, their age and palaeodynamics of dune massifs

According to the visual identification during the measurement procedure in the field, intervals with low MS values are characteristic for sand layers composed mostly of quartz and feldspar, with the highest values invariably associated with thin HMC interlayers (up to 4-5cm). MS values are presented in Annex No. 5.

Table 5. Results of infrared optically stimulated luminescence (IR-OSL) dating and radioactivity data of sand samples from the sites of Naglis dune and Vingis dune.

No.	Locality	Depth, meters below surface	Lab. No	Field No	U (ppm)	Th (ppm)	K (%)	IR-OSL age (ka)
1	Naglis dune	0.5	RLQG 2102-112	KOPOS-1	0.01	0.86	0.66	2.2 ± 0.2
2	-“-	0.5	RLQG 2103-112	KOPOS-2	0.20	0.93	0.64	1.7 ± 0.2
3	-“-	0.5	RLQG 2104-112	KOPOS-3	0.96	1.82	0.77	1.4 ± 0.1
4	-“-	0.5	RLQG 2105-112	KOPOS-4	0.22	1.29	0.79	1.3 ± 0.1
5	-“-	0.5	RLQG 2106-112	KOPOS-5	0.82	1.92	0.80	1.1 ± 0.1
6	Vingis dune	0.7	RLQG 2107-112	KOPOS-6	0.08	1.47	0.75	2.8 ± 0.2
7	-“-	0.7	RLQG 2108-112	KOPOS-7	0.25	0.55	0.74	2.4 ± 0.2
8	-“-	0.7	RLQG 2110-112	KOPOS-8	0.36	0.59	0.82	2.3 ± 0.2
9	-“-	0.7	RLQG 2109-112	KOPOS-9	0.31	0.82	0.73	2.3 ± 0.2
10	-“-	0.7	RLQG 2111-112	KOPOS-10	0.66	1.03	0.86	2.2 ± 0.2

At the site of Naglis dune (Figure 4.3.2) noticeable reflectors are palaeosols at 9 and 34 m along the profile. Both reflections dip to the SE at $\sim 8^\circ$ (older) and 6° (younger palaeosol). A few secondary reflectors correspond to thin SE-dipping HMC horizons, similar to those at the site of Vingis dune. The interpretation of GPR reflectors is based on the exposures of the aeolian sections along GPR transects, as well as in the shallow tranches excavated for IR-OSL sampling.

The IR-OSL dating results of the Naglis site demonstrate that the age of sand layers gradually increases from NW to SE – from 1.1 ± 0.1 ka to 2.2 ± 0.2 ka (Figure 4.3.2, Table 5).

The measurements of MS along Naglis profile show a range of values from 5-10 to 500-1000 mSI (with one anomaly –2027.5 mSI). At the Naglis site, relatively low values of MS were characteristic for the NW (upwind) part of the profile, whereas anomalies >800 -1000 mSI were common in the SE part of the profile. MS values are presented in Annex No. 6.

The results of GPR imaging demonstrate the subsurface situation of the exposed palaeosols and HMC horizons, providing a means of their mapping and connection in nearby dune sections. The values of magnetic susceptibility not only provide useful

4. Geological layering of the palaeosols, their age and palaeodynamics of dune massifs

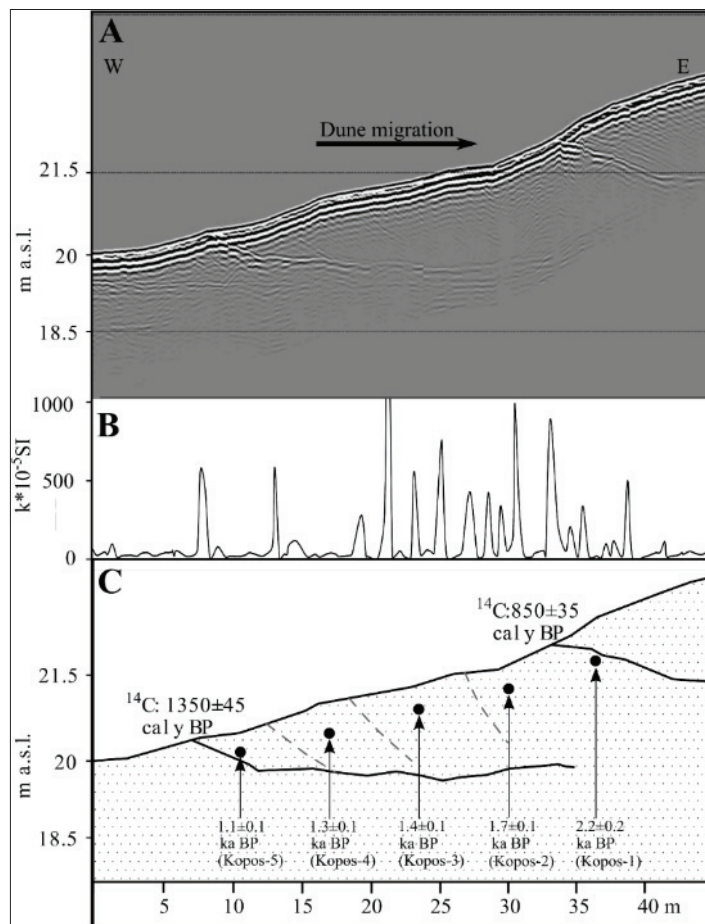


Figure 4.3.2. Profile of detailed investigations in the site of Naglis dune: A – ground penetrating radar (GPR) image (radarogram), B – magnetic susceptibility (MS) curve, C – interpretation of radarogram. In the latter section palaeosols are marked by solid lines, interlayers with high concentration of heavy minerals – by dashed lines; radiocarbon age of the palaeosols is indicated above the line identifying the surface. Black dots indicate sampling locations for IR-OSL dating. Distance along horizontal scale is marked from the beginning of the GPR profile.

independent data of mineralogical anomalies, but also contribute to the interpretation of specific reflections in the GPR data.

The results of investigations obtained by different methods of absolute chronology complement each other (^{14}C AMS dating of palaeosols and IR-OSL dating of intervening sand horizons) (Figures 4.3.1 and 4.3.2).

4. Geological layering of the palaeosols, their age and palaeodynamics of dune massifs

Interpretation

Radiocarbon dating suggests that the dune section investigated in detail at the Vingis site represents the aeolian activity that post-dates a stable phase that ended $\sim 3400 \pm 35$ cal y BP (older palaeosol). This dune sequence accumulated over a relatively short time span – between 2.4 and 2.2 ka according to IR-OSL dating results (Figure 4.3.3). After aeolian activity settled down, a new palaeosol (dated as 2430 ± 25 cal yr BP) started to form. Only an anomalous IR-OSL sample (2.8 ± 0.2 ka) located directly below the younger palaeosol (Figure 4.3.1, KOPOS-6) contradicts this interpretation.

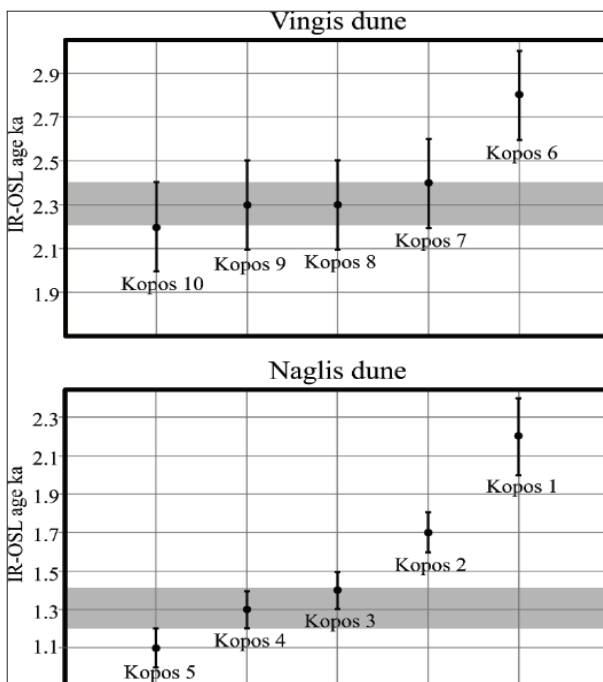


Figure 4.3.3. Results of IR-OSL dating from the sites of the Vingis and Naglis dunes. The most likely periods of aeolian sedimentation are indicated by a grey stripe.

The aeolian activity at the site of Naglis dune is more difficult to interpret. The IR-OSL dating results show that sand accumulation took place over a relatively long-time span that began before 2.4 ka and continued until 1000 years BP (Figure 4.3.3). Reviewing IR-OSL data of Naglis dune, three samples fall within the relatively short time span before ~ 1.4 -1.2 ka BP (Figure 4.3.3, samples KOPOS-3, 4 and 5). Therefore, it is likely that this time span reflects the actual age of aeolian sedimentation. These three IR-OSL samples do not contradict the results of ^{14}C AMS dating of palaeosols, i.e. 1350 ± 45 and 850 ± 35 cal yr BP, respectively.

4. Geological layering of the palaeosols, their age and palaeodynamics of dune massifs

The most problematic issue of the IR-OSL data interpretation relates to the fact that the oldest dates at both sites (KOPOS-1 and KOPOS-6) were obtained from the stratigraphically youngest sand horizon. One explanation relates to a possible influence of pedogenic processes, given that the oldest dates come from the samples collected directly beneath the palaeosol horizons. As shown in Table 5, a very low content of uranium (0.01 and 0.08 ppm) is characteristic for both samples (KOPOS-1 and KOPOS-6). This could have influenced the results of IR-OSL dating. The prevalence of uranium in sandy sediments is associated with common soluble salts (UO_2)² such as nitrate, chloride, acetate, sulphate, and carbonate that could be easily dissolved during soil-forming processes (Boyle, 1982). As a result, uranium could be transported (eluviated) into underlying sediments. Considering the morphology of the ancient dune, the sample KOPOS-1 at the site of Naglis dune (Figure 4.3.2) could have been partly influenced by Late Holocene pedogenesis. However, assuming the average of uranium content values between 0.20-0.96 ppm (average: 0.47 ppm), the corrected age could be younger by only 200 years if no U migration during the soil-forming processes had occurred. Therefore, pedogenesis is unlikely to explain the old age of stratigraphically youngest samples in both areas. Thus, an alternative explanation is proposed.

One possible scenario which explains IR-OSL dating peculiarities is the following. The initial stage of dune movement occurred in mild environmental conditions with predominantly low and moderate winds. At this stage the finest sand fractions were transported to the slipface of the dune. In these conditions transportation took long enough to cause full bleaching. Consequently, the IR-OSL age of sand interlayers deposited during the initial stage shows the real age of sedimentation (2.4 – 2.2 ka at the Vingis site, Figure 4.3.1, KOPOS-7, KOPOS-8, KOPOS-9, KOPOS-10 and 1.4 – 1.2 ka at the Naglis site, Figure 4.3.2 KOPOS-3, KOPOS-4, KOPOS-5).

Anomalous IR-OSL dates, corresponding to 2.8 ka at the Vingis site (KOPOS-6) and 2.2 – 1.7 ka at the Naglis site (KOPOS-1, KOPOS-2), could be explained by rapid sand transportation during a relatively stormy period (Hilgers, 2007): sand was deflated from the primary dune, quickly transported and deposited, there was little to no time for bleaching, thereby the “old” IR-OSL signal retained (i.e. with progenetic palaeodose-related effects in mineral lattice).

A scenario with two different transportation conditions could explain the anomalously old dates at both sites coinciding with stratigraphically younger dune sand. This scenario is supported by higher MS value readings.

Using multi-dating methods of absolute geochronology and making comparison between them in the frame of a single research requires considering dating errors. During this study two methods of dating were used: ^{14}C AMS and IR-OSL, each having different accuracy rates and errors that vary from decades (for ^{14}C AMS) to centuries (for IR-OSL).

Besides, lumps of charcoal from palaeosols for ^{14}C AMS sampling were used. Considering that the development of the soil horizon in organic-poor sand takes up to 600 – 800 years (Peyrat, 2007), dates taken from charcoal represent only several de-

4. Geological layering of the palaeosols, their age and palaeodynamics of dune massifs

cades from this long soil-forming period. Moreover, it must be considered that dated charcoal represents the latest stage of soil-forming period when there was enough organic-rich material for a higher plant vegetation.

At Naglis dune the older palaeosol is dated 1350 ± 45 cal y BP and the sand layer above is dated 1.1 ± 0.1 ka. With respect to the factors mentioned above it is possible to admit that these dates are relatively reliable.

4.4 Palaeogeographic reconstructions

Several palaeogeographic reconstructions of palaeodune morphology for different phases of dune development in the massif of Dead (Grey) Dunes have been carried out. The reconstructions have been created for smaller areas, depending on how widely the palaeosols of similar age were preserved.

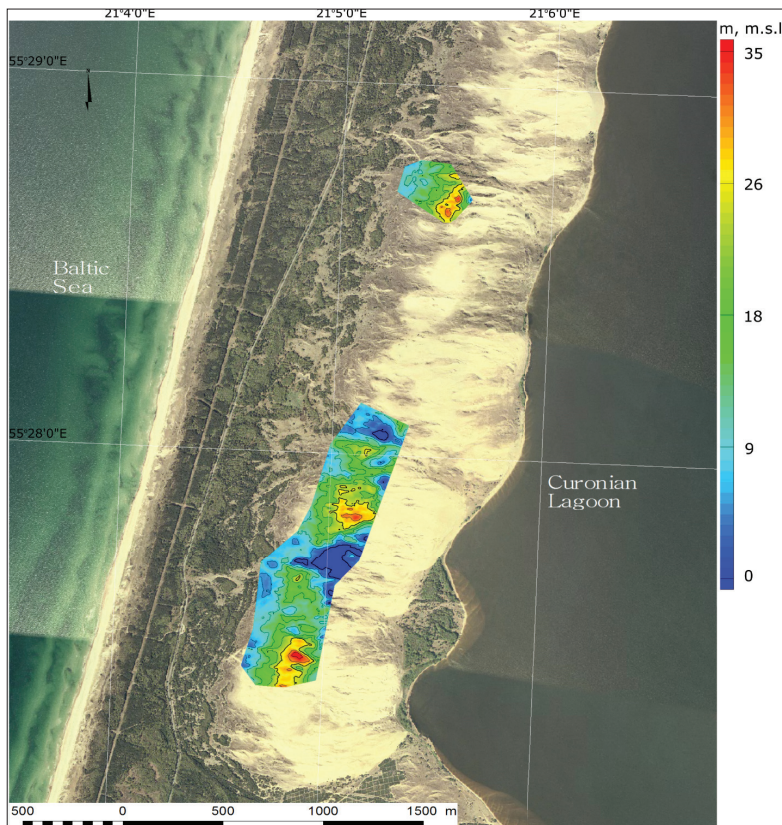


Fig 4.6.1. Palaeogeographic reconstruction of the Dead (Grey) Dunes massif (fragments) about 1000 calendar years BP. Colour indicates palaeosol surface elevation above sea level (m, m.s.l.).

4. Geological layering of the palaeosols, their age and palaeodynamics of dune massifs

Figure 4.6.1 shows the palaeomorphology of dune massif approximately 1000 years BP. The altitudes close to 0 m m.s.l. was, very possible, characteristic for the eastern base of dune massif and former Lagoon Palve. The eastern base of palaeo-dunes was situated almost near to the central part of the recent Curonian Spit. The maximum altitude of a dune massif did not exceed 35 m. m.s.l., its width reaches approximately 200 – 300 meters. The palaeo-dune massif was not consistent, composed of a several smaller dunes.

The palaeogeographic reconstruction for a dune approximately 3500 years BP is presented in Figure 4.6.2. The eastern base of palaeo-dune was situated almost near the central part of the current Curonian Spit. The maximum altitude of a dune massif did not exceed 25 m. m.s.l. the dune massif was composed of several smaller dunes. The reconstructed areas are very small, because palaeosols of this age survived very fragmentally.

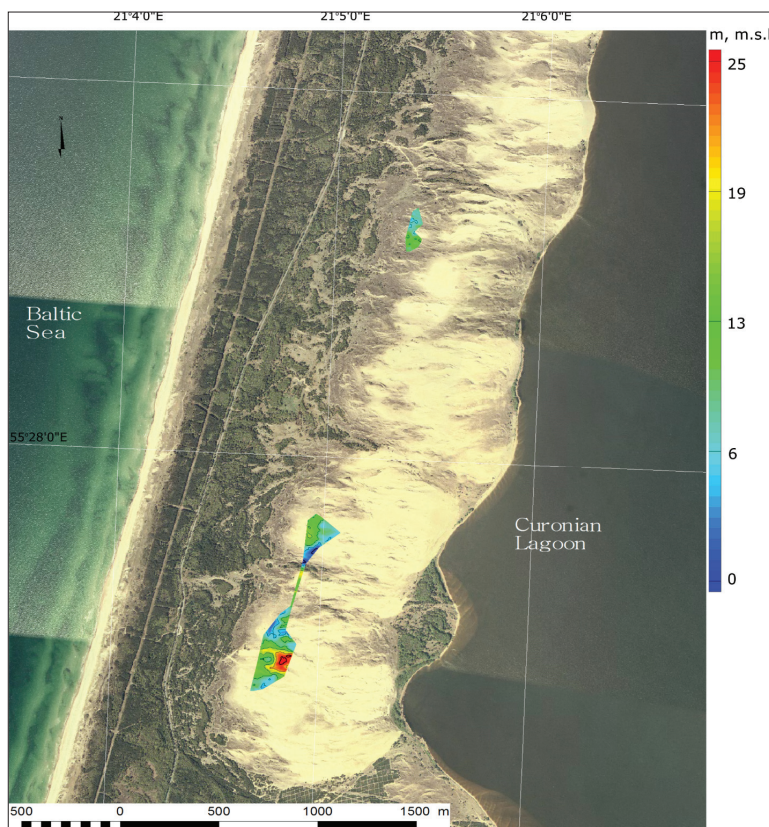


Fig 4.6.2. Palaeogeographic reconstructions of the Dead (Grey) Dunes massif (a few fragments) about 3500 calendar years BP. Colour indicates palaeosol surface elevation above sea level (m, m.s.l.).

4. Geological layering of the palaeosols, their age and palaeodynamics of dune massifs

According to the presented reconstructions, the eastern base of the dune ridge was approximately at the same position from 3500 to 1000 years BP, which was near the central (axial) part of the Curonian Spit, along the western slope of the present Great Dune Ridge. The highest altitudes of palaeosols in the Curonian Spit were fixed at more than 40 m above the present sea level (Michaliukaite, 1962), but according to our palaeo reconstructions, based on the results of GPR survey, the height of palaeodunes did not exceed 35 meters (Figures 4.6.1, 4.6.2, 4.6.3). Figure 4.6.3 presents the inner structure of the present dune, along cross-section V-V', as well as the topography of a palaeodune. The dune cross-section shows that a width of the particular dune was approximately 250 meters, height reached near 17 m. More examples of GPR data with a visible palaeodune presented in Annex No.7.

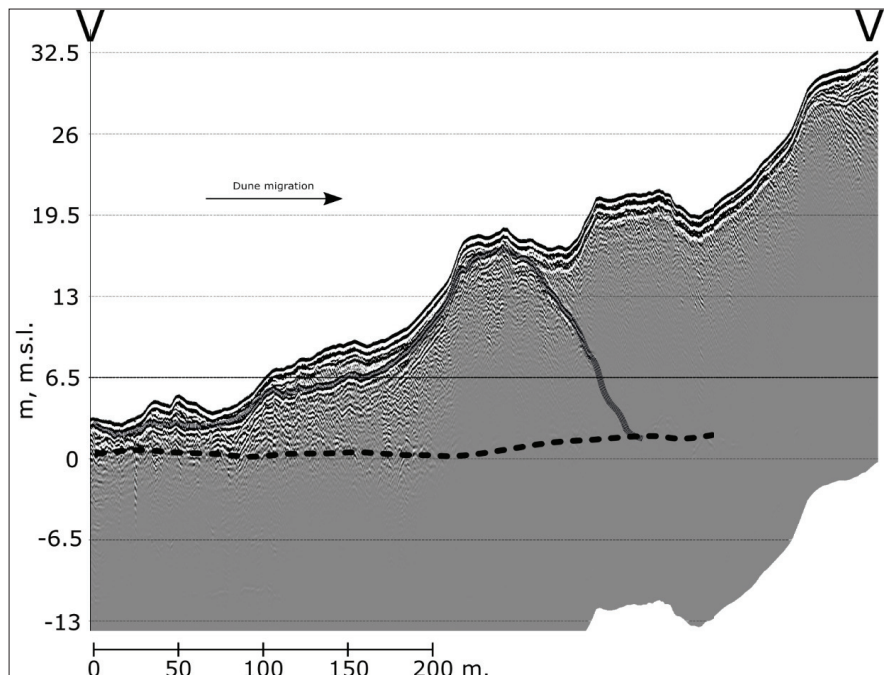


Fig 4.6.3. GPR cross-section with a visible palaeodune. GPR profile with altitudes corrected according to LIDAR data. The groundwater table is indicated by a dashed line, the buried palaeosol – by a grey line. Height of the palaeodune – 17 meters.

The palaeogeographic reconstruction of the eastern base of the dune massif indicates that during the last 1000 years a significant dune transgression occurred (Figure 4.6.4). In the time span of 2500 years (from 3500 to 1000 calendar years BP) dunes shifted only a few hundred meters (approximately 180 m), while over the last 1000 years dunes have moved by nearly 500 meters.

4. Geological layering of the palaeosols, their age and palaeodynamics of dune massifs

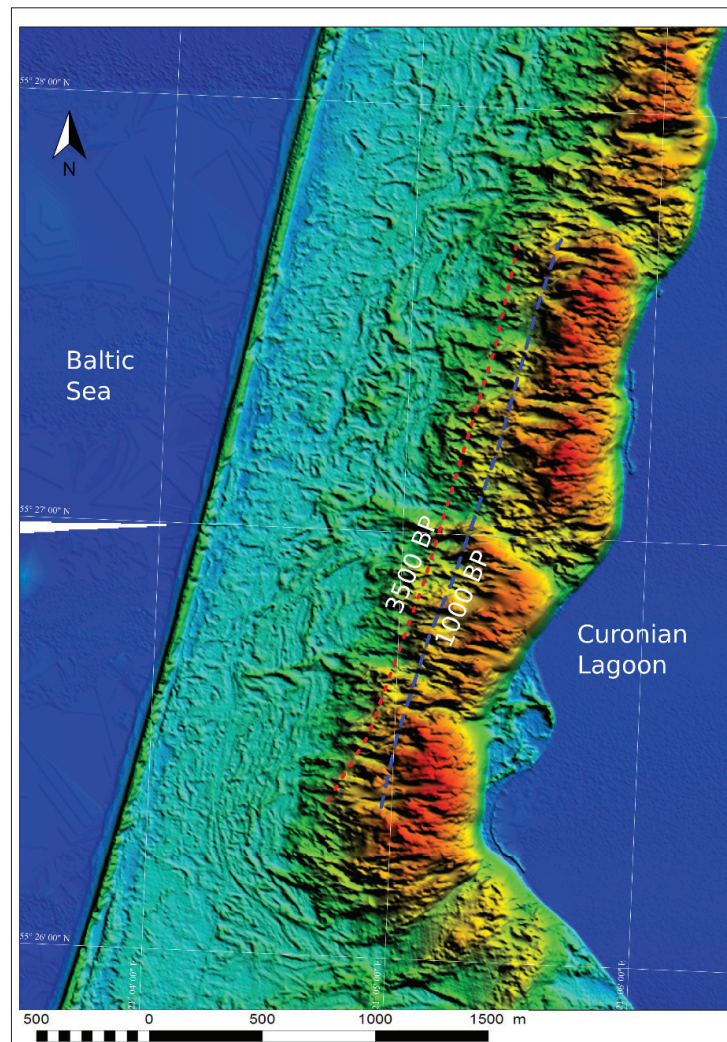


Figure 4.6.4. Generalized position of the ancient palaeodune massif eastern base in the southern part of the Dead (Grey) Dunes massif for the different time periods.
A red dashed line represents the palaeodune eastern base 3500 years BP, a blue dashed line – the palaeodune eastern base 1000 years BP.

5

Discussion

5.1 Dune evolution and climate change

The results obtained suggest that there is no relationship between global temperature fluctuations and palaeosol formation in the Curonian Spit, i.e. global temperature changes have not been the main factor that influenced the soil-forming processes. It is possible to assume, that, instead, local events triggered formation of the palaeosol. Almost all of the samples of palaeosol contain charcoals, as it was suggested by previous investigations (Gudelis, 1998b; Gaigalas & Pazdur, 2008), the forest fires served as a catalyst for palaeosol formation.

HMC layers found in the Naglis and Vingis dune profiles indicate increased near-surface wind velocity and can be associated with storms (Buynevich, 2012; Pupienis *et al.*, 2017). Thus, storms may have been playing the main role in dune transgression. Ground-penetrating radar images and magnetic susceptibility trends within aeolian sediments demonstrate a variation in heavy mineral concentration that can be related to local palaeo-climatic conditions (relatively calm, windy, or stormy near-surface regime) what existed during the dune accumulation. Aeolian reactivation phases were stimulated by the local factors (e.g., forest fires and deforestation), covered limited areas and lasted no longer than one or two centuries.

Investigations during the XX century led to the dominant opinion that aeolian reactivation and deposition were linked with large-scale changes in Holocene climate (Borowka

5. Discussion

1975). These periods of uninterrupted aeolian activity (“aeolodynamic stages”, Gudelis 1998b) were estimated to last thousands of years. The results of this study confirm recent findings (Moe *et al.*, 2005; Buynevich *et al.*, 2007a; Gaigalas & Pazdur, 2008; Tolksdorf & Kaiser, 2012) that suggest that dune reactivation was primarily triggered by local factors, such as abrupt climatic shifts and storminess, natural (or human-induced) forest fires, and (in historical times) deforestation that lasted tens to hundreds of years.

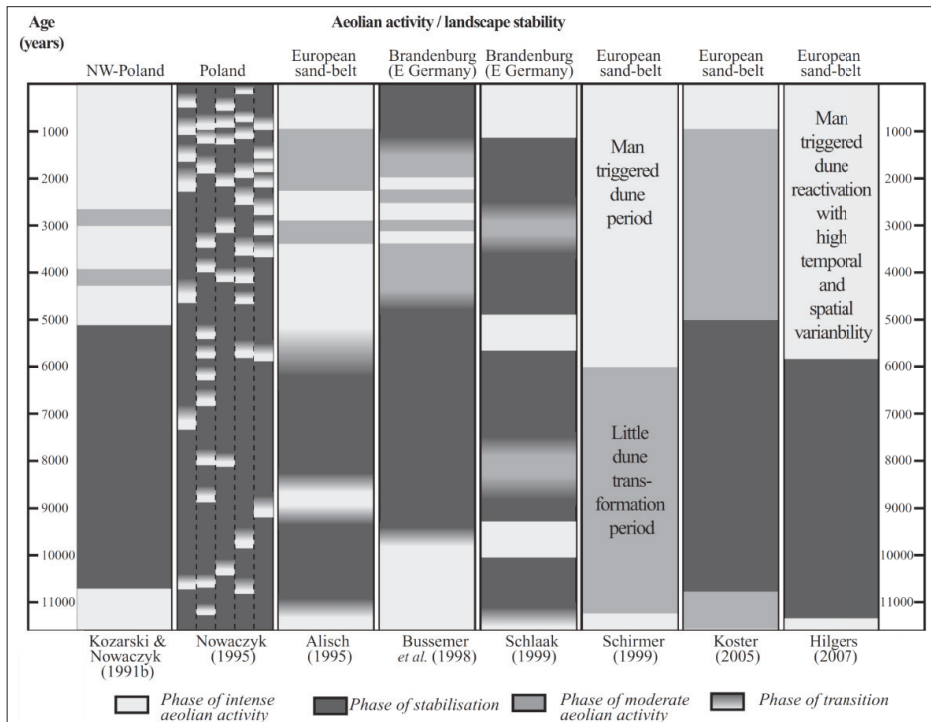


Figure 5.1.1 Comparison of Holocene aeolian activity and landscape stability in the European sand-belt and its sub regions (after Tolksdorf & Kaiser, 2012; modified).

Tolksdorf and Kaiser (2012) study based on dated aeolian sands and palaeo-surfaces shows complex phases of aeolian activity and landscape stabilization, during the Holocene. Figure 5.1.1. shows general comparison of aeolian activity and stability phases in European sand belt. Distinguished phases have no relationship, this can be caused by human impact or natural processes such as natural fires and windthrow.

5.2 Ecogeology and dune formation

Oldest palaeosols were not found during this survey, but dates obtained in the literature suggests that oldest palaeosol samples dates approximately to 5700 years BP. Considering that development of the soil horizon in organic-poor sand takes up to 800 years (Peyrat, 2007), it is possible to maintain, that palaeosol started to form more than 6500 years BP. This data consistent with archaeological findings dated to 5370 – 5800 years BP (archaeological data presented in the annex No.4, 47 – 53). Archaeological data consist of two samples taken from fireplace dated approximately to 5300 – 5400 years BP (Rimantienė, 1999) and five samples of ceramic shards dated to 5600 – 5800 years BP (Piličiauskas *et al.*, 2011). Hence, by this time human settlements already existed in the Curonian Spit. According aforementioned data, by 5800 years BP, soil forming processes were already advanced and accumulated enough organic-rich material for a higher plant vegetation.

Modelling of ancient dune ridge in the Grey (Dead) Dune massif shows that until 500 years BP eastern base of the Curonian Spit dune massifs remained in approximately the same position, close to the central part of the present Curonian Spit, i.e. along the present western (wind-ward) slope of the Great Dune Ridge (Figure 5.2.1). Ancient dune massifs evenly covered the entire area of the Curonian Spit. The Great Dune Ridge has formed only starting from the XVI century due to an extremely high aeolian activity influenced by destructive human practices. How it happened?

According to historical data, at around 1675 AD more than 50 % of the Curonian Spit was covered with vegetation or forest. Less than a hundred years later (AD 1733/1760) deforestation began initiated by pasturing, combined with forest fires and, possibly, timber export, which may have resulted in a new erosion and sand dune activity until a reforestation project initiated around 1850 AD (Moe *et al.*, 2005, Savukyniene *et al.*, 2003) (Figure 5.2.1). As a result, a number of villages located along the Curonian Lagoon coast was buried by advancing dunes and have to move from place to place (Bučas, 2001). For example, in 1786 the shifting dunes reached the village Karvaičiai (Karwaiten) and by the year 1797 the village was completely buried under the sand and became one of the 14 Curonian Spit villages destroyed by to shifting dunes (<http://genwiki.genealogy.net>).

Thus, as a result of human activity the ecogeological situation (ecogeology is a discipline which examines the interaction between the geological environment and the human living environment) was essentially changed and from during XVII – XIX centuries dramatic changes occurred in the Spit: parabolic dunes which dominated since the Holocene were destroyed by shifting sand and replaced by shifting barchans. As the chain of shifting barchans was moving eastwards, the interface between dune ridge and the lagoon (i.e. an area entitled as a Lagoon Palvė) rapidly decreased. There are not enough geological data precisely determinate what was the geomorphological situation

5. Discussion

along the lagoon coast before these events. According to some palaeo-geographic reconstructions (Figure 5.2.2) it was a wide Lagoon Palvè (occupying about half the width of the Spit) were a number of settlements were located (Povilanskas, 2009).

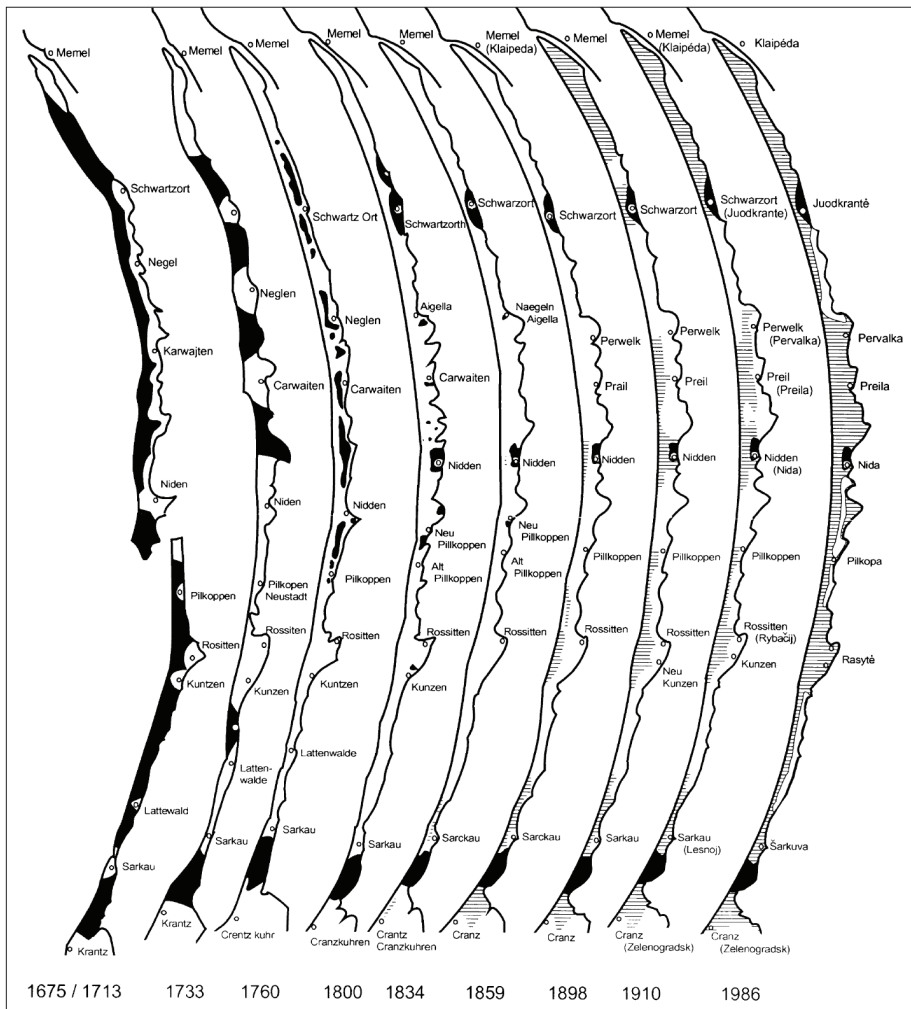


Figure 5.2.1. The history of deforestation and reforestation of the Curonian Spit from 1675 to 1986 AD. Black areas – old forest, hatched area – reforestation (Savukynienė et al., 2003).

5. Discussion

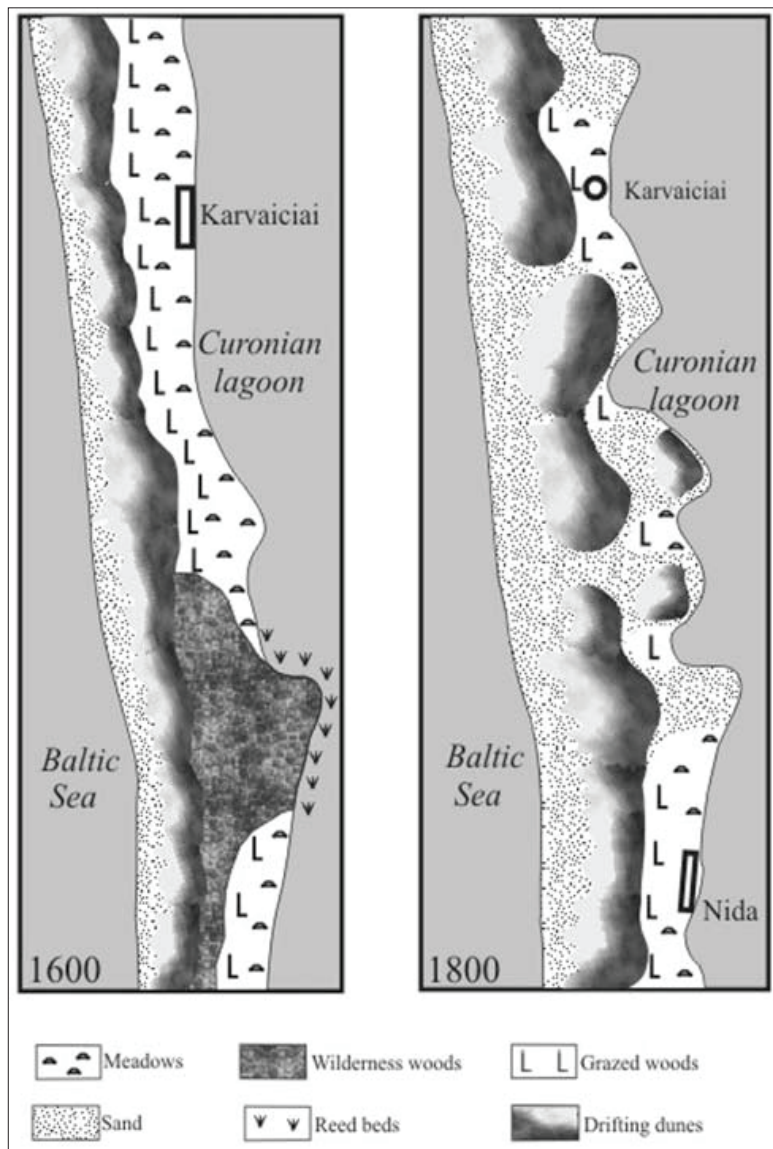


Figure 5.2.2. Landscape development in the Curonian Spit, 1600–1800 AD (Povilanskas, 2009).

The later, starting from the end of the XVIII century, reconstruction of the Curonian Spit dunes development, based on the more reliable cartographic materials and other historical documents (Wichdorff, 1919; Kazakevicius, 1989-1990; Povilanskas, 2009; and others), is more obvious and does not cause any major discussions.

Conclusions

1. Palaeosols in the Dead (Grey) Dune massif have survived fragmentarily, mainly in the southern part of the massif, along the western (windward) slope of the Great Dune Ridge.
2. The results of the radiocarbon dating of palaeosols range from modern times to approximately 5700 calendar years BP. The detailed analysis of the received data did not allow distinguishing separate soil-forming generations and supported the idea of V. Gudelis (1998a) that it was only one long continuous period of permanent formation of palaeosols. A bigger amount of radiocarbon (^{14}C) analysis collected during the latest several decades enable to extend the beginning of this period from 4000 to 6500-6700 calendar years BP. An uneven distribution of radiocarbon (^{14}C) ages of palaeosols can be explained by the fact that the palaeosols of particular age were better developed, better survived during the activation of aeolian processes, or are more often outcropping in the recent aeolian relief: as a result, the unequal number of samples was collected from the different palaeosol layers during various studies.
3. According to the palaeo-reconstructions, the eastern base of the former Curonian Spit dunes was at approximately the same position during the last 5000 years, which was near the central (axial) part of the Spit, along the western (windward) slope of the present Great Dune Ridge. The palaeogeographic

Conclusions

reconstruction of the eastern base of palaeo-dune massif indicates that over the time span of 2500 years (from 3500 to 1000 years BP) dunes shifted only a few hundred meters (approximately 180 m), whereas over the last 1000 years dunes moved nearly 500 meters.

4. The reactivation of aeolian processes and re-deposition of dunes in the Curonian Spit started at least in the mid-Holocene and have not been linked with long-lasting climate fluctuations that occurred during this period. The aeolian reactivations were stimulated by the local factors (e.g., forest fires and deforestation), covered limited areas, the sand of dunes was dislocated from a few to few tens of meters, and it lasted no longer than for one or two centuries.
5. The ground-penetrating radar images and magnetic susceptibility trends within aeolian sediments that separate palaeosols of different age demonstrate the variations in heavy-mineral content that can be related to palaeoclimatic conditions (relatively calm, windy, or stormy near-surface regime) that existed during the dune accumulation.
6. The Great Dune Ridge formed starting only at the end of XVI century due to an extremely high aeolian activity influenced by the destructive human practices – the essential changes of the ecogeological situation in the entire Curonian Spit. As a result, the parabolic dunes which dominated since the Holocene were destroyed by shifting sand and transformed into the single dune ridge.

References

- Alisch, M. 1995. Das äolische Relief der mittleren Oberen Allerniederung (Ostniedersachsen). Spät- und postglaziale Morphogenese, Ausdehnung und Festlegung historischer Wehsande, Sandabgrabungen und Schutzaspekte. Kölner Geographische Arbeiten 62, 176 pp.
- Alley, R. B. 2004. GISP2 Ice Core Temperature and Accumulation Data. IGBP PAGES/World Data Center for Palaeoclimatology Data Contribution #2004-013. NOAA/NGDC Palaeoclimatology Program, Boulder CO, USA.
- Berendt, G. 1869. Geologie des Kurischen Haffes und seiner Umgebung. Könisberg.
- Bitinas, A., Mažeika, J., Buynevich, I. V., Damušytė, A., Molodkov, A., Grigienė, A. 2017. Constraints of Radiocarbon Dating in Southeastern Baltic Lagoons: Assessing the Vital Effects. In: J. Harff, K. Furmańczyk and H. van Storch (eds.). *Coastline Changes of the Baltic Sea from South to East – Past and Future Projections*. Springer, 137–171.
- Bitinas, A., Damušytė, A., Molodkov, A. 2011. Geological structure of the Quaternary sedimentary sequence in the Klaipėda Strait, southeastern Baltic. In: J. Harff, S. Bjørck and P. Hoth (eds.). *Baltic Sea Basin Book Series: Central and Eastern European Development Studies*, Springer, 133–146.
- Bitinas A., Damušytė A., Stančikaitė M. 2000. Antro lygio kvartero geologinis kartografiavimas 1:50 000 masteliu Šilutės plote. Lietuvos geologijos tarnyba, Vilnius.

References

- Blazhchishin, A. I. 1998. Palaeogeography and evolution of late Quaternary sedimentation in the Baltic Sea. Kaliningrad. Jantarnyj Skaz (In Russian).
- Borowka, R. K. 1975. Problem of the morphology of fossil dune forms on the Łeba bar. *Quaestiones Geographicae*, 2, 39–51.
- Boyle, R. W. 1982. Geochemical prospecting for thorium and uranium deposits. Developments in Economic Geology, Vol 16. Elsevier, Amsterdam (Netherlands).
- Bronk Ramsey, C. 2001. Development of the radiocarbon calibration program OxCal. *Radiocarbon*, 43, 2A, 355–63.
- Bučas, J. 2001. Curonian Spit National Park. Savastis, Vilnius. (In Lithuanian with English summary).
- Buynevich, I. V., Savarese, M., Curran, H. A., Bitinas, A., Glumac, B., Pupienis, D., Kopczinski, K., Dobrotin, N., Gnivecki, P., Park Boush, L, and Damušytė, A. 2017. Sand incursion into temperate (Lithuania) and tropical (the Bahamas) maritime vegetation: georadar visualization of target-rich aeolian lithosomes. *Estuarine, Coastal and Shelf Science*, 195 (5), 69–75.
- Buynevich, I. V. 2012. Morphologically induced density lag formation on bedforms and biogenic structures in aeolian sands. *Aeolian research*, 7, 11–15.
- Buynevich, I. V., Bitinas, A., Damušytė, A., Pupienis, D. 2010. Unique Baltic outcrops reveal millennia of ecological changes. *EOS Trans. Am. Geophys. Union* 91(11), 101–102.
- Buynevich, I. V., Bitinas, A., Pupienis, D. 2007a. Lithological anomalies in a relict coastal dune: Geophysical and palaeoenvironmental markers. *Geophysical Research Letters*, 34, L09707.
- Buynevich, I. V., Bitinas, A., Pupienis, D. 2007b. Reactivation of coastal dunes documented by subsurface imaging of the Great Dune Ridge, Lithuania. *Journal of Coastal Research*, SI 50, 226–230.
- Buynevich, I. V., Jol, H. M., FitzGerald, D. M. 2009. Coastal Environments. In: Jol, H. M. (ed.). GPR: Radar Theory and Applications. Elsevier, 299–322.
- Chichiagova, O. N., Cherkinski, A. E. 1988. Radiocarbon investigations in geographical survey. In: The materials of Radiometric Laboratory of Geographical Institute of Academy of Science of USSR, Part 1. Moscow, 6–79. (In Russian)
- Damušytė A. 2011. Post-glacial geological history of the Lithuanian coastal area. Summary of doctoral dissertation, Physical sciences, geology (05P). Vilnius.
- Daniels, D. J. 1996. Surface – penetrating radar. The Institution of Electrical Engineers, UK.
- Fedorowicz S., Zielinski P., Wysiecka G. and Holub B. 2012. Phases of aeolian accumulation on the Vistula Spit (Southern Baltic Sea) in the light of TL dating and analysis of a digital elevation model. *Geological Quarterly*, 56 (2), 345–352.
- Gaigalas, A., Banys, J., Gulbinskas, S., Savukyniene, N. 1991. The radiocarbon age of the buried soils in the dunes of the Kuršių Nerija spit. In: Gaigalas, A. (ed.). Geo-

References

- chronological and isotopic-geochemical investigations in the Quaternary geology and archaeology. Vilnius, 8–13. (In Russian with English summary).
- Gaigalas, A., Pazdur, A. 2008. Chronology of buried soils, forest fires and extreme migration of dunes on the Kuršių Nerija spit (Lithuanian coast). Landform Analysis, 9, 187–191.
- Gerasimov, I. P., Zavelski, F.S. 1980. Radiocarbon investigations in the Radiometric Laboratory of Geographical Institute of Academy of Science of USSR. Bulletin of Quaternary Research Commission, 50, 206–213. (In Russian)
- Gudelis, V. 1989–1990. Lithology of old parabolic dunes of the Curonian Spit and the coastal dynamics of the late Litorina Sea. The Geographical Yearbook, 25–26, 13–17. (In Lithuanian)
- Gudelis, V. 1998a. The Lithuanian offshore and coast of the Baltic Sea. Lithuanian Academy of Sciences Monograph, Vilnius. (In Lithuanian)
- Gudelis, V. 1998b. A Catastrophic Dune Forest Fire on the Kuršių Nerija spit (Lithuanian Coast) and its Impact on the Coastal Population in the Late Neolithic Time. Pact, 54, 45–50.
- Gudelis, V., 1955. Lietuvos TSR Baltijos pajūrio geologinės raidos vėlyvajame glaciiale ir postglaciale (holocene) pagrindiniai etapai. Vilniaus Valst. V. Kapsuko varo universiteto mokslo darbai, VII, Biologijos, geologijos ir geografijos mokslų serija, III, 119–139.
- Gudelis, V., Klimaviciene, V., Savukyniene, N. 1993. Old buried forest soils in the Kuršiu Nerija spit and their palynological pattern. In: Gudelis, V. (ed.) Baltic Sea coastal dynamics and palaeogeography issues, 2, Academia, Vilnius, 64–93. (In Lithuanian with English summary).
- Gudelis, V., Michaliukaite, E. 1976. The old parabolic dunes of the Curonian Spit. Geographia Lituanica, Vilnius, 59–63. (In Russian).
- Guobytė, R. 2007. Lietuvos kvartero geologinio ir geomorfologinio žemėlapių legendos 1:50 000 masteliu. Vilnius, Lietuvos geologijos tarnyba, 43 p.
- Gupta, S. K., Polach, H. A. 1985. Radiocarbon Dating Practices at ANU. Canberra: Radiocarbon Laboratory, Research School of Pacific Studies, Australian National University, Canberra. 176 pp.
- Hilgers, A. 2007: The chronology of Late Glacial and Holocene dune development in the northern Central European lowland reconstructed by optically stimulated luminescence (OSL) dating. Ph.D. thesis, University of Cologne, 353 pp.
- Kabailienė, M. 1959a. Augalijos raida vėlyvajame ledynmetyje ir poledynmetyje Lietuvos ir pietinės Latvijos pajūrio zonoje. Geografinis metraštis, 12, 477–505.
- Kabailienė, M. 1959b. Lietuvos ir pietinės Latvijos Baltijos pajūrio raida vėlyvajame ledynmetyje ir poledynmetyje diatomėjų floros tyrimų duomenimis. Lietuvos TSR MA Geologijos ir geografijos institutas, Moksliniai pranešimai, Geologija, Geografija, X, 2 sąs., 175–213.

References

- Kabailienė, M., 1967. The development of the spit of Kuršių nerija and the Kuršių marios bay. In: Kabailienė, M. (ed.), On Some Problems of Geology and Palaeogeography of the Quaternary Period in Lithuania, Transactions, vol. 5. Mintis, Vilnius, 181-207. (In Russian with Lithuanian and English summaries).
- Kabailienė, M., 1995. Lagoon marl exposures at Nida. In: Kabailienė, M. (Ed.), Natural Environment, Man and Cultural History on the Coastal Areas of Lithuania: Excursion Guidebook of the NorFa Course in the Baltic Countries, September 20-22, 1995, Vilnius, 40-43.
- Kaminskas, D., Rudnickaitė, E., Vaikutienė, G., Bitinas, A., Grigienė, A., Buynevich, I. V., Damušytė, A., Pupienis, D., Šnkūnas, P. 2018. Middle and Late Holocene palaeoenvironmental developement of the Curonian Lagoon, Lithuania. Quaternary International.
- Kaminskas, D., Bitinas, A., 2013. Rare earth elements of Holocene sediments in the south-Eastern baltic region (Nida VI borehole, Lithuania). *Geologija*, 55 (1) (81), 1-7.
- Kazakevicius, S. 1989-1990. Dynamics of the Curonian Spit coastal development (cartographic analysis). *Geographical Yearbook*, 25-26, 46-56.
- Koster, E. A. 2005. Recent advances in luminescence dating of Late Pleistocene (cold-climate) aeolian sand and loess deposits in Western Europe. *Permafrost and Periglacial Processes*, 16, 131-143.
- Kovaliukh, N. N., Skripkin, V.V. 1994. An Universasl technology for oxidation of carbon-containing materials for radiocarbon dating. In: Abstarct and papers of conference on geochronology and dendrology of old town>s and radiocarbon dating of archaeological findings. Vilnius, Lithuania, 31 October - 4 November. Vilnius University press, 37-42.
- Kozarski, S., Nowaczyk, B. 1991a. The late Quaternary climate and human impact on aeolian processes in Poland. *Zeitschrift für Geomorphologie Neue Folge*, Supplement 83, 29-37.
- Labuz, T. A., Grunewald, R., Bobykina, V., Chubarenko, B., Česnulevičius, A., Bautrėnas, A., Morkūnaitė, R., Tõnisson, H. 2018. Coastal dunes of the Baltic Sea shores: a review. *Quaestiones Geographicae*, 37(1), 47-71.
- Lavrushin, J. A. 1993. Deglacjacja ostatniego lądolodu na obszarze Perybałtickim. In: Florek, W (ed). *Geologia i geomorfologia środkowego Pobrzeża i południowego Bałtyku*. Wyższa Szkoła Pedagogiczna w Słupsku, Słupsk, 37-57.
- Libby, W. F., Anderson, E. C., Arnold, J. R. 1949. Age determination by radiocarbon content: world-wide assay of natural radiocarbon. *Science*, 109, Issue 2827, 227-228.
- Linčius, A. 1993. The secret of the lagoon marl, *Geologijos akiračiai*, 1 (9), 29-33. (In Lithuanian with English summary).
- Mauring, E., Ronning, J. S., Gellein, J. 1994. Geophysical surveyng of five locations of Lithuania. NGU Report No. 94.092, Trondheim.
- Michaliukaite, E. 1962. The old dunes and palaeosols of the Curonian Spit. The *Geographical Yearbook* 5, 377-390. (In Lithuanian)

References

- Moe, D., Savukyniene, N., Stancikate, M. 2005. A new 14C (AMS) date from former heathland soil horizons at Kuršiu Nerija, Lithuania. *Baltica*, 18, 23–28.
- Molodkov, A., Bitinas, A., Damušytė, A. 2010. IR-OSL studies of till and inter-till deposits from the Lithuanian Maritime Region. *Quaternary Geochronology*, 5, 263–268.
- Molodkov A, Bitinas A. 2006. Sedimentary record and luminescence chronology of the Lateglacial and Holocene Aeolian sediments in Lithuania. *Boreas*, 35, 244 – 254.
- Nowaczyk, B. 1995. The age of dunes in Poland – selected problems. *Quaestiones Geographicae*, SI 4, 233–239.
- Paul, K. H. 1944. Morphologie und Vegetation der Kurischen Nehrung. *Nova Acta Leopoldina*, 132 (96), Halle (Sante). (In German)
- Peyrat, J. 2007. Development, properties and classification of dune soils in the Curonian Spit National Park, Russian part. *Geologija*, 59, 59–64.
- Piličiauskas, G. 2015. Coastal Lithuania during the Neolithic. In.: A hundred years in the archeological discoveries in Lithuania, 96–109.
- Povilanskas, R. 2009. Spatial diversity of modern geomorphological processes on a Holocene Dune Ridge on the Curonian Spit in the South-East Baltic. *Baltica*, 22 (2), 77–88.
- Povilanskas, R., Baghdasarian, H., Arakeylyan, S., Satkunas, J., Taminskas, J. 2009. Secular morphodynamic trends of the Holocene dune ridge on the Curonian Spit. *Journal of Coastal Research*, 25, 209–215.
- Preusser, F., Degering, D., Fuschs, M., Hilgers, A., Kaderet, A., Kalsen, N., Krbetshek, M., Richter, D., Spencer, J. 2008. Luminescence dating: basics, methods and applications. *Eiszeitalter und Gegenwart Quaternary Science Journal*, 57/1-2, 95–149.
- Pupienis, D., Buynevich, I.V., Ryabchuk, D., Jarmalavičius, D., Žilinskas, G., Fedorovič, J., Kovalevac, O., Sergeevic, A., Cichon-Pupienis, A. 2017. Spatial patterns in heavy-mineral concentrations along the Curonian Spit coast, southeastern Baltic Sea. *Estuarine, Coastal and Shelf Science*, 195, 41–50.
- Raukas, A. 2011. Evolution of aeolian landscapes in North-Eastern Estonia under environmental changes. *Geographia Polonica*, 84, SI Part 1, 117–126.
- Reimer, P. J., Baillie, M. G. L., Bard, E., Bayliss, A., Beck, J. W., Blackwell, P. G., Bronk Ramsey, C., Buck, C. E., Burr, G. S., Edwards, R. L., Friedrich, M., Grootes, P. M., Guilderson, T. P., Hajdas, I., Heaton, T. J., Hogg, A. G., Hughen, K. A., Kaiser, K. F., Kromer, B., McCormac, F. G., Manning, S. W., Reimer, R. W., Richards, D. A., Southon, J. R., Talamo, S., Turney, C. S. M., Van der Plicht, J., Weyhenmeyer, C. E. 2009. IntCal09 and Marine09 radiocarbon age calibration curves, 0–50,000 years cal BP. *Radiocarbon*, 51, (4), 1111–1150.
- Rimantiene, R. 1999. Curonian Spit at a glance of an archaeologist. Academy of Arts Press, Vilnius. (In Lithuanian)
- Savukyniene, N., Moe, D., Usaityte, D. 2003. The occurrence of former heathland vegetation in the coastal areas of the south-east Baltic sea, in particular Lithuania: a review. *Veget Hist Archaeobot*, 12, 165–175.

References

- Schlaak, N. 1999: Typical Aeolian Sand Profiles and Palaeosols of the Glien Till Plain in the Northwest of Berlin. In Schirmer, W. (ed.). Dunes and Fossil Soils, GeoArchaeoRhein 3, 97–105.
- Schumann, J. 1861. Die Wandernden Dunen auf Kurischen Nehrung. N. Preuss Prov., Blatt., 8. (In German).
- Sergeev, A., Sivkov, V., Zhamoida, V., Ryabchuk, D., Bitinas, A., Mažeika, J. 2015. Holocene organic-rich sediments within the Curonian Spit coast, the south-eastern Baltic Sea. *Baltica*, 28 (1), 41–50.
- Sergeev, A. Y., Zhamoida, V. A., Ryabchuk, D. V., Buynevich, I. V., Sivkov, V. V., Dorokhov, D. V., Bitinas, A., Pupienis, D. 2016. Genesis, distribution and dynamics of lagoon marl extrusions along the Curonian Spit, southeast Baltic Coast. *Boreas*, 46, 69–82.
- Starkel, L. (ed.). 1990. Evolution of the Vistula river valley during the last 15000 years Vol. III. Synthesis, Prace Geograficzne IGiPZ PAN, Special Issue 5, Warsaw.
- Šimoliūnas J., 1939. Klaipėdos uostas. Kaunas, Technika.
- Tamkutonis, S. 1960. Gintaro paieškos šiaurinėje Kuršių marių dalyje (Nidos paieškinės partijos ataskaita už 1959 m.). Geologinė paieškų-žvalgybos ekspedicija, Inv. Nr. 1419, Vilnius.
- Tolksdorf, J. F. and Kaiser, K. 2012. Holocene aeolian dynamics in the European sand-belt as indicated by geochronological data. *Boreas*, 41, 408–421.
- Tornquist, A. 1910. Geologie von Ostpreussen. Berlin.
- Van Dam, R. L., Hendrickx, J. M. H., Cassidy, N. J., North, R. E., Dogan, M., Borchers, B. 2013. Effects of magnetite on high-frequency ground-penetrating radar. *Geophysics*, 78, No. 5.
- Valiukevičienė, O., Gasiūnienė, V. E. 1995. Ar Lietuva gintaro šalis? Lietuvos geologijos tarnybos informacinis leidinys, Vilnius.
- Viliamas, VI. 1932. Kuršių nerija: slenkančios kopos ir jų įtaka sodyboms. Sakalas, Kaunas.
- Wentworth, C. K. 1922. A scale of grade and class terms of clastic sediments. *J. Geol.*, 30, 377 – 390.
- Wichdorff, von H. 1919. Geologie der Kurischen Nehrung. Preuss. Abh. D. Preuss Geol. Landesanstalt, Neue Folge, H. 77.
- Rimša, V. 1994. Gintaro telkinių paieškos šiaurinėje Kuršių marių dalyje bei Juodkrantės gintaro telkinio įvertinimus. AB "Vilniaus geologija". Inv. Nr. 4347, Vilnius. 137 pp.
- Šimėnas J. J. 1989. Baltijos jūros dugno geologinė sandara (ataskaita apie geologinio kartagrofavimo M 1:200000 rezultatas Baltijos jūros šelfo tarybinėje dalyje, prie LTSR teritorijos, topografiniuose lapuose N-34-II, N-34-III ir N-34-IV, 1986-89 metais). Naftos žvalgybos ekspedicija, Inv. Nr. 4038, Vilnius.
- <http://genwiki.genealogy.net/Karwainen>, 2/2/2018
- <https://www.geoportal.lt>, 2/28/2018
- <https://www.radiocarbon.com>, 1/25/2018

Annexes

Annexes

Annex No.1. Borehole No. 30 used in GPR data interpretation

Borehole no.		30		OSL dates, years
Elevation (m, a.s.l)		21		
Bottom depth, m	Index	Index in Fig. 2.2	Lithology	
14.1	v IV	A	Various sand	≥ 500
22.7	m IV	B	Fine grained sand	≥ 1000
26.7	m IVPL	C	Various sand	≥ 1500

Annex No.2. Control boreholes used to identify GPR reflections

Borehole No.	Coordinates WGS84		Detected horizon
B1	21° 04' 38.3261" E	55° 26' 08.4781" N	Coarse sand layer
B2	21° 04' 42.0000" E	55° 26' 09.0000" N	Palaeosol, dated, Vs-2245
B3	21° 05' 00.6913" E	55° 26' 05.4871" N	Palaeosol
B4	21° 04' 39.1015" E	55° 26' 25.2147" N	Palaeosol
B5	21° 04' 42.5562" E	55° 26' 25.1400" N	HMC
B6	21° 04' 43.0781" E	55° 26' 25.0395" N	Palaeosol
B7	21° 04' 50.4182" E	55° 26' 55.8639" N	Different direction slipface
B8	21° 04' 58.8560" E	55° 26' 55.4751" N	Palaeosol
B9	21° 05' 06.4480" E	55° 26' 54.8517" N	Different direction slipface
B10	21° 05' 32.2883" E	55° 27' 52.0355" N	Palaeosol, dated, Vs-2250
B11	21° 05' 42.1291" E	55° 28' 24.8717" N	Coarse sand layer
B12	21° 05' 13.4776" E	55° 27' 12.3667" N	HMC
B13	21° 06' 06.0745" E	55° 29' 00.0583" N	Different direction slipface
B14	21° 06' 16.8910" E	55° 29' 48.1984" N	Different direction slipface
B15	21° 06' 33.2443" E	55° 30' 34.8832" N	Coarse sand layer

Annexes

Annex No.3. Borehole No. 18685 used in GPR data interpretation

Borehole no.		18685	
Coordinates		21° 04' 08" E 55° 26' 30" N	
Elevation (m, m.s.l.)		2.5	
Bottom depth, m	Index	No. in Fig 3.7.2	Lithology
2.5	v IV	1	Aeolian sand. Various sand
12	m IVL	2	Marine sand. Various sand
13	l IV	3	Gyttja
28	lg III B	4	Glaciocustrine sand. Fine-grained sand
31	lg III B	5	Glaciocustrine clay
57.8	g II md	-	Moraine. loam, clay

Annex No.4. Results of radiocarbon (¹⁴C) dating of palaeosols in the Curonian Spit

No.	Lab. index	Coordi-nates WGS84 / location	Sampling site, Palaeosol code, depth, etc.	Method, analysed matter	Project / publication	¹⁴ C age, years (BP) (±1s)	Calibrated age (1s range)
1.	Vs-2088	Vingio dune	“Oldest” palaeosol	Bulk, soil humus	This study	3180±120	3560-3316 BP (59.2%) 3310-3262 BP (9.0 %)
2.	Vs-2214	55° 26' 42" 21° 04' 53"	Palaeosol-1	Bulk, soil humus	-,-,-	3545±70	3913-3720 BP (68.2%)
3.	Vs-2216	55° 26' 55" 21° 04' 55"	Palaeosol-2	Bulk, charcoal	-,-,-	675±70	606-556 BP (36.9 %) 668-624 BP (31.3%)
4.	Vs-2239	55° 26' 28" 21° 04' 56"	Palaeosol, G	Bulk, wood	-,-,-	420±40	518-459 BP (63.1%) 348-340 BP (5.1%)
5.	Vs-2240	55° 26' 35" 21° 04' 48"	Palaeosol, K	Bulk, charcoal	-,-,-	1055±195	1174-788 BP (68.2%)

Annexes

No.	Lab. index	Coordinates WGS84 / location	Sampling site, Palaeosol code, depth, etc.	Method, analysed matter	Project / publication	¹⁴ C age, years (BP) ($\pm 1s$)	Calibrated age (1s range)
6.	Vs-2241	55° 26' 29" 21° 04' 45"	Palaeosol, F	Bulk, charcoal	-,-	3455±60	3778-3678 BP (40.5%) 3828-3788 BP (16.5%) 3669-3640BP (11.3%)
7.	Vs-2242	55° 27' 40" 21° 05' 31"	Palaeosol-13, exposure, depth 0.6 m	Bulk, wood	-,-	605±50	648-584 BP (54.2%) 568 550 BP (14.0%)
8.	Vs-2243	55° 26' 31" 21° 04' 49"	Palaeosol, I	Bulk, charcoal	-,-	1225±60	1184-1070 BP (52.0%) 1240-1204 BP (16.2%)
9.	Vs-2244	55° 26' 24" 21° 04' 42"	Palaeosol, D	Bulk, charcoal	-,-	765±110	796-640 BP (60.4%) 590-564 BP (7.0%) 891-887 BP (0.9%)
10.	Vs-2245	55° 26' 09" 21° 04' 42"	Borehole No. 2, depth 1.7 m	Bulk, soil humus	-,-	1735±150	1826-1516 BP (63.3%) 1458-1442 BP (2.3%) 1860-1850 BP (1.4%) 1432-1422 BP (1.2%)
11.	Vs-2249	55° 26' 53" 21° 05' 02"	Palaeosol, N	Bulk, soil humus	-,-	1785±80	1818-1684 BP (46.6%) 1678-1615 BP (21.6%)
12.	Vs-2250	55° 27' 49" 21° 05' 32"	Palaeosol-21, exposure, depth 0.6 m	Bulk, soil humus	-,-	410±95	523-426BP (41.4%) 392-319 BP (26.8%)
13.	Vs-2251	55° 27' 41" 21° 05' 22"	Palaeosol, V	Bulk, soil humus	-,-	930±90	927-765 BP (68.2%)

Annexes

No.	Lab. index	Coordi-nates WGS84 / location	Sampling site, Palaeosol code, depth, etc.	Method, analysed matter	Project / publication	¹⁴ C age, years (BP) ($\pm 1s$)	Calibrated age (1s range)
14.	Vs-1764	Lesnoje	Palaeosol TN 21/1	Bulk, soil humus	Bitinas, pers. com.	2430±50	2494-2357 BP (50.5%) 2682-2640 BP (14.1%) 2610-2599 BP (3.6%)
15.	Vs-1763	-,-	Palaeosol TN 21/2	Bulk, soil humus	-,-	1510±90	1422-1318 BP (43.6%) 1515-1459 BP (21.1%) 1442-1432 BP (3.5%)
16.	Vs-1768	-,-	Palaeosol TN 21/3	Bulk, soil humus	-,-	1780±80	1815-1614 BP (68.2%)
17.	Not specified	Dead (Grey) dunes	Palaeosol, NP-V4	AMS, charcoal	Buynevich, pers. com	3400±35	3692-3612 BP (62.3%) 3600-3590 BP (5.9%)
18.	-"-	-"-	Palaeosol, KNP-V4A	AMS, charcoal	-,-	2430±25	2486-2362 BP (66.9%) 2648-2645 BP (1.3%)
19.	-"-	-,-	Palaeosol 1	AMS, charcoal	-,-	780±30	725-682 BP (68.2%)
20.	-"-	-,-	Palaeosol 3	AMS, charcoal	-,-	3130±40	3399-3327 BP (60.3%) 3286-3270 BP (7.9%)
21.	-"-	-,-	Palaeosol 4	AMS, soil humus	-,-	4990±40	5748-5655 BP (62.4%) 5844-5830 BP (5.8%)
22.	-"-	-"-	Palaeosol	AMS, charcoal	-,-	660±30	587-565 BP (35.1%) 665-644 BP (33.1%)
23.	-"-	-,-	-"-	AMS, charcoal	-,-	1330±35	1298-1258 BP (55.0%) 1202-1186 BP (13.2%)

Annexes

No.	Lab. index	Coordinates WGS84 / location	Sampling site, Palaeosol code, depth, etc.	Method, analysed matter	Project / publication	¹⁴ C age, years (BP) ($\pm 1s$)	Calibrated age (1s range)
24.	12919	Vinkis dune	Vinkis 2, depth 0.75 m	Bulk, charcoal	Gaigalas & Pazdur, 2008	420 \pm 45	520-455BP (59.9%) 348-334BP (8.3%)
25.	12920	-,-	Vinkis 3, depth 0.75 m	Bulk, soil humus	-,-	970 \pm 50	870-797 BP (45.0%) 932-898 BP (23.2%)
26.	17430	-,-	Vinkis 4, depth ~3 m	Bulk, wood	-,-	125 \pm 95	150-56 BP (30.5%) 270-186 BP (26.8%) 46-12 BP (11.0%)
27.	GdS-570	Naglis dune	Naglis 1, depth 0.3 m	Bulk, soil humus	-,-	1050 \pm 30	974-930 BP (68.2%)
28.	GdS-571	-,-	Naglis 2, depth 0.43 m	Bulk, charcoal	-,-	590 \pm 30	637-592 BP (51.5%) 562-547 BP (16.7%)
29.	GdS-572	-,-	Naglis 3, depth 0.49	Bulk, wood	-,-	630 \pm 30	599-560 BP (42.1%) 655-631 BP (26.1%)
30.	Not specified	Dead (Grey) dunes	Palaeosol P1	AMS, charcoal	Buynevich <i>et al.</i> , 2007	850 \pm 35	792-725 BP (68.2%)
31.	-,-	-,-	Palaeosol P2	AMS, charcoal	-“-	1350 \pm 45	1310-1256 BP (57.0%) 1202-1185 BP (9.9%) 1247-1244 BP (1.3%)
32.	TUa-4763	55°28' 25" 21°05' 37"	Exposure, depth 4-10 cm	AMS, charcoal	Moe <i>et al.</i> , 2005	735 \pm 40	698-658 BP (68.2%)

Annexes

No.	Lab. index	Coordi-nates WGS84 / location	Sampling site, Palaeosol code, depth, etc.	Method, analysed matter	Project / publication	¹⁴ C age, years (BP) ($\pm 1s$)	Calibrated age (1s range)
33.	TUa-4762	-,-	Exposure, depth 47-59 cm	AMS, charcoal	-,-	1900 \pm 40	1898-1813 BP (67.0%) 1750-1746 BP (1.2%)
34.	Not specified	Pervalka	Palaeosol 3	Bulk, soil humus	Gaigalas <i>et al.</i> , 1991	560 \pm 70	641-590 BP (37.5%) 564-523 BP (30.7%)
35.	-,-	-,-	Palaeosol 4	Bulk, soil humus	-,-	1040 \pm 90	1060-902 BP (56.2%) 864-828 BP (9.1%) 812 800 BP (2.9%)
36.	-,-	Nida	Palaeosol	Bulk, wood	-,-	3470 \pm 70	3834-3680 BP (60.0%) 3666-3642 BP (8.2%)
37.	-,-	Pilkopa	-,-	Bulk, wood	-,-	290 \pm 90	476-284 BP (64.6%) 167-154 BP (3.6%)
38.	-,-	-,-	-,-	Bulk, wood	-,-	340 \pm 90	480-310 BP (68.2%)
39.	-,-	Vingiakopė	Palaeosol 3	Bulk, peat	-,-	1200 \pm 90	1186-1054 BP (47.5%) 1256-1202 BP (15.9%) 1027-1010 BP (4.8%)
40.	-,-	SW from Juodkrante	Palaeosol	Bulk, wood	Gerasimov <i>et al.</i> , 1980; Chichagova & Cherka-sin, 1988	500 \pm 70	632-598 BP (16.4%) 560-494 BP (51.8%)
41.	-,-	Vingiakope	Palaeosol I	Bulk, wood	-,-	630 \pm 90	664-550 BP (68.2%)

Annexes

No.	Lab. index	Coordinates WGS84 / location	Sampling site, Palaeosol code, depth, etc.	Method, analysed matter	Project / publication	¹⁴ C age, years (BP) ($\pm 1s$)	Calibrated age (1s range)
42.	-,-,-	-,-,-	Palaeosol II	Bulk, wood	-,-,-	1140 \pm 90	1145-965 BP (64.5%) 1170-1158 BP (3.7%)
43.	-,-,-	-,-,-	Palaeosol III	Bulk, wood	-,-,-	2960 \pm 90	3260-2996 BP (68.2%)
44.	-,-,-	-,-,-	Palaeosol IV	Bulk, wood	-,-,-	4025 \pm 90	4645-4410 BP (58.4%) 4801-4762 BP (7.2%) 4693-4675 BP (2.7%)
45.	-,-,-	N from Pervalka	Upper Palaeosol	Bulk, soil humus	Gudelis & Michaliukaitė, 1976	2450 \pm 120	2544-2360 BP (43.2%) 2700-2635 BP (15.6%) 2616-2584 BP (7.4%) 2572-2562 BP (2.0%)
46.	-,-,-	-,-,-	Lower Palaeosol	Bulk, soil humus	-,-,-	4390 \pm 110	5065-4850 BP (51.2%) 5271-5184 BP (15.5%) 5120-5112 BP (1.5%)
Archaeological findings							
47.	Vs-321	Nida	Fireplace	Bulk, charcoal	Rimantienė, 1999	4630 \pm 120	5483-5275 BP (45.1%) 5580-5528 BP (8.4%) 5180-5123 BP (8.2%) 5110-5068 BP (6.5%)

Annexes

No.	Lab. index	Coordi-nates WGS84 / location	Sampling site, Palaeosol code, depth, etc.	Method, analysed matter	Project / publication	¹⁴ C age, years (BP) ($\pm 1s$)	Calibrated age (1s range)
48.	Vs-631	-,-	-,-	Bulk, charcoal		4620 \pm 110	5476-5273 BP (45.7%) 5182-5122 BP (9.6%) 5576-5540 BP (5.7%) 5110-5066 BP (7.3%)
49.	Hela-2467	Nida, 55° 17' 52.53" 20° 58' 48.46"	Ceramic shards	AMS, charred crust	Piličiauskas <i>et al.</i> , 2011	5041 \pm 34	5890-5806 BP (50.7%) 5766-5734 BP (17.5%)
50.	Hela-2474	-,-	-,-	-,-	-,-	5005 \pm 34	5750-5661 BP (54.1%) 5855-5829 BP (14.1%)
51.	Hela-2469	-,-	-,-	-,-	-,-	4946 \pm 34	5714-5642 BP (55.8%) 5630-5613 BP (12.4%)
52.	Hela-2468	-,-	-,-	-,-	-,-	4917 \pm 34	5659-5600 BP (68.2%)
53.	Hela-2475	-,-	-,-	-,-	-,-	4854 \pm 34	5614-5583 BP (52.2%) 5643-5629 BP (11.8%) 5498-5492 BP (4.3%)

Annexes

Annex No.5. Magnetic susceptibility (MS) measurements at the Vingis dune site

X, m	k*10 ⁻⁵ SI	X, m	k*10 ⁻⁵ SI	X, m	k*10 ⁻⁵ SI
0	7.96	10.2	17.17	20.4	10.58
0.3	19.16	10.5	10.55	20.7	8.6
0.6	13.24	10.8	10.58	21	7.26
0.9	18.54	11.1	15.21	21.3	25.12
1.2	12.56	11.4	23.79	21.6	8.59
1.5	9.28	11.7	11.85	21.9	8.61
1.8	11.89	12	12.51	22.2	24.47
2.1	16.51	12.3	19.17	22.5	9.9
2.4	28.44	12.6	23.79	22.8	24.48
2.7	24.45	12.9	20.52	23.1	7.96
3	33.73	13.2	32.42	23.4	29.07
3.3	23.81	13.5	19.42	23.7	10.6
3.6	17.2	13.8	16.54	24	41.65
3.9	15.26	14.1	10.6	24.3	18.47
4.2	11.89	14.4	12.57	24.6	11.84
4.5	12.56	14.7	15.19	24.9	14.5
4.8	15.87	15	14.53	25.2	10.58
5.1	6.65	15.3	12.56	25.5	11.24
5.4	11.92	15.6	17.19	25.8	21.15
5.7	14.52	15.9	31.11	26.1	19.88
6	10.59	16.2	18.55	26.4	15.24
6.3	10.62	16.5	12.56	26.7	35.73
6.6	13.24	16.8	11.24	27	48.3
6.9	5.97	17.1	4.75	27.3	53.58
7.2	11.27	17.4	11.87	27.6	25.77
7.5	31.09	17.7	21.14	27.9	16.51
7.8	9.96	18	9.3	28.2	6.58
8.1	19.85	18.3	10.57	28.5	12.53
8.4	12.59	18.6	13.87	28.8	11.27
8.7	15.83	18.9	15.84	29.1	9.91
9	5.96	19.2	26.46	29.4	7.29
9.3	15.24	19.5	17.87	29.7	25.84
9.6	18.58	19.8	10.59	30	15.27
9.9	5.33	20.1	16.51		

Annexes

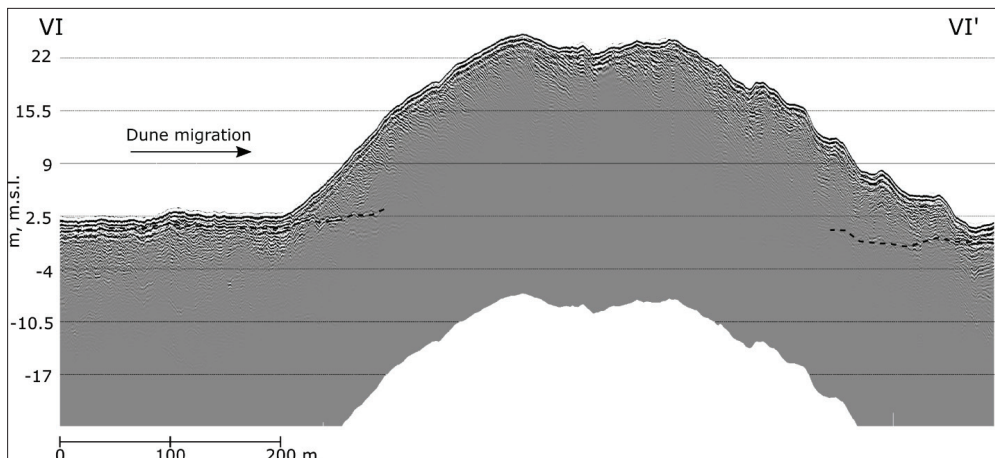
Annex No.6. Magnetic susceptibility (MS) measurements at the Naglis dune site

X, m	k*10 ⁻⁵ SI	X, m	k*10 ⁻⁵ SI	X, m	k*10 ⁻⁵ SI
0	9.81	12.2	5.3	26	55.55
0.1	58.16	12.5	27.13	26.3	21.11
0.4	19.52	12.7	25.79	26.5	329.96
0.9	40.95	12.8	82	26.9	46.23
1.1	25.77	13.2	111.71	27.3	140.17
1.4	89.75	13.5	84.63	27.4	967.46
1.7	7.93	14	10.56	27.7	314.76
2	17.17	14.5	25.68	28	24.43
2.3	19.14	14.8	9.26	28.5	9.9
2.6	20.44	15.3	29.76	28.7	33.09
3	15.2	15.6	34.35	29.3	48.29
3.3	33.07	15.9	23.11	29.4	14.54
3.7	35.67	16	11.88	29.7	869.6
4	18.52	16.7	18.48	30.2	207.66
4.3	18.48	16.9	29.69	30.7	44.96
4.5	27.12	17.5	269.75	31	198.41
4.9	37.68	17.8	12.56	31.5	11.25
5	35.69	17.9	13.19	31.8	327.38
5.3	42.92	18.6	11.9	32.2	15.25
5.3	50.93	19	290.93	32.7	15.9
5.4	14.52	19.2	2027.5	33	4.56
5.5	46.94	19.5	12.5	33.3	91.94
5.7	42.99	19.8	28.93	33.6	16.52
6.2	13.22	20	47.66	33.8	110.43
6.7	21.78	20.3	9.93	34.4	23.17
6.9	54.24	20.7	11.88	34.7	486.74
7.1	555.46	20.9	541.6	35	10.56
7.4	433.14	21.3	27.14	35.8	11.22
7.7	10.56	21.7	52.9	36.5	35.08
8.2	72.71	22	42.99	36.8	38.34
8.7	10.55	22.2	34.36	37.1	106.47
9	14.5	22.6	656.66	37.2	15.2
9.6	12.6	22.7	730.75	37.5	14.55

Annexes

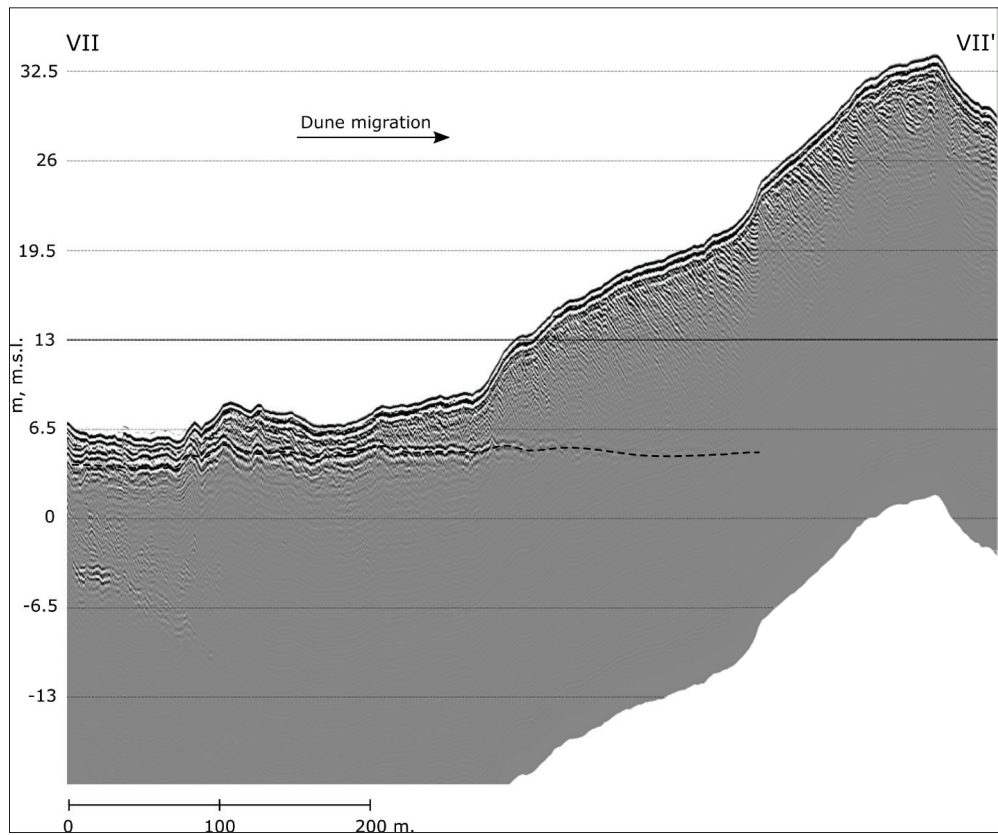
X, m	$k \cdot 10^{-5}$ SI	X, m	$k \cdot 10^{-5}$ SI	X, m	$k \cdot 10^{-5}$ SI
10	21.81	23	17.2	38	22.46
10.3	35.75	23.7	17.83	38.2	36.4
11	15.2	24	45.4	38.3	25.84
11.3	23.79	24.5	417.33	38.7	45
11.7	62.19	25	16.54	39	35
11.8	142.85	25.4	25.8	39.5	23.81
11.9	568.09	25.7	411.97	40	56.22

Annex No.7. GPR cross-sections



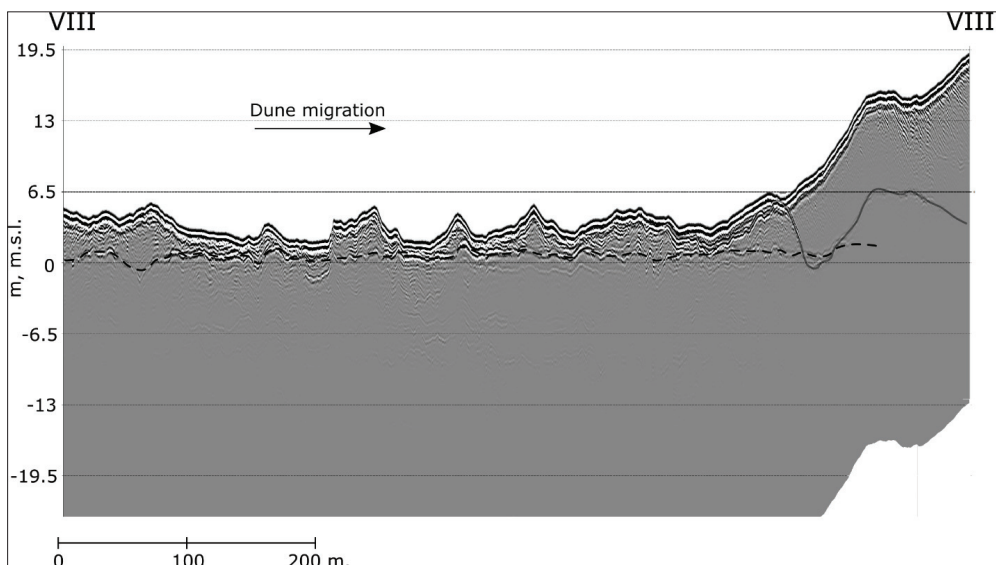
GPR cross-section VI – VI' (for location see Fig. 3.3.2). Northern part of the survey area. Ground water table and slipfaces are clearly visible, no palaeosols are found. The groundwater table is indicated by a dashed line.

Annexes



GPR cross-section VII – VII' (for location see Fig. 3.3.2). Northern part of the survey area.
Ground water table and slipfaces are clearly visible, no palaeosols are found.
The groundwater table is indicated by a dashed line.

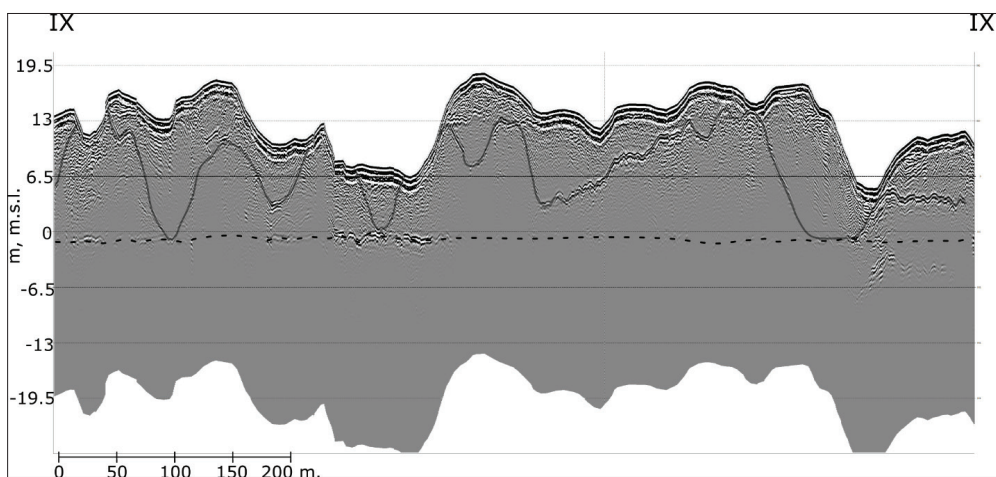
Annexes



GPR cross-section VIII – VIII' (for location see Fig. 3.3.2) with a visible palaeodune. GPR profile with altitudes corrected according to LIDAR data.

The groundwater table is indicated by a dashed line, the buried palaeosol – by a grey line.

The relative height of the palaeodune is up to 6 meters.



GPR cross-section IX – IX (for the location see Fig. 3.3.2) with the visible palaeodunes.

GPR profile with altitudes corrected according to LIDAR data. The groundwater table is indicated by a dashed line, the buried palaeosol (K, 981 ± 193 cal. years BP) – by a grey line.

The relative height of the palaeodunes is up to 15 meters

Santrauka

ĮVADAS

Temos aktualumas

Kuršių nerija yra vienas unikaliausių Lietuvos kampelių tiek kultūrine, tiek geologine prasme. Geologiniu požiūriu – tai „gyvas“, iki šiol besiformuojantis darinys, kurį sudaro eolinės (vėjo sunešamos) nuogulos. Kuršių nerijos nacionalinis parkas, kaip UNESCO sąraše esanti kultūrinio kraštovaizdžio vertybė, yra vienas iš labiausiai lankomų turistinių objektų Lietuvoje. Nors Kuršių nerijoje buvo atlikta daug mokslinių tyrimų, iki šiol nėra galutinai aiški šio pusiasalio geologinio vystymosi raida. Didelė dalis nerijos susiformavo intensyviai veikiant eoliniams procesams: XVI–XIX a., iškirtus miškus, smėlis užpustė 14 kaimų. XIX a., siekiant apsaugoti nuo užpustumyo žvejų gyvenvietes, Kuršių nerija buvo apželdinta. Tuo pat metu, palei visą nerijos jūros krantą, pradėta kurti apsauginį kopagūbrį. Mirusių (Pilkujų) kopų masyvas, esantis tarp Juodkrantės ir Pervalkos, iki šiol išlaikė savo pirmykštį kraštovaizdį, nėra padengtas augalija ir gali būti naudojamas kaip natūrali eolinių procesų laboratorija. Čia, vykstant smėlio išpusťymo (deflacijos) procesui, žemės paviršiuje atsidengia paleodirvožemiai, kurie liudija buvus aktyvių ir pasyvių (stabiliių) kopų formavimosi laikotarpių (fazių) kaitą. Ramius tarpsnius, kuomet kopų paviršių padengdavo augmenija ir susiformuodavo dirvožemio sluoksnis, periodiškai keisdavo eolinio aktyvumo laikotarpiai, kurių metu dirvožemiai

buvo suardomi arba padengiami naujai supustomo smėlio sluoksniu. Priežastys, lėmios periodinį fazių aktyvumą (galimi klimato pokyčiai, natūralūs ar žmogaus veiklos sukelti gaisrai ir kt.) iki šiol yra diskusijų objektu. Informacija apie Kuršių nerijos geologinį vystymąsi ir vėjo dinamiką turi ne tik mokslinę vertę, bet ir praktinį pritaikymą plėtojant miesto infrastruktūrą, vertinant marių pakrančių stabilumą, nustatant saugomų teritorijų ribas, kuriant turinius maršrutus bei reguliuojant turistų srautus ir kt.

Kuršių nerija yra ekologiškai jautri teritorija su nemažai saugomų teritorijų. Dėl to, tiriant kuršių nerijos geologinę sandarą bei čia vykstančius procesus, ne visus tradicinius geologinius lauko tyrimo metodus buvo galima panaudoti. Tyrimų kompleksas, susidedantis iš modernių neinvazinių geofizinių ir geochronologinių tyrimo metodų, apėmė geofizinius lauko tyrimus georadaru (GPR), LIDAR duomenų panaudojimą, paleodirvožemiu datavimą radiokarboniniu (^{14}C) bei eolinių smėlių absoliutaus amžiaus nustatymą optiškai stimuliuotos luminescencijos (IR-OSL) metodais, tai pat kopų reljefo įvairiaisiais praeties laikotarpiais rekonstravimą.

Tyrimo tikslas ir pagrindiniai uždaviniai

Šio tyrimo tikslas – išnagrinėti Kuršių nerijos kopų geologinę sandarą, nustatyti kopų raidos ypatumus bei tai lėmusius veiksnius holocene metu, taip pat įvertinti esamas hipotezes apie palaidotų dirvožemiu formavimo procesus.

Siekiant numatyto darbo tiksls išsikelti tokie uždaviniai:

1. kartograuoti paleodirvožemius ir nustatyti jų erdvinį pasiskirstymą;
2. nustatyti paleodirvožemiu amžių ir išskirti galimas paleodirvožemiu generacijas;
3. atlikti kopų masyvo paleoreljefo rekonstrukcijas įvairiems praeties laikotarpiams;
4. įvertinti eolinių procesų paleodinamikos greitį ir pobūdį;
5. nustatyti pagrindinius veiksnius, lėmusius Kuršių nerijos kopų raidą.

Naujumas

Tyrimai parodė, kad, pasitelkus naujausias šiuolaikines technologijas (georadarą kartu su aukšto tikslumo GPS sistema), galima itin detaliai ir tiksliai fiksuoti paleodirvožemiu reljefą, neatliekant grėžimo ar kasimo darbų, kas yra svarbu vykdant darbus saugomose teritorijose. Tuo būdu, padengus tiriamajį plotą detaliu georadaro profilių tinklu, galima itin aukštu patikimumu atkurti tiriamajame plote aptinkamą palaidotų dirvožemiu paviršių, kuris tiksliai atitiktų buvusių kopų paleoreljefą stabiliuoju jų formavimosi periodu. Tokio detalumo paleorekonstrukciniai darbai Lietuvoje iki šiol nebuvu atliekami.

Darbo mokslinė ir praktinė reikšmė

Nors iki šiol nėra galutinai aiški šio pusiasalio geologinio vystymosi raida, akivaizdu, kad didesnioji nerijos dalis susiformavo intensyviai veikiant eoliniams procesams.

Tad eolinių, o taip pat ir dirvodaros procesų supratimas gali padėti geriau suvokti Kuršių nerijos geologinė raidos ypatumus. Gauta informacija gali būti panaudota ir kitų panašių Baltijos jūros nerijų (pvz. Lebos, Helio, Vyslos) vystymuisi rekonstruoti.

Kadangi Kuršių nerijos nacionalinis parkas, kaip UNESCO sąraše esanti kultūrinio kraštovaizdžio vertybė, yra vienas iš labiausiai lankomų turistinių objektų Lietuvoje, tai gauti tyrimų rezultatai, o ypač atliktos paleogeografinių sąlygų rekonstrukcijos, gali būti pagrindu iš esmės atnaujinat informacinę medžiagą šio parko lankytojams.

Šiandien turimi duomenys liudija, kad su palaidotais dirvožemiais siejamuose geologiniuose sluoksniuose, ypač žemai gruntu grunto vandens lygio, yra išlikusių gerai išsilaikeusių akmens ir bronzos amžiaus archeologinių radinių. Todėl projekto metu gauta nauja informacija apie paleodirvožemių paplitimą būtų naudinga ir šiais objektais besidomintiems archeologams.

Darbo rezultatų aprobabimas

Šio darbo rezultatai buvo pristatyti dešimtyje tarptautinių konferencijų ir šešiuose nacionalinėse seminaruose ir doktorantūros studentų konferencijose.

Tarptautinės konferencijos:

Dobrotin, N. Reconstruction of palaeodynamics of the Curonian Spit dunes based on the ground-penetrating radar (GPR) survey and LIDAR data. ECSA 51th International Symposium “Research and management of transitional waters”, Klaipeda, Lithuania, September 2012.

Dobrotin, N., Bitinas, A., Michelevičius, D., Damušytė, A. Reconstruction of palaeodynamics of the Curonian Spit dunes based on the ground-penetrating radar (GPR) survey and geochronological data. 11th Colloquium on Baltic Sea Marine Geology, m/s “Silja Serenade”, 18-19.09.2012.

Bitinas, A., Molodkov, A., Buynevich, I. V., Damušytė, A., Dobrotin, N., Gregoriuskienė, V., Mažeika, J., Pupienis. D. Aeolian landscape evolution in the Curonian Spit, Baltic Sea. The Baltic Sea a Mediterranean of Northern Europe: In the Light of Natural Sciences, Archaeological and Historical Research from Ancient to Medieval Times, 4-7 June 2014, Gdańsk, Poland.

Bitinas, A., Molodkov, A., Buynevich, I., V., Damušytė, A., Dobrotin, N., Gregoriuskienė, V., Mažeika, J., Pupienis. D. Dune palaeodynamics and chronological control, Curonian Spit, South-eastern Baltic. 9th Baltic Sea Science Congress „New Horizons for Baltic Sea Science“, 26-30 August 2013, Klaipeda, Lithuania.

Buynevich, I.V., Gnivecki, P., Curran, H.A., Savarese, M., Bitinas, A., Dobrotin, N., Pupienis, D., Boush, L.P., Brūniņa, L., Damušytė, A., Lloyd, G., Brake, M., Felgar, C. Geoarchaeological implications of biogenically-induced GPR signal interference in Baltic and Bahamian coastal dunes: comparative sedimentology and internal structure. 10th Baltic Sea Science Congress, Riga, Latvia, 15-19 June 2015.

Buynevich, I.V., Bitinas, A., Tõnisson, H., Brūniņa, L., Pupienis, D., Dobrotin, N., Damušytė, A., Molodkov, A., Vilumaa, K., Vandel, E., Anderson, A., Orviku. K. Early stage of mega-ridges at cape Kolka, Latvia. 10th Baltic Sea Science Congress, Riga, Latvia, 15-19 June 2015.

Buynevich, I.V., Gregorauskienė, V., Bitinas, A., Damušytė, A., Dobrotin, N., Pupienis, D., Pickett, W.J. Diagnostic magnetic susceptibility signatures of episodic pedogenesis in aeolian slipface sequences, Great Dune Ridge, Lithuania. 10th Baltic Sea Science Congress, Riga, Latvia, 15-19 June 2015.

Buynevich, I.V., Bitinas, A., Tõnisson, H., Brūniņa, L., Pupienis, D., Dobrotin, N., Damušytė, A., Vilumaa, K., Vandel, E., Anderson, A. Coastal relicts in the Baltic woods: Early stage palaeo-shorelines of cape Kolka, Latvia. North-eastern Section - 50th Annual Meeting of the Geological Society of America, 23–25 March 2011, Bretton Woods, New Hampshire, USA.

Buynevich, I.V., Bitinas, A., Pupienis, P., Damušytė, A., Brūniņa, L., Sivkov, V., Dobrotin, N., Tõnisson, H., Orviku. K. Paraglacial mega-barriers of the Baltic Sea: a decade of collaborative research. North-eastern Section - 50th Annual Meeting of the Geological Society of America, 23–25 March 2011, Bretton Woods, New Hampshire, USA.

Dobrotin, N. Palaeodynamics of Curonian Spit eastern coastline during the Holocene according GPR data. 11th Baltic Sea Science Congress, Rostock, Germany, June 2017.

Nacionalinės konferencijos:

Dobrotin, N. Kuršiu nerijos kopų geologinė raida ir jos ryšys su klimato kaita holoceno metu. Seminar at Faculty of Natural Sciences and Mathematics, Klaipėda University, Klaipėda, Lithuania, September 2013.

Bitinas, A., Dobrotin, N., Michelevičius, D., Damušytė, A. Kuršių Nerijos kopų geologinė raida. Jūros ir krantų tyrimai 2013. Klaipėda, Lithuania, April 2013.

Dobrotin, N. Kuršiu nerijos kopu geologinė raida ir jos ryšys su klimato kaita holoceno metu. Seminar at the Faculty of Natural Sciences and Mathematics, Klaipėda University, Klaipėda, Lithuania, September 2013.

Bitinas, A., Dobrotin, N. Kuršių nerijos kopos: susiformavimas, vystymasis, dabartiniai geologiniai procesai. Kuršių nerijos nacionalinio parko įkūrimo 25-mečio konferencija „Kuršių nerijos kraštovaizdžio pokyčiai“. Nida, Lithuania, 3-4 November 2016.

Dobrotin, N. Palaeodynamics of Curonian Spit eastern coastline during the Holocene according GPR data. Seminar at Faculty of Natural Sciences and Mathematics, Klaipėda University, Klaipėda, Lithuania, March 2017.

Dobrotin, N. Kuršių nerijos rytinio kranto paleodinamika holoceno metu pagal georadarą ir ^{14}C datavimo duomenis. Annual Conference of PhD Geology Students, Faculty of Chemistry and Geosciences, Vilnius University, Vilnius, Lithuania, November 2017.

Šios disertacijos rezultatai buvo paskelbti keturiose mokslinėse publikacijose:

Dobrotin, N., Bitinas, A., Michelevičius, D., Damušytė, A., Mažeika, J. 2013. Reconstruction of the Dead (Grey) Dune evolution along the Curonian Spit, Southeastern Baltic, Bulletin of the Geological Society of Finland, 85, 49–60.

Buynevich, I.V., Savarese, M., Curran, H.A., Bitinas, A., Glumac, B., Pupienis, D., Kopczynski, K., Dobrotin, N., Grievecki, P., Boush, L.P., Damušytė, A. 2017. Sand incursion into temperate (Lithuania) and tropical (the Bahamas) maritime vegetation: Georadar visualization of target-rich aeolian lithosomes, Estuarine, Coastal and Shelf Science.

Morkūnaitė, R., Bautrenas, A., Česnulevičius, A., Dobrotin, N., Baubinienė, A., Jankauskaitė, M., Kalesnikas, A., Mačilevičiūtė - Turlienė, N. 2018. Changes in quantitative parameters of active wind dunes on the south-east Baltic Sea coast during the last decade (Curonian Spit, Lithuania), Geological Quarterly, 62 (1).

Bitinas, A., Dobrotin, N., Buynevich, I.V., Molodkov, A., Damušytė, A., Pupienis, D. Coastal dune dynamics along the northern Curonian Spit, Lithuania: toward an integrated database (in press, accepted).

SANTRUMPU SARAŠAS

Santrumpa	Paaškinimas
¹⁴ C method	radiokarboninis datatavimas
m.s.l.	vidutinis jūros (dabartinės) lygis
AD	Anno Domini, kalendoriniai metai
AMS method	radiokarboninis datatavimas naudojant atominę masės spektrometriją
BP	prieš dabartį
GD	Mirusios (Pilkosios) kopos, arba Pilkosios kopos
GDR	Didysis kopagūbris
GISP2	globali temperatūros kreivė; pagal Greenland Ice Sheet Project 2
GPR	georadaras
GPS	globali pozicionavimo sistema
HMC	sunkiųjų mineralų koncentracija
IR-OSL	datavimas optiškai stimuliuotos luminescencijos metodu
ka	amžius (tūkstančiais metų)
LIDAR	didelės skyros reljefinių žemėlapių sudarymo metodas
MS	magnetinis imlumas
NP	nacionalinis parkas
AK	apsauginis kopagūbris
SAR	sintetinės apertūros radaras

TYRIMO MEDŽIAGA IR METODAI

Tyrimų rajonas

Kuršių nerija – tai 98 km ilgio pusiasalis, skiriantis Baltijos jūrą nuo Kuršių marių. Kuršių nerija yra pietrytinėje Baltijos jūroje dalyje ir driekiasi nuo Sembos pusiasalio iš šiaurė. Kuršių nerijos kopos yra aukščiausios šiaurės Europoje ir siekia 60–70 m (Gudelis, 1998a). Tyrimo objektu pasirinktos Mirusios (Pilkosios) kopos, esančias tarp Juodkrantės ir Pervalkos (2.4 A pav.).

Kuršių nerijoje kvartero darinių storis labai priklauso nuo prekvartero paviršiaus pobūdžio bei šiuolaikinio reljefo. Kvartero nuogulų vidutinis storis siekia 80–100 m, o vietomis, po kopų masyvais, gali siekti iki 140 m. Kvartero nuogulų ir nuosėdų stratigrafija pateikta 3.2.1 paveiksle. Labiausiai paplitusios eolinės nuosėdos (v IV) dengia beveik visą Kuršių nerijos teritoriją (Bitinas ir kt., 2000) ir susideda iš perklostytų limnoglacialinių, fliuvioglacialinių, limninių ir jūrinių nuosėdų. Didysis kopagūbris, siekiantis 50–60 m, aukščiausiam taške – 67,2 m virš jūros lygio, susideda iš perpustyty Litorinos, Post-Litorinos ir dabartinės jūros nešmenų. Eolines nuoguldas daugiausiai sudaro smulkus ir vidutinio rupumo feldšpatinis-kvarcinis rudai geltonas smėlis. Didžiajame kopagūbryje eolinėse nuogulose aptinkami palaidoti paleodirvožemiai, o taip pat smėlio sluoksniai su didesne sunkiųjų mineralų koncentracija bei glaukonito kiekiu.

Geomorfologija

Kuršių nerijos jūrinis krantas yra lygus ir taisyklingai įgaubtas, tuo tarpu rytinis (marių) krantas – išraižytas ragais ir įlankom. Ragai pakrypę iš šiaurės rytus, kas rodo pietvakarinį vėjų ir srovių vyraujančią kryptį. Kuršių nerija plačiausia ties ragais ir siekia 3,8 km plotį (Bulvikio ragas šalia Nidos), siauriausia – siauriau Šarkuvos (plotis iki 0,4 km.).

Kuršių nerija geomorfologiniu požiūriu gana diferencijuota, o jos pagrindiniai morfologiniai elementai yra orientuoti išilgai nerijos. Tai lémė kranto ir eolinių procesų kryptingumas. Išskiriami 4 genetiniai–morfologiniai nerijos ruožai (3.2.1 A pav.):

1) Jūros paplūdimys su apsauginiu paplūdimio kopagūbriu. Jūros paplūdimio plotis siekia 25–70 m. Apsauginis paplūdimio kopagūbris siekia 15 m. aukštį.

2) Jūrinė palvė. Tai kauburėta ir gubrėta lyguma tarp apsauginio paplūdimio kopagūbrio ir Didžiojo kopagūbrio, sudaryta reliktinio eolinio smėlio, likusio vėjui išpusčius čia buvusias parabolines kopas. Eolinio smėlio storis apie 6–7 m, palvė virš jūros lygio pakilusi apie 2–5 metrus.

3) Didysis kopagūbris. Stambiausia Kuršių nerijos reljefo forma. Kopos ištisusios rytiame nerijos krante šiaurės–pietų kryptimi. Kopagūbrio plotis kinta nuo 0,4 iki 1,2 km. Vidutinis aukštis apie 30–40 m. Didysis kopagūbris nėra vientisas – jį atskirus

masyvus jį skaldo kloniai ir defliacinių raguvos. Būdingas lėkštas ilgas vakarinis šlaitas ir plati viršukalnė bei pakopiškas, neaukštasis nuobirinis šlaitas.

4) Marių palvė ir paplūdimys. Šios reljefo formos silpnai išsivysčiusios, daug kur jų visai nėra. Dažniausiai 3–6 m pločio smėlio paplūdimiai paplitę nerijos raguose ir įlankose.

Georadaro veikimo principas

Georadaras – tai sintetinės apertūros radaro sistema, skirta popaviršinių atspindžių tyrimams: trumpas elektromagnetinis impulsas išspinduliuojamas į tiriamąją aplinką, dalis impulso pasiekia sluoksnį ar objektą, kurio santykinė dielektrinė skvarba skiriasi nuo aplinkos, atsispindi ir grįžta atgal, kur atspindys fiksuojamas priemimo antena; kita impulso dalis keliauja toliau, kol pasiekia kitą sluoksnį ar objektą, ir t.t. (3.3.1 pav.). Kuo didesnis dviejų sluoksninių dielektrinių konstantų skirtumas, tuo didesnė energijos dalis atsispindi ir tiriamoji riba (ar objekto) matomas ryškiau.

Kopų tyrimas georadaru

Projekto pirmajame darbų etape tiriamasis plotas buvo padengtas retu georadaro profilių tinklų – matavimų profiliai buvo išdėstyti apytiksliai kas 500 metrų (3.3.2 pav.). Atlirkus gautų duomenų apdorojimą, buvo išskirti plotai, kur aptinkami paleodirvožemiai, kurie vėliau buvo padengti tankesniu georadaro profilių tinkleliu – atstumas tarp profilių buvo apie 200 metrų. Projekto darbų metu georadaro profiliais padengtas apytikriai 15 km² plotas, kas sudaro apie 180 km georadaro profilių.

Tyrimai buvo atliekami „RADAR Systems“ georadaru „Zond 12-e“. Matavimams buvo naudojama 300 MHz antena su 400 V impulsų generatoriumi. Atliekant tyrimus buvo naudojamas 500 ns langas. Naudojant bandomuosius gręžinius, nustatyta smėlio santykinė dielektrinė skvarba: $\epsilon_r=5.33$ (gręžinių duomenys pateikti priede Nr. 2).

Magnetinis imlumas

Magnetinio imlumo (MS) matavimai buvo atliekami *in situ*, šalia georadaro profilių. Tyrimui buvo naudotas Bartington MS3 matuoklis su MS2K jutikliu (Buynevich ir kt., 2007a). MS buvo matuojamas 30 cm intervalais, vietose, kur pastebimas akivaizdus litologinis skirtumas (stambesnė frakcija, sunkiųjų mineralų koncentracijos, paleodirvožemiai), buvo atliekami papildomi matavimai. Tai leido tiesiogiai palyginti tam tikro sluoksnio magnetines savybes (pirmiausia magnetito kiekį) su jų elektromagnetinio signalo atsaku georadaro duomenyse. Magnetinio imlumo vertės pateiktos priede Nr. 5 ir priede Nr. 6.

Paleodirvožemiu datavimas radiokarboniniu (^{14}C) metodu

Palaidotų dirvožemiu amžiui nustatyti buvo surinkti 25 mèginiai datavimui radiokarboniniu (^{14}C) metodu, iš kurių 13 – išanalizuoti. Mèginiai paimti iš vizualiai matomų skirtingų paleodirvožemiu sluoksnių kopų šlaituose, o taip pat ir iš smelyje palaidotų paleodirvožemiu. Pastarieji mèginiai paimti atsižvelgiant į geofizinių tyrimų rezultatus, dirvožemius pasiekus perkasose bei panaudojus rankinio gréžimo priemones. Visi paimti mèginiai datuoti Gamtos tyrimų centro Geologijos ir geografijos instituto Radioizotopinių tyrimų laboratorijoje (laboratorijs vadovas prof. hab. dr. Jonas Mažeika).

Datavimui paimti mèginiai laboratorijs buvo susmulkinami ir apdorojami rûgštis-šarmo-rûgštis technologija, kad bûtu pašalinti karbonatų bei humidinių rûgščių taršalai. Po to mèginyje likës visas organinës kilmës karbonatų kiekis buvo panaudotas benzenui išgauti (Kovaliukh & Skripkin, 1994). Specifinis ^{14}C aktyvumas benzene buvo matuojamas skystas scintiliacijos (LSC) metodu (Gupta & Polach, 1985; Arslanov, 1985) prietaise Tri-CarbÒ 3170TR/SL. Nustatytas paleodirvožemio mginis radiokarboninis amžius buvo perskai-

iuotas / kalendorin/ amžis naudojant ^{14}C kalibracinę programą OxCal v. 3.1 (Bronk Ramsey, 2001) ir kalibracinę kreivę IntCal09 (Reimer et al., 2009). Pagal šią metodiką buvo perskaičiuoti ir visi projekte panaudoti ankstesnių tyrimų metu gauti radiokarboninio datavimo rezultatai (priedas Nr. 4).

Smelių datavimas OSL metodu

Eolinių nuogulų amžiui bei jų sedimentacijos greičiui nustatyti skirtingais holocene laikotarpiais buvo paimti smelio mèginiai datavimui optiskai stimuliuotos luminescencijos (OSL) metodu – naudota IR-OSL metodo modifikacija t.y. kai liuminescencijai sužadinti naudojamas infraraudonųjų spindulių (IR – infrared) šaltinis. Analizei buvo paimta po 5 mèginius dviejuose profiliuose, statmenuose skirtingo amžiaus palaidotų dirvožemiu horizontams. Mèginiai paimti kasiniuose, iš 0,5-0,7 metrų gylio. Smelių absoliutaus amžiaus nustatymas OSL metodu atliktas Talino technologijos universiteto Geologijos instituto Kvartero geochronologijos laboratorijs (laboratorijs vadovas dr. Anatoly Molodkov). Datavimas OSL metodu yra sudetingas ir daug laiko reikalaujantis procesas – jo aprašymas yra pateiktas specialiose tam tikslui skirtose publikacijose (Molodkov, Bitinas, 2006; Molodkov et al., 2007; Jaek et al., 2007a, 2007b; 2008).

Georadarо duomenų interpretavimas ir paleogeografinės rekonstrukcijos

Interpretuojant gautus duomenis buvo labai svarbu įvesti pataisas pagal dabartinių kopų reljefą – tuo tikslu buvo naudojami LIDAR nuotraukos duomenys. Įvedus minėtias korektūras, buvo identifikuojamas gruntuinio vandens horizontas ir kiti ryš-

kiausiai atspindintys horizontai (paleodirvožemai, sunkiųjų mineralų sankaupos, ir kt.). Gruntinio vandens horizontas visame tiriamajame plote išsilaičio apytiksliai tame pačiame gylyje, kas leidžia lengvai interpretuoti gautus duomenis. Paveiksle 3.7.1 A dalyje parodyti pirminiame georadaro profilyje išskirti atspindintys horizontai, o B dalyje pateikti tie patys duomenys, tik jau su atlirkta auksčio korekcija.

Kartais georadaro duomenyse užfiksuočiai paleodirvožemiu atspindžiai ir smėlio sluoksniai su sunkiaisiais mineralais turi panašią formą ir amplitudę (Buynevich ir kt., 2007a). Siekiant atskirti paleodirvožemius, 15 atspindžių užfiksotų georadaro duomenyse buvo patikrinti kontroliniai gręžiniai (3.2.1 pav, B1 – B15). Paveiksle 3.7.3 pateiktas georadaro profilio fragmentas II – II', šiame pavyzdyme matomi 5 skirtinių atspindžiai: (1) grūtinio vandens horizontas, (2) paleodirvožemis, (3) sunkiųjų mineralų koncentracija, (4) smėlio klostymas, (5) riba tarp skirtinės vėjo krypčių su klotu smėlio sluoksnį. Atspindžiai (2) ir (3) turi panašias amplitudes, ir tik išgręžus bandomuosius gręžinius (B5 ir B6) paaiškėjo, kad pirmasis atspindys (2) yra paleodirvožemis, o kitas (3) – sluoksnis su didesne sunkiųjų mineralų koncentracija. Visi bandomieji gręžiniai pateikti priede Nr. 2.

Georadaro tyrimo duomenys parodė, kad kai kuriose vietose paleodirvožemio paviršius kerta grūtinio vandens paviršių. Tokios vietas interpretuotos kaip buvusi ankstesnioji Didžiojo kopagūbrio rytinio šlaito papėdė (3.7.4 pav.).

Kadangi GPR tyrimai atskleidė, kad Mirusiu (Pilkuijų) kopų masyve paleodirvožemai yra išlikę arba tik paskirais fragmentais, arba tik labai lokaliose teritorijose, tad ir sudaryti atitinkamas paleorekonstrukcijas skirtinėmis praeities laikotarpiams buvo galima tik gana lokaliuose šio kopų masyvo plotuose (3.7.5 pav.). Sudarant minėtās paleorekonstrukcijas buvo naudojamas Halliburton GeoGraphix SeisVision programa.

Eolinės paleodinamikos vertinimas

Detalaus tyrimo plotai pasirinkti vietovėse, kur į paviršiuose plyti keli skirtinės amžiaus paleodirvožemai (3.2.1 pav., V ir N), datuoti (AMS) ankstesnių tyrimų metu (Buynevich ir kt., 2007a). Detalūs kompleksiniai tyrimai susidėjo iš nuosėdų litologinio aprašymo, lauko turimų georadaru, smėlio magnetinio imlumo matavimų, smėlio mėginių datavimų IR-OSL metodu. Pasirinktuose plotuose georadaro profilis buvo užrašomas statmenai žemės paviršiuje atsidengiančių paleodirvožemų lėšai. Profilių pradžios ir pabaigos koordinatės:

Vingio kopos plotas: $55^{\circ} 27' 35.07''$ N, $21^{\circ} 05' 20.13''$ E – $55^{\circ} 27' 36.44''$ N, $21^{\circ} 05' 23.98''$ E;

Naglio kopos plotas: $55^{\circ} 26' 47.64''$ N, $21^{\circ} 05' 01.51''$ E – $55^{\circ} 26' 48.88''$ N, $21^{\circ} 05' 04.15''$ E.

Siekiant atpažinti kuo daugiau atspindžių, tyrimų georadaro duomenys buvo lyginami su magnetinio imlumo duomenimis. Eolinės sedimentacijos greičio nustatymui buvo datuojami smėlio mėginių, paimtų tarp gretimų paleodirvožemų.

REZULTATAI

Paleodirvožemiu amžius ir paplitimas

Projekto lauko tyrimai vyko paraleliai atliekant tyrimus georadaru bei vizualiai (lauko maršrutų metu) kartografuojant kopų paviršiue atsidengiančius paleodirvožemius. Kartografavimo metu pastebėta, kad paleodirvožemiu atodangos nėra tolygiai paplitusios visame tyrimų plote, o didžioji jų dalis koncentruojasi pietinėje tiriamojo ploto dalyje (4.1.1 ir 4.1.2 pav.).

Atlikus paleodirvožemiu kartografavimą ir išskyrus paleodirvožemius georadaro profiliuose, buvo atrinkta 13 ryškiausiai išsiskiriančių paleodirvožemiu fragmentų, iš kurių paimti mèginių datavimui radiokarboniniu metodu. Datuotų mèginių paëmimo vietų altitudës varijuoja nuo 9 iki 33 m virš dabartinio jūros lygio. Šio datavimo duomenys pateikti 4-oje lentelëje. Atlikus datavimus, paaiškėjo, kad šešių paleodirvožemiu amžius patenka į 400–900 metų prieš dabartį (PD) intervalą, keturi mèginiai – į 1000–2000 metų PD intervalą, o dar trys mèginių sutelpa į 3400–3900 metų PD laikotarpi.

Paleodirvožemiu amžiaus ir genezës interpretacija

Be 13 tyrimo metu datuotų mèginių, literatûroje buvo rasta dar 40 Kuršių nerijos dirvožemiu datų (visas datuotų paleodirvožemiu sąrašas pateiktas priede Nr. 4). Visi 53 datuoti dirvožemiai sutelpa laiko intervale nuo 5800 metų PD iki kelių šimtų metų PD.

Visų Kuršių nerijoje datuotų paleodirvožemiu kompleksinë analizë leido išskirti 4 paleodirvožemiu formavimosi periodus (generacijas): 1) 5800–4500 metų PD; 2) 3900–3100 metų PD; 3) 2600–2400 metų PD, ir 4) nuo 1900–400 metų PD (4.2.1 pav.). Išskirtos dirvožemiu generacijos skiriasi nuo Gaigalo ir Padzur (2008) išskirtų generacijų, kadangi pastarojo tyrimo metu buvo naudota didesnë radiokarboninių datavimų duomenų imtis.

Išskirtas paleodirvožemiu generacijas buvo bandoma susieti su pasaulinës oro temperatûros kaita holocene metu. Buvo analizuojama hipotezë, kad eolinių procesų reaktyvacija holocene viduryje gali būti susijusi su globaliu temperatûros pokyčiu tuo metu. Dël informacijos stokos apie klimatą (oro drëgnumą, vėjo stiprumą, ir kt.) per pastaruosius 6000 tûkst. m., buvo apsiribota tik gautų duomenų sugretinimu su globalia temperatûros kreive GISP2 (4.2.2 pav.). Buvo nustatyta, kad nėra jokio ryšio tarp išskirtų paleodirvožemiu formavimosi generacijų ir globalaus atšilimo bei atšalimo laikotarpių.

Pagal ankstesnius tyrimus dirvožemio formavimasis smëlingoje aplinkoje gali trukti net iki 800 metų (Peyart 2007). Paveikslas 4.2.3 paaïskina, kaip gali kisti datuoto dirvožemio amžius, priklausomai iš kurio dirvožemio dalies paimtas mèginiys: amžius tarp viršutinës ir apatinës dirvožemio dalies gali skirtis iki 800 metų. Atsižvelgiant į tai, kad dauguma datavimui skirtų mèginių imama iš viršutinio paleodirvožemio sluoksnio, kuriame randama dau-

giausia organikos, radiokarboninis datavimas reprezentuoja vėlyviausią dirvožemio vystymosi stadiją. Padarius prielaidą, kad datuotas paleodirvožemis galėjo pradeti vystytis 800 metų anksčiau, nei kad rodo gautas jo amžius, dirvožemiu formavimosi generacijų ribos buvo atitinkamai pakoreguotos. Paveikslas 4.2.4 rodo paleodirvožemio radiokarboninio datavimo rezultatus, o rodyklemis parodyta galima paleodirvožemio formavimosi pradžią. Tad, atsižvelgiant į dirvožemio formavimosi ir datavimo ypatumus, anksčiau išskirtų generacijų ribos buvo praplėstos (4.2.5 pav) apie 800 metų, dėl ko visos anksčiau išskirtų paleodirvožemiu formavimosi generacijų ribos persidengė. Tai leidžia teigti, kad visos minėtos 4-ios generacijos gali būti sujungtos į vieną nepertraukiamą paleodirvožemiu formavimosi generaciją. Šie rezultatai paneigia Gaigalo ir Padzur (2008) publikuotą kelių dirvodaros generacijų modelį ir patvirtina Gudelio (1998a) pateiktą modelį (hipotezę), kad skirtinį palaidoti paleodirvožemai formavosi vieno ilgo dirvodarinių procesų periodo metu. Mūsų tyrimo metu gautas didesnis duomenų kiekis leido minėtą periodą praplėsti nuo 4000 metų PD (Gudelis 1998a) iki 6500–6700 metų PD.

Eolinių procesų paleodinamika

Paleodinamikos tyrimams pasirinkti du plotai: Vingio kopos poligonas ir Naglio kopos poligonas.

Vingio kopų poligone tyrimų georadarui duomenyse aiškiai matosi du paleodirvožemiai (4.3.1 pav.), kurių datuotas amžius yra 3400 ± 35 kal. metų PD ir 2430 ± 25 kal. metų PD. IR-OSL metodu datuotų smėlio mèginių amžius varijuoja nuo 2200 ± 200 metų iki 2800 ± 200 metų (5 lentelė, KOPOS-6 – KOPOS-10). Georadarui užraše taip pat matomi silpnesni atspindžiai, kurie sutampa su magnetinio imlumo maksimumais, sukeltais smėlio sluoksnių su didesniu sunkiųjų mineralų kiekiu.

Naglio kopų poligone tyrimo georadarui duomenyse aiškiai išsiskiria du paleodirvožemiai (4.3.2 pav.), kurių amžius – 1350 ± 45 kal. metų PD ir 850 ± 35 kal. metų PD. Tarp dirvožemio sluoksnių esančio ir IR-OSL metodu datuotų smėlio amžius varijuoja nuo 1100 ± 100 metų iki 2200 ± 200 metų (5 lentelė, KOPOS-1 – KOPOS-5). Kaip ir pirmu atveju, georadarui užraše taip pat išsiskiriantis silpnesni atspindžiai sutampa su magnetinio imlumo maksimumais, kuriuos sukélė smėlio sluoksniai su didesne sunkiųjų mineralų koncentracija.

IR-OSL datavimų interpretacija pateikta 4.3.3 paveiksle. Atmetus kelias anomalias datas, datavimo rezultatai rodo, kad smèliai tarp dviejų dirvožemiu susiklostę per gan trumpą laiko tarą, t.y. apytikriai per 200 metų. Šiuos duomenis patvirtina ir nustatytois aukštostas kai kurių smėlio sluoksnelių magnetinio imlumo vertės, kurias sukelia ypač didelė sunkiųjų mineralų koncentracija sluoksnyje – tai byloja buvus intensyvaus eolinio aktyvumo (audringus) periodus.

Paleogeografinės rekonstrukcijos

Paleogeografinės rekonstrukcijos atliktos vienodo amžiaus paleodirvožemiu paplitimo plotuose. Paveiksle 4.4.1 pateikta apytiksliai 1000 metų PD laikotarpio paleogeografinė rekonstrukcija. Kopų masyvas ne vientisas, sudarytas iš kelių atskirų kopų. Kopų plotis siekia 200–300 metrų, aukštis – 35 metrus.

Paveiksle 4.4.2 pateikta apytiksliai 3500 metų PD laikotarpio paleogeografinė rekonstrukcija. Čia kopų masyvas taip pat ne vientisas, sudarytas iš kelių atskirų kopų, aukštis siekia 25 metrus.

Paveiksle 4.4.3 pavaizduota užpustyta paleokopa. Jos plotis siekia 250 m, aukštis – apie 17 m.

Paveiksle 4.4.4 vaizduojamas Kuršių nerijos kopų masyvo rytinio šlaito papédės persistūmimas per pastaruosius 3500 metų. Maždaug prieš 3500 metų kopų masyvo rytinio šlaito papédė buvo ties centrine nerijos dalimi, o apytikriai 1000 metų PD ši papédė dar maždaug 180 metrų buvo persistūmusi rytų kryptimi. Tad per paskutinius 1000 metų Kuršių nerijos kopų masyvo rytinio šlaito papédė patyrė esminius pasikeitimus – buvo perstumta daugiau kaip 500 metų į rytus.

REZULTATU APTARIMAS

Kopų evoliucija ir klimato pokyčiai

XX a. vykdyti tyrimai suformavo vyraujančią nuomonę, kad kopų reaktyvacija susijusi su dideliais klimato pokyčiais holocene metu (Borowka 1975). Eolinio aktyvumo periodai (eoladinaminės stadijos; Gudelis 1998b) truko tūkstančius metų. Gauti rezultatai rodo, kad globalios pasaulinės temperatūros kitimas nebuvo pagrindinis dirvožemiu formavimosi faktorius Kuršių nerijoje. Lokalūs veiksnių (audros, miškų gaisrai) turėjo didesnę įtaką dirvožemiu formavimuisi. Daugumoje palaidotų dirvožemiu aptinkama medžio anglies, tad jau anksčiau vykdytų tyrimų metu manyta (Gudelis, 1998b; Gaigalas ir Pazdur, 2008), kad lokalūs miško gaisrai galėjo padėti formuotis dirvožemiams.

Sluoksnių su didesne sunkiuju mineralų koncentracija, aptikti Naglio ir Vingio kopų poligonuose, rodo buvus laikotarpių su padidėjusių pažeminio vėjo greičiu, ir tai gali būti siejama su audromis (Buynevich, 2012; Pupienis ir kt., 2017). Audros galėjo būti pagrindinis veiksnys, lėmęs kopų transgresiją. Tyrimų georadarų duomenys ir magnetinio imlumo matavimų rezultatai rodo, kad eolinėse nuogulose, skiriančiose skirtingo amžiaus paleodirvožemius, yra sluoksnių su didesne sunkiuju mineralų koncentracija. Didesnis sunkiuju mineralų kiekis nuosėdose gali būti siejamas su paleoklimatinėm sąlygom (ramiom, vejuotom ar audringom) kopų akumuliacijos metu. Tyrimų duomenys rodo, kad kopų reaktyvaciją

paskatino lokalūs veiksniai (miškų gaisrai, miškų kirtimas ir t.t.), ji apėmė nedideles teritorijas, o eolinio suaktyvėjimo periodai tėsdavosi kelis šimtus metų.

Ekogeologija ir kopų formavimasis

Seniausias Kuršių nerijoje aptiktas paleodirvožemis datuojamas 5700 metų PD, tačiau atsižvelgiant į galimą dirvodaros trukmę (apie 800 metų; Peyrat, 2007), galima teigti, kad dirvožemis galėjo pradėti formuotis ir maždaug prieš 6500 metų. Šie duomenys sutampa su archeologinių tyrimų duomenimis (Rimantienė, 1999; Piličiauskas ir kt., 2011). Laužaviečių turinio ir keramikos dataivimai rodo, kad Kuršių nerija jau buvo apgyvendinta 5300–5800 metų PD, tad tuo metu jau turėjo būti pakankamai išsvystės dirvožemis ir tam tikra augmenija, sudaranti palankias sąlygas gyvybei vystytis.

Atliktos paleorekonstrukcijos rodo, kad kopų masyvo rytinio šlaito papėdės padėtis iki 500 metų PD beveik nekito ir buvo ties centrine dabartinės Kuršių nerijos ašimi (t.y. ties dabartinio Didžiojo kopagūbrio vakarinio šlaito papėde). Senosios kopos vienodai dengė visa Kuršių nerijos teritoriją. Didysis kopagūbris susiformavo tik XVI amžiuje, dėl destruktyvios žmogaus veiklos paskatinto eolinio aktyvumo.

Pagal istorinius duomenis, 1675 metais apie 50 % nerijos buvo padengta augmenija. Maždaug po 100 metų (1733–1760 metais) prasidėjo intensyvus miškų naikinimas paruošiant erdves ganykloms, taip pat dėl gaisrų ir galimo intensyvaus medienos eksporto. Augmenijos sunykimas paskatino eolinį aktyvumą, kuris tesėsi iki 1850 metų, kuomet prasidėjo miškų atsodinimas (Moe ir kt., 2005, Savukyniene ir kt., 2003) (5.2.1 pav.). Laikotarpyje tarp miškų kirtimo ir atsodinimo buvo užpustytą 14 Kuršių nerijos gyvenviečių. Gerai dokumentuotas Karvaičių kaimo užpustumasis: 1786 metais slenkančios kopos pasiekė gyvenvietę, o 1797 metais gyvenvietė buvo galutinai palaidota po smėliu.

XVII–XIX a. dėl žmogaus intensyvios ūkinės veiklos Kuršių nerijos ekogeologinė padėtis pakito dramatiškai: parabolinės kopos, dominavusios nuo pat vidurinio holoceno, buvo sunaikintos judančio smėlio ir transformavosi į judančius barchanus. Dėl judančių barchanų marių palvė susiaurėjo ir galiausiai vietomis visai sunyko. Tačiau kol kas nepakanka duomenų, kurie leistų tiksliai nustatyti buvusias marių kranto bei kitas geomorfologines ribas. Pagal kai kurias paleogeografinės rekonstrukcijas (5.2.2 pav.) Kuršių nerijoje dominavo plati marių palvė (užimanti apie pusę nerijos pločio), kurioje buvo dauguma gyvenviečių (Povilanskas, 2009).

IŠVADOS

1. Paleodirvožemai išliko fragmentiškai, daugiausiai pietinėje Mirusių (Pilkųjų) kopų dalyje, vakarinėje Didžiojo kopagūbrio šlaito papédėje.
2. Radiokarboninio (^{14}C) datavimo rezultatai rodo, kad paleodirvožemiu amžius siekia 5700 metų prieš dabartį. Detalios surinktų duomenų analizės metu nepavyko išskirti atskirų dirvožemiu formavimosi generaciją, o gauti duomenys patvirtina V. Gudelio (1998a) vieno ilgai trukusio dirvodaros proceso modelį. Paleodirvožemiu radiokarboninių datavimų gausa leido praplėsti šį dirvodaros periodą nuo 4000 metų PD iki 6500–6700 metų PD. Nevienodos paleodirvožemiu datų pasiskirstymas gali būti paaškinamas tuo, kad kai kurie dirvožemai yra geriau išsvystę, taip pat daugiau jų atodangų yra aptinkama dabartiniame kopų reljefe, kas ir nulémė detalesnį jų ištirtumą (t.y. buvo surinktas didesnis mėginių skaičius).
3. Atliktos paleorekonstrukcijos rodo, kad kopų masyvo rytinio šlaito papédės padėtis per pastaruosius 5000 metų beveik nekito ir buvo ties centrine Kuršių nerijos ašimi (ties dabartinio Didžiojo kopagūbrio vakarinio šlaito papėde). Paleorekonstrukcijos byloja, kad laikotarpiu tarp 3500 ir 1000 metų prieš dabartį kopų masyvo rytinė papédė pasislinko tik maždaug 180 metrų, o jau vien per pastaruosius 1000 metų kopos buvo perstumtos daugiau nei 500 metrų rytių kryptimi.
4. Eolinių procesų reaktyvacija ir kopų perpustymas prasidėjo maždaug Holoceno viduryje. Reaktyvacija nesusijusi su ilgai trukusiais globalaus klimato pokyčiais. Tyrimo duomenys rodo, kad kopų eolinė reaktyvacija paskatino lokalūs veiksniai (miškų gaisrai, miškų kirtimas ir t.t.), ji apėmė nedideles teritorijas, tešesi nuo kelių dešimčių iki kelių šimtų metų, o kopos buvo perstumiamos tik keliasdešimt metrų.
5. Tyrimų georadaro duomenys bei smėlių magnetinio imlumo matavimų rezultatai eolinėse nuogulose skiriančiose skirtingo amžiaus paleodirvožemius, rodo sluoksnius su didesne sunkiuju mineralų koncentracacija, didesnis sunkiuju mineralų kiekis gali būti siejamas su paleoklimatinėm sėlygom kopų akumuliacijos metu (ramiom, vejuotom ar audringom).
6. Didysis kopagūbris susiformavo tik XVI amžiuje dėl destruktyvios žmogaus ūkinės veiklos paskatinto kopų eolinio aktyvumo. Parabolinės kopos, dominavusios Kuršių nerijoje didžiąją Holoceno laikotarpio dalį, buvo sunaikintos judančio smėlio ir transformavosi į vientisą kopagūbrių.

Klaipėdos universiteto leidykla

Nikita Dobrotin

EVOLUTION OF THE CURONIAN SPIT DUNES

Doctoral dissertation

KURŠIŲ NERIJOS KOPŲ RAIDA

Daktaro disertacija

Klaipėda, 2018

SL 1335. 2018 08 23. Apimtis 8,48 sąl. sp. l. Tiražas 28 egz.

Išleido ir spausdino Klaipėdos universiteto leidykla, Herkaus Manto g. 84, 92294 Klaipėda

Tel. (8 46) 398 891, el. paštas: leidykla@ku.lt; interneto adresas: <http://www.ku.lt/leidykla/>

